AFADIN AND RHOA CONTROL PANCREATIC ENDOCRINE

MASS VIA LUMEN MORPHOGENESIS

APPROVED BY SUPERVISORY COMMITTEE

Ondine Cleaver, Ph.D.

Thomas Carroll, Ph.D.

Jane Johnson, Ph.D.

Eric N. Olson, Ph.D.

DEDICATION

To my dad Emir B. Azizoglu, my mom Gonul Azizoglu, my grandma Ayse Demir, my aunts Guler and Guner Demir, my husband Arnaldo Carreira-Rosario, and my Puerto Rican family, Marian Rosario-Hernandez, Fernando Carreira-Reyes and Alayla Carreira-Rosario

I would like to first acknowledge my mentor Ondine Cleaver, who has provided me with constant support and encouragement throughout grad school. Her constructive feedback was crucial to my success. I am especially thankful to her for setting a great example for being persistent, developing a thick skin, and, very important to me, being collaborative. She will always be my role model, not only as a mentor and a scientist, but also as a wife, a mother and for all the other roles she plays. I would also like to acknowledge my second mentors Denise Marciano and Tom Carroll, who have given me tremendous support, advised me on any challenge I faced, and provided critical feedback throughout my studies. I have been very lucky to have Ondine, Denise and Tom on my side. I would like to thank current and past Cleaver lab members for their scientific input and friendship. Special thanks to Leilani Marty Santos and

Stryder Meadows for helping me make the right choice by joining the lab and for training me after I joined; to David Barry for his critical questions and advice; to Caitlin Braitsch for being a great friend, for encouraging me at all times and her advice on everything and anything; to Simon Lee for being my aisle-mate for some time and keeping me sane through hard times; to Edward Daniel for his scientific feedback and being a great friend; to Annie Ryan for sharing my excitement for science, setting an example as a hardworker and always encouraging me.

I am truly grateful to my Thesis Committee: Drs. Tom Carroll, Jane Johnson and Eric Olson, for their vital suggestions and support. Their encouragement was key to my success. I am especially grateful to them for their open door policy, for being available despite their busy schedules whenever I needed them, their advice and support as I decide on my next step post-graduation.

I would like to thank the Department of Molecular Biology, especially the whole NA8 floor, for providing an excellent, collaborative environment to do science. I am also very thankful to the Genes, Development and Disease community for their feedback during retreats and Work In Progress seminars, which contributed tremendously to my training and scientific development.

I want to thank my husband Arnaldo Carreira for being who he is and supporting me throughout. Special thanks to my three amazing friends, Varsha Bhargava, Victor Palacios and Upa Mukhopadhyay, for teaching me so much and for being who they are. None of this would have been possible without these four people in my life. Finally, I would like to thank my family in Turkey and in Puerto Rico, and my friends in Dallas and back in Turkey, for providing me with an essential support system.

AFADIN AND RHOA CONTROL PANCREATIC ENDOCRINE MASS VIA LUMEN MORPHOGENESIS

by

DICLE BERFIN AZIZOGLU

DISSERTATION / THESIS

Presented to the Faculty of the Graduate School of Biomedical Sciences

The University of Texas Southwestern Medical Center at Dallas

In Partial Fulfillment of the Requirements

For the Degree of

DOCTOR OF PHILOSOPHY

The University of Texas Southwestern Medical Center at Dallas

Dallas, Texas

May 2018

AFADIN AND RHOA CONTROL PANCREATIC ENDOCRINE MASS VIA LUMEN MORPHOGENESIS

Publication No. _____

Dicle Berfin Azizoglu

The University of Texas Southwestern Medical Center at Dallas, 2018

Supervising Professor: Ondine Cleaver, Ph.D.

Pancreas is a vital organ responsible for digestion and blood glucose homeostasis in vertebrates. Pancreatic endocrine cells secrete hormones that regulate blood glucose levels, while exocrine cells secrete digestive enzymes. In mice, all pancreatic cell types derive from an early set of multipotent progenitors, cells of the early pancreatic bud. These progenitors complete differentiation by birth. Coincidental with differentiation, the bud epithelium forms and remodels lumens. Previous studies suggest that lumen morphogenesis is critical to endocrine and exocrine cell fate. Furthermore, recent studies show that a central network of lumens (termed core plexus) is the birthplace of most endocrine progenitors. To date, it

remains unclear how pancreatic lumens form and remodel, and which aspects of lumen morphogenesis influence cell fate. Importantly, models testing the function of the central lumen network as an endocrine niche are lacking. My thesis work identifies mechanisms underlying lumen formation and remodeling, and shows that central lumen network morphogenesis impacts pancreatic endocrine mass. Through this work, I find that loss of the scaffolding protein Afadin disrupts *de novo* lumenogenesis and lumen continuity in the tip epithelium. Co-depletion of the actomyosin regulator RhoA and Afadin results in defects in the central lumens and arrests lumen remodeling. This arrest leads to prolonged perdurance of the central lumen network over developmental time, and expansion of the endocrine progenitor population and, eventually, endocrine mass. Thus, my thesis work uncovers essential roles of Afadin and RhoA in pancreatic central lumen morphogenesis, which subsequently determines endocrine cell mass.

TABLE OF CONTENTS

PRIOR PUBLICATIONS

Azizoglu DB, Braitsch C, Marciano DK, Cleaver O. Afadin and RhoA control pancreatic endocrine mass via lumen morphogenesis. Genes Dev. 2017 Dec 1;31(23-24):2376-2390 *(featured on cover).*

Azizoglu DB, Chong DC, Villasenor A, Magenheim J, Barry DM, Lee S, Marty-Santos L, Fu S, Dor Y, Cleaver O. Vascular development in the vertebrate pancreas. Dev Biol, 2016 Dec 1;420(1):67-78.

Azizoglu DB, Cleaver O. Blood vessel crosstalk during organogenesis-focus on pancreas and endothelial cells**.** Wiley Interdiscip Rev Dev Biol. 2016 Sep;5(5):598-617 *(featured on cover).*

Daniel E, **Azizoglu DB**, Ryan AR, Walji TA, Chaney CP, Sutton GI, Carroll TJ, Marciano DK, Cleaver O. Spatiotemporal heterogeneity and patterning of developing renal blood vessels. Angiogenesis. 2018 Apr 7. doi: 10.1007/s10456-018-9612-y. (Epub ahead of print)

Barry DM, Koo YS, Norden PR, Wylie LA, Xu K, Wichaidit C, **Azizoglu DB**, Zheng Y, Cobb MH, Davis G, Cleaver O. Rasip1-Mediated Rho GTPase Signaling Regulates Blood Vessel Tubulogenesis via Non-Muscle Myosin II. Circ Res. 2016 Sep 16;119(7):810-26.

Chang CL, Hsieh TS, Yang TT, Rothberg KG, **Azizoglu DB**, Volk E, Liao JC, Liou J. Feedback regulation of receptor-induced Ca2+ signaling mediated by E-Syt1 and Nir2 at endoplasmic reticulum-plasma membrane junctions. Cell Rep. 2013 Nov 14;5(3):813-25.

LIST OF FIGURES

LIST OF APPENDICES

LIST OF ABBREVIATIONS

ADIP – Afadin DIL Domain-Interacting Protein

$Afa^{KO}RhoA^{HET}$ – $Afa^{f/f}$;$RhoA^{f/+}$; $Pdx1^{Cre}$

Afa^{pancKO} – $Afa^{f/f}$; $Pdx1^{Cre}$

aPKC – Atypical protein kinase C

Cdc42 – division cycle 42

Crb3-GFP – $Crumbs3^{GFP/+}$

Crumbs – Crumbs 1, Cell Polarity Complex Component

DBA – Dolichos biflorus agglutinin

DIL – dilute

DKO – $Afa^{f/f}$; $RhoA^{f/f}$; $Pdx1^{Cre}$

E – embryonic day

EGFR – Epidermal Growth Factor Receptor

EMT – epithelial-to-mesenchymal transition

F-actin – filamentous actin

FHA – Forkhead-association

Hnf1b – Hepatocyte nuclear factor 1 beta

Hnf6 – Hepatocyte nuclear factor 6

MDCK – Madin Darby Canine Kidney

Neurog3 – Neurogenin 3

Nkx6.1 – NK6 homeobox 1

NMII – non-muscle myosin II

P – postnatal day

Par3 – Partitioning Defective 3

Par6 – Partitioning Defective 6

Pdx1– Pancreatic and duodenal homeobox 1

Podxl – podocalyxin

Ptf1a – Pancreas specific transcription factor, 1a

RA – Ras association

Rab8 – Ras-Associated Protein Rab8

Rab11 – Ras-Associated Protein Rab11

Rac – Rac Family Small GTPase

Rap1 – Ras-Related Protein Rap1

Rasip1 – Ras interacting protein 1

Rho – Ras Homolog Family

RhoA – Ras Homolog Family Member A

R26 – Rosa26

Snail2 – Snail Family Transcriptional Repressor 2

Sox9 – SRY (Sex-determining region Y) box 9

Tcf2 – Transcription Factor 2 (same as Hnf1b)

TEM – transmission electron microscopy

TJ – tight junction

ZO1 – zonula occludens 1

CHAPTER ONE

INTRODUCTION TO PANCREAS DEVELOPMENT AND LUMEN MORPHOGENESIS

Blood sugar homeostasis and proper digestion of food both rely on a functional pancreas. Pancreas serves these functions through three major cell types; endocrine cells that release sugar-regulating hormones into the circulation, acinar cells that secrete digestive enzymes into the ducts, and ductal cells that line the ducts and help digestion. These cell types all differentiate during embryonic development (Pan and Wright 2011). Deficiencies in pancreatic cell function cause diabetes or exocrine insufficiency which can be treated, if we could supply patients with the relevant cell type. However, our poor understanding of how these cells differentiate prevents us from generating them efficiently and consistently well in the lab (Pan and Wright 2011). Elucidation of mechanisms underlying pancreatic differentiation is a crucial step towards generating functional pancreatic cells *in vitro*. By studying pancreas development, we can delve into the native environment of the differentiating cells, find out where and how each cell decides on a specific fate, and eventually use this knowledge towards developing treatments for pancreatic diseases.

Early pancreas and its microlumens

Mature pancreas is a highly branched organ made up of tubes (or ducts, i.e. mature lumens). To get to this mature form, the embryonic pancreas coordinates branching morphogenesis

and tubulogenesis (or lumen morphogenesis) with differentiation during development (Villasenor et al. 2010; Pan and Wright 2011). We can only fully understand where and how the cells differentiate into specific pancreatic lineages by putting them in their native context: an epithelium in the process of branching and forming tubes. Mouse pancreas represents a good model system to study these developmental processes and pancreatic differentiation, as it shares high similarity with the human pancreas (Pan and Wright 2011; Jennings et al. 2015).

In the mouse, the dorsal pancreatic epithelium gets specified following signals from the mesoderm, the notochord and the aorta, and starts expressing Pancreatic And Duodenal Homeobox 1 (Pdx1). Pancreatic bud formation initiates with mesenchyme-dependent proliferation and thickening of the Pdx1-expressing epithelium along the gut endoderm at embryonic day (E) 9.5. Upon budding, the pancreatic epithelium becomes stratified. Now, the bud consists of outermost layer cells in contact with the nearby mesenchyme, innermost layer cells surrounding the primary gut lumen, and non-polarized cells in-between **(Figure 1.1)**. This cell mass is multipotent until E12.5; it gives rise to all the lineages of the pancreas, and determines both the final endocrine and exocrine masses (Gu et al. 2002; Stanger et al. 2007; Pan and Wright 2011).

A subset of pancreatic cells gets distinguished from the rest through formation of small discontinuous cavities, called microlumens, at E10.5. To open these microlumens, cells rearrange their junctions and undergo apico-basal polarization **(Figure 1.1)**. Then, the cells organize into a flower-like arrangement, called rosettes. The microlumen opens in the center of the rosette. These microlumens extend and fuse into a mostly continuous network of

interconnected lumens at around E12.5 **(Figure 1.1)**. This arrangement of lumens with no hierarchy is termed the plexus (Kesavan et al. 2009; Villasenor et al. 2010; Bankaitis et al. 2015). As development proceeds, the plexus remodels through unknown mechanisms into a continuous hierarchical tree by postnatal day (P) 0 **(Figure 1.1)** (Bankaitis et al. 2015).

Coincidental with lumen development, the multipotent pancreatic progenitors decide on their fates and start differentiating (Pictet et al. 1972; Zhou et al. 2007; Pan and Wright 2011). Cells in "tip" epithelia of an E12.5 (or later) pancreas commit to the acinar lineage which serves digestion in the mature pancreas. The remaining "trunk" cells are bipotential and give rise to the other two pancreatic lineages through E12.5-P0, i.e. ductal cells that line the ducts and endocrine cells that regulate glucose metabolism **(Figure 1.2)** (Pan and Wright 2011).

Close relationship between lumen development and differentiation, both temporally and spatially, is intriguing. This brings up the question "Does lumen development provide cues for differention in the pancreas?" Indeed, in a pancreas-specific *Cdc42* mutant mouse model, lumen morphogenesis is defective starting at the microlumen stage, and this is accompanied by a skewed acinar to endocrine cell ratio later on (Kesavan et al. 2009). The authors of this study argued that the *Cdc42* mutant epithelium is overexposed to the basement membrane due to absence of lumens. This basement membrane overexposure was proposed to induce acinar fate. Although this idea is consistent with the findings of the study, it has not been tested in other models. Besides this study, there have not been other models that directly tested whether lumen development affects pancreatic differentiation. However, correlation between abnormal differentiation and deficient lumen morphogenesis in general is striking: Many pancreatic mutant models with defective differentiation display abnormal tube

morphology, including the classical *Pdx1*-null model with pancreatic agenesis (Kang et al. 2009; Zhang et al. 2009; Hale et al. 2014; Bankaitis et al. 2015; De Vas et al. 2015; Marty-Santos and Cleaver 2016). Altogether, these studies strongly suggest that lumen morphogenesis is a crucial part of pancreas development and may have a role in guiding differentiation of the pancreatic lineages.

Differentiating pancreas and its remodeling lumens

The first indication of differentiation in the pancreas is trunk-tip compartmentalization at E12.5. This sets the next series of events for the first lineage bifurcation: specification of the acinar and ductal bipotential progenitor lineages **(Figure 1.2)**. This also marks the beginning of the "secondary transition", referring to the production of endocrine cells that will form most of the endocrine mass in the mature organ. The pancreas at the stage of trunk-tip compartmentalization is also referred to as "proto-differentiated". Here, the transcription factors Nkx6.1 and Ptf1a are induced in the trunk and tip domains, respectively, to promote the compartmentalization. These two transcription factors also repress each other, thereby suppressing the alternate differentiation program in their respective domains (Zhou et al. 2007; Schaffer et al. 2010; Pan and Wright 2011). By the time of trunk-tip compartmentalization, microlumens have fused to form a continuous plexus **(Figure 1.2)** (Villasenor et al. 2010). Therefore, pancreatic differentiation, acinar, endocrine or ductal, occurs in the presence of a plexus, while the plexus slowly remodels into a tree.

Despite their co-occurrence, while pancreatic differentiation has been extensively studied, mechanisms underlying lumenal plexus remodeling remain unknown. Bankaitis and

colleagues recently provided a thorough morphological characterization of the pancreatic lumens at E14.5-E18.5 (Bankaitis et al. 2015). This study described two regions, core and periphery, with morphologically distinct lumens in the developing pancreas. It further revealed that core and periphery undergo different lumen morphogenesis events. In the core, pancreas undergoes "plexus-to-duct transformation": The E14.5-E15.5 pancreas core mostly consists of a lumenal plexus. Starting at E16.5, this plexus slowly remodels into ducts. The appearance of these ducts is asynchronous throughout the pancreas, where a domain of plexus turns into a domain of hierarchical ductal branches, with the central duct being the first to form. At E18.5, a few isolated domains of plexi still remain. This remodeling gives rise to a hierarchical central ductal tree by birth. Unlike in the core, no plexi were observed in the periphery. Here, the lumens formed branches without going through the plexus state **(Figure 1.3)** (Bankaitis et al. 2015). Therefore, pancreatic core and periphery represent two regions where lumens undergo distinct morphological processes.

Overall, decades of work suggests that lumen morphogenesis and differentiation are closely linked during pancreas development. More recent studies indicate that pancreatic lumens undergo well-defined morphogenetic processes to remodel extensively. How this lumen remodeling occurs and is coordinated with differentiation remains unknown. Whether maintenance or differentiation of the progenitors is impacted by their lumenal environments is a mystery. Answering these questions will be critical for an in-depth understanding of pancreatic tip and trunk progenitor differentiation towards exocrine and endocrine lineages.

Endocrine pancreas development: Decide, get out and get together

Once the proto-differentiated epithelium has formed, tip cells have no choice but become acinar. Trunk cells, on the other hand, still have another choice to make: turn on endocrine or ductal fate. Trunk cells in bipotential state can be recognized by the expression of the transcription factors Sox9, Hnf1b and Hnf6. A subset of these progenitors up-regulates Neurog3 and commits to the endocrine lineage (Gradwohl et al. 2000; Jensen et al. 2000; Schwitzgebel et al. 2000; Gu et al. 2002). Neurog3 up-regulation is not just a marker, but is also known to be required and sufficient for endocrine fate commitment (Apelqvist et al. 1999; Gradwohl et al. 2000; Schwitzgebel et al. 2000). The remaining bipotential cells with no or low Neurog3 expression commit to the ductal fate. These cells express Sox9, Hnf1b and Hnf6; in other words, they retain the markers expressed in bipotential progenitors (Seymour et al. 2007; Solar et al. 2009; Schaffer et al. 2010).

Ductal versus endocrine fate decision arguably represents one of the most poorly understood events in pancreas development. What decides whether a bipotential progenitor will up-regulate Neurog3 and commit to the endocrine fate? Indeed, only a small percentage of bipotential progenitors commit to the endocrine lineage (Bankaitis et al. 2015). What decides which bipotential progenitors will do so?

Endocrine fate decision has been a subject of research for decades. Early studies provided evidence for an inhibitory role of the mesenchyme in this process (Gittes et al. 1996; Miralles et al. 1998a; Miralles et al. 1998b). These studies relied on embryonic pancreas explant cultures with and without the mesenchyme. Recent work based on *in vivo* studies argues that the pancreatic mesenchyme plays a mitogenic role rather than a fate-inductive one (Pulkkinen et al. 2003; Landsman et al. 2011). Therefore, mesenchymal signals are not

required, nor is their absence sufficient to induce pancreatic fate decisions towards acinar or endocrine lineages.

Recent studies have begun to address mechanisms of endocrine fate induction by studying the type and number of cell divisions that give rise to endocrine and remaining bipotential progenitors. Work by Kim and colleagues showed that bipotential progenitors can undergo three types of divisions: an asymmetric division producing one bipotential and one endocrine cell, a symmetric division to produce two bipotential cells, or a symmetric division to produce two endocrine cells (Kim et al. 2015). The dynamics of cell division and fate commitment observed in this study suggested that endocrine fate was induced stochastically following asymmetric divisions, rather than relying on unequal partitioning of cellular contents. In the case of symmetric endocrine-yielding divisions, the cells seemed to turn on endocrine fate prior to cell division. This appears contrary to the general belief that endocrine progenitors are by large post-mitotic. However, this contradiction gets resolved, if one considers that the timing of Neurog3 induction in the context of cell cycle is critical, as the authors concluded. Then, there are two possible major outcomes as a result of different Neurog3 induction timing: 1) Neurog3 induction early during cell cycle following division will induce cell cycle exit and produce one endocrine cell, 2) Neurog3 induction late in the cell cycle will not induce cell cycle exit; the cell will commit and divide to produce two endocrine daughters (Kim et al. 2015). This study is the first to assess endocrine-yielding divisions in detail and define the relevant cell cycle dynamics. However, as stated by the authors, "…the molecular mechanisms of Neurog3 priming remain to be elucidated, especially whether it is under cell-intrinsic or extrinsic control…"

Recent work has also focused on mechanisms of regulating Neurog3 levels in the cell in order to gain insight into endocrine fate induction. Cell cycle was once again identified as a master regulator of this process. These work revealed that Neurog3 can be phosphorylated and degraded in a cell cycle-dependent manner (Azzarelli et al. 2017; Krentz et al. 2017). Lengthened G1 phase over developmental time was shown to be required for Neurog3 up-regulation and endocrine differentiation. The authors concluded that longer G1 phase leads to stabilization and accumulation of Neurog3, which then reaches high levels to initiate the endocrine differentiation program. This finding is in line with previous work suggesting that high Neurog3 levels are necessary to induce endocrine differentiation (Wang et al. 2010). Although this work nicely shows that endocrine differentiation can be driven by altered cell cycle dynamics, it does not address how only a subset of bipotential progenitors turn on endocrine fate. Cell cycle dynamics of bipotential progenitors were measured in bulk. Therefore, it remains unknown whether a subset of bipotential progenitors has different cell cycle dynamics than the rest, therefore turning on endocrine fate. Even so, what triggers bipotential cells to have varying cell cycle dynamics needs to be addressed. Thus, how regulation of cell cycle dynamics relates to induction of endocrine fate in only a subset of progenitors remains to be determined.

Once committed to endocrine fate, the progenitors give rise to five different subtypes of hormone-producing cells: glucagon-producing alpha, insulin-producing beta, somatostatin-producing delta, pancreatic polypeptide producing PP, and ghrelin-producing epsilon cells. Individual endocrine progenitors are unipotent; they will only give rise to one endocrine-subtype (Desgraz and Herrera 2009). Furthermore, each subtype arises at different

developmental time points, in the following order: alpha cells (E9.5), beta cells (E10.5), delta cells (E15.5) and PP cells (P0) (Yamaoka and Itakura 1999). As committed progenitors initiate the appropriate endocrine-subtype differentiation program, they leave the ductal epithelium through delamination (Herrera et al. 1991; Bouwens and De Blay 1996; Jensen 2004). This occurs independently for individual progenitors. Following delamination, endocrine progenitors come together and form long stretches of clusters, remaining closely associated with the duct they delaminated from. These clusters then separate to give rise to the oval-shaped islets of Langerhans with peripheral alpha and inner beta cells short before birth (E18.5). The islets are no more closely associated with the ductal epithelium at birth (P0) **(Figure 1.4)** (Miller et al. 2009). Finally, each hormone-producing cell matures, as the islet morphology take its final shape. This process is referred to as isletogenesis.

Isletogenesis is required for proper endocrine function, and elucidating its mechanisms will be important for developing endocrine cell-related therapies (Gannon et al. 2000; Konstantinova et al. 2007). Delamination, the first step to form islets, relies on down-regulation of cell-cell adhesion and up-regulation of migratory/epithelial-to-mesenchymal transition (EMT) phenotype (Rukstalis and Habener 2007; Gouzi et al. 2011). The following steps, migration and clustering, involve modulation of cell-cell adhesion and EGFR pathways (Dahl et al. 1996; Miettinen et al. 2000). Endocrine differentiation program may initiate not only differentiation, but also the EMT program required for isletogenesis: The master endocrine differentiation factor Neurog3 has been shown to directly regulate expression of *Snail2*/*Slug*, major regulator of the EMT phenotype (Gouzi et al. 2011). Thus, delamination

and clustering of endocrine cells are strongly linked to, and in some cases may depend on, proper endocrine differentiation.

Thanks to the wealth of information on how endocrine differentiation occurs *in vivo*, there have been significant improvements in *in vitro* endocrine cell differentiation protocols. However, the lab-made endocrine cells fail to behave consistently well, and are not ready for therapeutic applications (Pagliuca et al. 2014; Massumi et al. 2016). One major point of divergence of *in vitro* protocols from the *in vivo* path is that these protocols do not induce differentiation through the bipotential progenitor state. Instead, they rely on direct differentiation of early, presumably multipotent, pancreatic progenitors to the endocrine lineage (Santosa et al. 2015). This may be one of the reasons why the resulting cells do not function as predicted consistently when transplanted *in vivo*. Indeed, our poor understanding of endocrine fate induction is undoubtedly a major obstacle in trying to make *in vivo*-like endocrine cells. *In vitro* protocols can be designed to take the *in vivo* path to definitively generate the best *in vivo*-like endocrine cells possible, once we identify the factors that induce endocrine fate *in vivo*.

Although signaling mechanisms that induce endocrine fate remain unknown, exciting recent work described a special microenvironment in the developing pancreas where most endocrine progenitors reside (Bankaitis et al. 2015). This study by Bankaitis and colleagues revealed higher endocrine yield from bipotential progenitors in the core plexus region (as defined in the previous section) compared to the periphery **(Figure 1.3)**. Furthermore, the core plexus resolves into a tree by birth, which nicely correlates with termination of endocrine progenitor generation. Finally, even though the authors have only analyzed past

E14.5, the plexus has been previously described to arise shortly after E12.5, which also nicely coincides with the beginning of secondary transition endocrine cell generation (Villasenor et al. 2010). Taken together, this work suggests that the core may act as a niche for endocrine differentiation (Bankaitis et al. 2015). However, no functional data was provided to test this idea. Thus, further studies are needed to address a potential function of the core plexus in endocrine cell generation.

In summary, the signaling mechanisms that specify endocrine fate remain elusive. Recently, core lumenal plexus has been proposed to act as a niche for endocrine differentiation. Identification of such a niche will undoubtedly improve our understanding of endocrine differentiation and will set the stage for elucidation of the underlying mechanisms. However, testing the function of the core plexus as an endocrine niche will require a better understanding of pancreatic lumen and plexus morphogenesis.

Conserved mechanisms of lumen morphogenesis

Tubes are formed during development in many tissue systems of metazoans, and are essential for function of many organs (Iruela-Arispe and Beitel 2013). In the pancreas, tube morphogenesis occurs coincidental with differentiation and has the potential to provide cues for fate decisions. Thus, it will be crucial to elucidate the mechanisms of pancreatic tubulogenesis to shed light on development of pancreatic cell types. Although cellular or molecular mechanisms underlying pancreatic tubulogenesis largely remain elusive, other organ systems in both mammalian and non-mammalian species undergo similar events (Hogan and Kolodziej 2002). A few of these have been used as model systems to study tube

morphogenesis. Here, I will highlight a series of findings in such model systems, and discuss their potential relevance in the context of pancreas development.

Microlumen emergence and coalescence seen in the pancreas is a common mechanism to form a single tube used across species and organs. Zebrafish gut, mammalian mammary and salivary glands, and hair follicle all rely on these cellular events to form a tube (Hogan and Kolodziej 2002). Here, initally unpolarized cells undergo apico-basal polarization to form *de novo* lumens isolated from each other. Following *de novo* lumen formation, lumens coalesce to form a single tube. Mechanisms underlying lumen coalescence have been investigated mostly through genetic approaches. These work revealed key players in the zebrafish gut and drosophila trachea.

In the zebrafish gut, mutation of *aPKC* homolog *has* leads to formation of multiple lumens as opposed to a continuous single lumen due to delayed or aberrant apical junction formation (Horne-Badovinac et al. 2001). Two other zebrafish mutant models, for the Hedgehog signaling receptor *smoothened* and the transcription factor *Tcf2*, or *Hnf1b,* display very similar lumen discontinuity phenotypes (Bagnat et al. 2007; Alvers et al. 2014). Hnf1b was shown to act through regulation of gap junction protein expression to ensure continuous lumen formation (Bagnat et al. 2007). In the pancreas, Hnf1b is expressed in progenitors lining lumens, and its depletion leads to cystic duct formation (De Vas et al. 2015). Therefore, the role of involved molecular factors may be conserved in the pancreas, and studying these factors may provide insight into pancreatic lumen development.

Lumen morphogenesis in the Drosophila tracheal system, although not similar to pancreas in its early steps, also relies on lumen coalescence (Lee and Kolodziej 2002). Here, lumen

coalescence occurs through junction formation between cells on their basolateral side, which then triggers F-actin assembly through RhoA activity at the site of junction. Next, F-actin assembles in a track that radiates outwards in the apposing cells, and this creates a path for the apical membrane of each cell to expand on and colaesce. Thus, lumen coalescence requires junction rearrangement and F-actin assembly directed by RhoA activity in the Drosophila trachea (Lee and Kolodziej 2002). Given high conservation of the involved molecules across metazoa, it will be interesting to determine whether pancreatic lumen coalescence relies on similar mechanisms.

Unlike the initial steps of *de novo* lumen formation and coalescence, morphogenesis of a lumenal plexus and remodeling of this plexus into a hierarchical tree in the pancreas seem to be much more uncommon. Another system well-known to develop this way is a specialized epithelium, the endothelium of the vasculature. In many examples of vasculogenesis, i.e. *de novo* formation of vasculature, endothelial cells initially form a plexus of tubes (Drake et al. 1997; Drake and Fleming 2000). Then, this plexus remodels into hierarchically organized specialized vessels, arteries, arterioles, veins, venules, and capillaries. The process of plexus-to-hierarchical vessel remodeling is poorly understood, like pancreatic plexus remodeling itself. It is interesting, however, that the pancreatic tube morphogenesis goes through a similar, rarely seen plexus state. During vascular development, the plexus may serve as an intermediate prior to specification of vessels, enabling vascular function needed for survival of the embryo (Hogan and Kolodziej 2002). By contrast, the function of pancreatic tubes is not needed until birth, where the plexus has already remodeled into a tree (Bankaitis et al. 2015). It is tempting to hypothesize that the pancreatic plexus may play an unexpected role in

development of the organ, rather than functioning as tubes per se. Based on the findings of the Bankaitis et al study (discussed in the previous section), it is possible that the plexus serves as a niche for endocrine differentiation. This and other ideas need to be tested to better understand whether the plexus state of lumens has any function in the developing pancreas.

While the molecular mechanisms identified in other systems may shed light on pancreatic lumen coalescence, cellular events underlying this process are largely unknown and need further study. Do pancreatic lumens coalesce through cell-cell junction formation and apical membrane expansion? Is cell migration involved? What is the role of spindle orientation during cell division in this process? Addressing these questions will be crucial for our understanding of tube development and lumen remodeling, one of the most poorly defined events in pancreatic morphogenesis.

De novo lumen formation: Molecular mechanisms

Before lumens coalesce, they need to form *de novo* in many tissues, such as the developing pancreas, kidney and vasculature (Kesavan et al. 2009; Villasenor et al. 2010; Xu et al. 2011; Yang et al. 2013). *De novo* lumen formation has been shown to depend on junction rearrangement, apical membrane generation and vesicle exocytosis (Hieda et al. 1996; Nanba et al. 2001; Datta et al. 2011). Indeed, these events have been found to occur in the developing pancreas (as discussed in the "Early pancreas and its microlumens" section of this chapter). Although the underlying molecular mechanisms have not been investigated, studies in other systems are likely to inform *de novo* lumen formation mechanisms in the pancreas (Kesavan et al. 2009; Villasenor et al. 2010).

The most well-studied aspect of *de novo* lumen formation can be considered apical polarity (Hogan and Kolodziej 2002; Datta et al. 2011). Since *de novo* lumen formation relies on apical polarity, any cellular process or molecular factor needed for apical polarity will also be needed for *de novo* lumen formation. These include the well-established apical determinants Par and Crumbs complexes. These proteins are conserved all the way down to C. *elegans*, and are required for polarity across metazoan phyla (Thompson 2013). Since the role of these factors in apical polarity, as well as the role of apical polarity in *de novo* lumen formation, is rather well-studied, I will not review those findings here. A much less understood problem is, what are the determinants of *de novo* lumen formation (and not apical polarity per se)?

In vitro studies have identified a set of molecular factors needed for *de novo* lumen formation. This work has mostly relied on a 3-dimensional culture system using Madin Darby Canine Kidney (MDCK) cell lines. This model system provides high spatial detail and temporal control, as well as easy accessibility for genetic manipulations. Through decades of work in MDCK cultures, a molecular model of *de novo* lumen formation has emerged **(Figure 1.5)** (Bryant et al. 2010).

To form lumens, MDCK cells first aggregate (as they start off as single cells in this system) and form junctions **(Figure 1.5)** (Bryant et al. 2010). Then, Par complex protein Par3 and members of the exocyst complex localize to the junctional foci along with junctional complex proteins. Next, apical membrane formation is initiated. Exocyst components and Par3 re-localize from junctional foci to the pre-apical domain, initiating interactions with the Par complex proteins aPKC and Par6. This event triggers exocytosis of the apically targeted vesicles mediated by Cdc42, Rab11 and Rab8. Exocytosis generates the apical membrane

and eventually the lumen **(Figure 1.5)** (Bryant et al. 2010). Thus, lumen formation occurs as a result of junction reorganization, apical membrane formation and exocytosis.

One of the first steps of *de novo* lumen formation, junction reorganization, requires coordinated activity of polarity complexes, Rho GTPases and the actin cytoskeleton (Shin et al. 2006; Citi et al. 2014). These complexes are also involved in other processes, such as cell-cell adhesion or polarity determination (Shin et al. 2006; Citi et al. 2014). This represents a challenge in studying junction reorganization process in the context of lumen formation. Such a study requires strictly transient manipulation of the multi-functional junction reorganization factors. There is, however, evidence for junction reorganization prior to lumen formation *in vivo*, including in mammalian mammary glands and the zebrafish gut (Hieda et al. 1996; Horne-Badovinac et al. 2001; Hogan and Kolodziej 2002). Epithelial junction reorganization occurs early during pancreas development, as well, suggesting that it likely precedes pancreatic *de novo* lumen formation (Villasenor et al. 2010).

Following junctional reorganization, cells generate the apical membrane through exocytosis of apical components at the pre-apical domain. The molecular machinery that initiates apical membrane formation has been extensively studied in the MDCK system. During lumen formation by MDCK cells, a Rab11-Rabin8-Rab8 cascade activates the Rho GTPase family member Cdc42 and drives vesicular exocytosis at the preapical domain (Bryant et al. 2010). Exocyst complex localizes to the pre-apical domain, and is thought to mediate the exocytosis of apical vesicles (Bryant et al. 2010). The motor protein MyosinV has also been shown to be involved in apical exocytosis, presumably directing vesicular trafficking towards the pre-apical domain (Hogan and Kolodziej 2002; Massarwa et al. 2009; Roland et al. 2011). These

processes altogether ensure proper targeting of apical cargo and formation of the apical membrane. In fact, exocytosis is not only required for apical membrane formation, but also localization of apical polarity determinants, suggesting a feedback mechanism for establishing apical polarity and forming the apical membrane (Datta et al. 2011).

In line with the findings in the MDCK system, loss of function of the identified exocytosis mediators leads to exocytosis defects in mice and humans. In the developing pancreas, Cdc42 depletion leads to accumulation of intracellular vesicles (Kesavan et al. 2009). *Rab8* mutant mice similarly show exocytosis defects in the intestine, and develop "intracellular lumens" reminiscent of microvillus inclusion disease seen in humans (Sato et al. 2007). Likewise, *MyosinV* mutations are associated with microvillus inclusion disease in children, suggesting a role for MyosinV in trafficking of apical vesicles in humans (Muller et al. 2008). These findings provide evidence that the molecular factors identified in the MDCK system are relevant to lumen formation in developing tissues of mice and humans.

Mechanisms of *de novo* lumen formation have also been studied in the vasculature. One of the most crucial lumen formation events occurs in the aorta. The aorta has to open a lumen early in development for survival of the embryo. Recent work has elucidated mechanisms underlying this process (Xu et al. 2011; Barry et al. 2016). Here, an endothelial-specific scaffolding molecule, Rasip1, was identified as a master regulator of lumen formation, or a "lumen master" (Xu et al. 2011). Rasip1 regulates this process by activating Cdc42, which in turn regulates non-muscle myosin II (NMII) to mediate actomyosin constriction (Barry et al. 2016). This signaling is required for clearance of junctions between cells to be able to open the lumen. Once the lumen is formed, Rasip1 is required to maintain lumen size, where it

acts through RhoA, once again, to activate NMII (Barry et al. 2016). Although junction clearance has not been proposed to occur in most other *de novo* lumen forming systems, the molecular machinery involving Cdc42, actomyosin and RhoA seems to be well-conserved across systems. This brings up the idea that, even though different systems form *de novo* lumens through different cellular mechanisms, they may re-use evolutionarily established molecular regulators to do so.

The developing kidney is another system where *de novo* lumen formation is critical. How lumen morphogenesis in the kidney is regulated has only recently been addressed. Afadin, a junction-cytoskeleton linker molecule, has been found as required for timely lumen formation and coalescence in the renal vesicle (Yang et al. 2013). In the absence of Afadin, cells of the renal vesicle partially mis-localize or lack enrichment of apical determinants, fail to form an apical membrane and a lumen with correct timing. Lumens do develop in these mutants, however with a delay, and mostly fail to recover from coalescence defects (Yang et al. 2013). Afadin bears striking similarity to the vascular-specific lumen-master Rasip1 in its domain structure and interaction partners. Both proteins contain Ras-association (RA), dilute (DIL), and Forkhead-association (FHA) domains, and have been consistently shown to interact with Rap1 (Hoshino et al. 2005; Sato et al. 2006; Post et al. 2013; Wilson et al. 2013; Gingras et al. 2016; Bonello et al. 2018). Thus, Afadin and Rasip1 represent two cousin molecules with highly similar functions as lumen masters in epithelium and endothelium, respectively. Given this conservation, it will be important to investigate the role of epithelial Afadin during *de novo* lumen formation in other systems, including the developing pancreas.

Once the lumen is formed, maintaining the lumen at the right place and size requires physical force generation and proper spindle orientation in the lumen-surrounding cells (Datta et al. 2011). RhoA and actomyosin contractility regulate the subapical physical force, thereby facilitating lumen maintenance in the aorta (Barry et al. 2016). Proper spindle orientation, on the other hand, depends on many factors, some of which have been established as junction reorganizers, polarity determinants, or exocytosis mediators, such as Afadin, Cdc42, Par3 and aPKC (Tawk et al. 2007; Jaffe et al. 2008; Hao et al. 2010; Qin et al. 2010; Rodriguez-Fraticelli et al. 2010; Carminati et al. 2016; Gao et al. 2017; Rakotomamonjy et al. 2017). Due to their multifunctional nature, identifying the role of these molecules in lumen formation versus spindle orientation is challenging. Additionally, proper cell division orientation and lumen formation may be inter-dependent and can overlap in time. Indeed, this brings up an interesting problem in trying to elucidate mechanisms of lumen formation and maintenance in general: These processes share many molecular factors, and they cross-talk. Therefore, it is not trivial to dissociate these two events and identify molecular factors involved in one versus the other. Experimentation with tight spatiotemporal control will be needed to tease apart lumen formation and maintenance mechanisms. Eventually, both of these processes need to act together to form a proper tube.

Altogether, these studies provide in-depth molecular insight into lumen formation and maintenance in different systems. Although the relevance of these factors to pancreatic lumen morphogenesis remains unknown, I predict that most of the identified mechanisms will be relevant to the developing pancreas, given the conservation of the involved molecular machinery across organ systems and metazoan phyla.

Plexus morphogenesis and endocrine differentiation: Is there a connection?

Plexus morphogenesis and endocrine differentiation: They initiate together, they end together, and both occur only transiently during development. The question becomes, does plexus morphogenesis provide guidance for endocrine differentiation?

Abnormal pancreatic lumen initiation causes major defects in epithelial integrity before affecting cell fate, as suggested by previous work (Kesavan et al. 2009). This represents a challenge in trying to determine a direct relationship between lumen morphogenesis and cell fate. One way to tackle this question is to disrupt lumen morphogenesis in a way that will cause as little defects in epithelial integrity as possible. This could be achieved by altering lumen morphogenesis once early lumens have formed. This idea built the basis of my thesis work.

My study focuses on the question "Does plexus morphogenesis matter to endocrine differentiation?" To ask this question, I manipulated lumen morphogenesis using a genetic approach. I hypothesized that pancreatic lumen morphogenesis relies on the conserved molecular factors required for lumen morphogenesis in other systems (as introduced in the section "*De novo* lumen formation: Molecular mechanisms" of this chapter). Indeed, I was able to identify pancreas-specific *Afadin* single mutant and *Afadin;RhoA* double mutant models that form initial lumens mostly fine, but fail in further steps of lumen morphogenesis. Depletion of Afadin led to lumen discontinuity in the pancreatic periphery, while Afadin;RhoA double depletion caused failure in remodeling of the core plexus. As a result, *Afadin;RhoA* double mutants exhibited prolonged maintenance of the plexus. Unlike the previously characterized *Cdc42* mutant model of defective pancreatic lumen formation,

Afadin and *Afadin;RhoA* mutants did not display any abnormalities in early epithelial integrity or branching. Strikingly, I found that the plexus arrest in *Afadin;RhoA* double mutants was accompanied by dramatic expansion of endocrine mass. Altogether, my findings suggest that the prolonged maintenance of the plexus promotes endocrine differentiation. Based on these findings, I propose that the transient pancreatic plexus acts as a niche for endocrine fate induction. I provide my experimental results that led to these conclusions in Chapter 3. I discuss the significance of these findings, address remaining questions, highlight alternative hypotheses and provide future directions in Chapter 4 for a better understanding of lumen morphogenesis and endocrine fate induction during pancreas development.

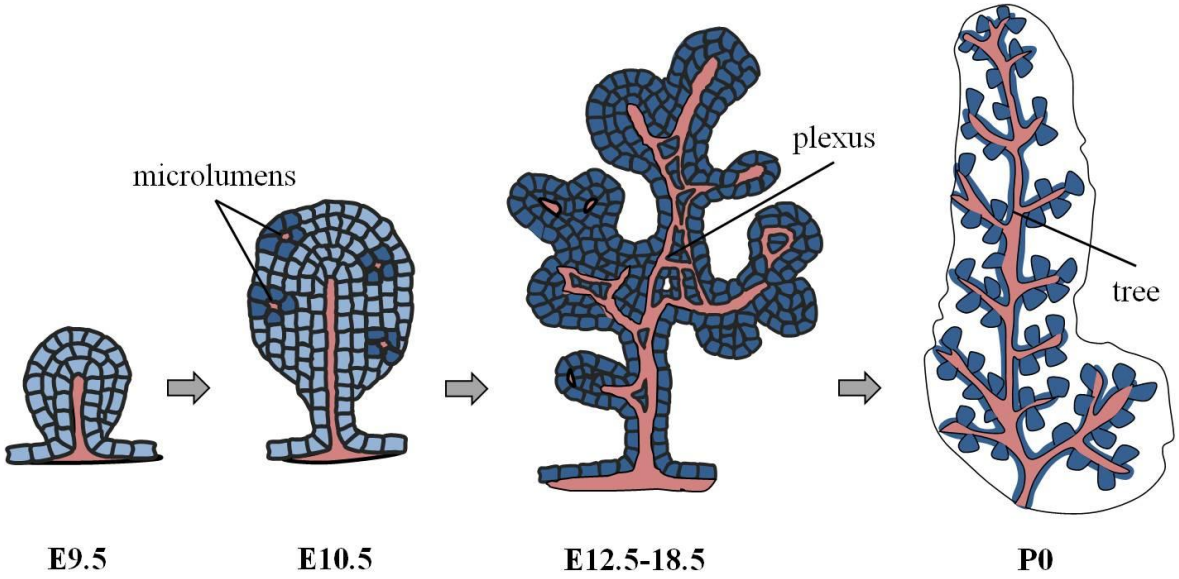

Figure 1.1. Lumen morphogenesis during pancreas development. Pancreas development initiates with budding of the specified epithelium along the endoderm at E9.5. At this stage, cells are non-polarized (light blue), with the exception of apical polarity of the innermost cells and presumably basal polarity of outermost cells. At E10.5, cells start gaining apical polarity and order themselves into flower-shaped structures, or rosettes (dark blue). These cells then open an isolated cavity in the rosette center, called microlumen (pink). Microlumens coalesce (or fuse) over developmental time and form a network of interconnected tubes by E12.5. This arrangement of lumens without hierarchy is termed "plexus". By birth, the plexus remodels into a continuous hierarchical tree.

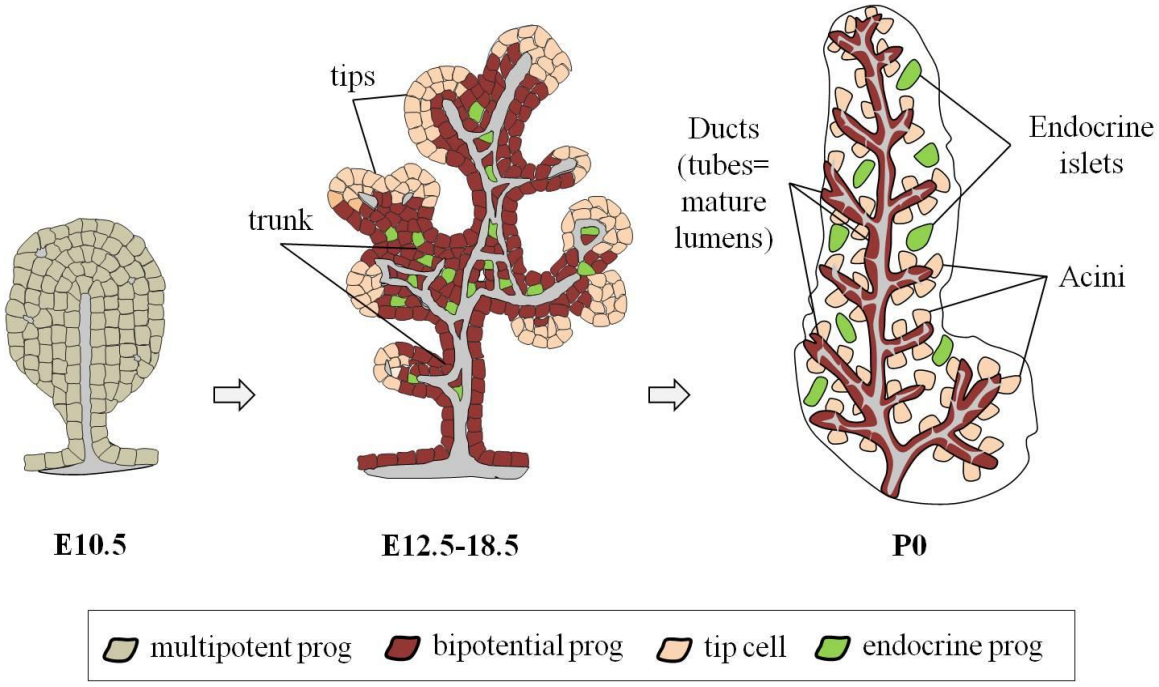

Figure 1.2. Pancreatic differentiation coincides with lumen morphogenesis. The developing pancreas at the microlumen stage (E10.5) is multipotent and gives rise to all the pancreatic lineages. Cells start making fate decisions upon tip-trunk compartmentalization in the epithelium at E12.5. By this time, a continuous plexus has formed. Cells at epithelial tips turn on acinar fate, while cells in the trunk are now bipotential and give rise to ductal and endocrine cells. Endocrine progenitors (shown in green) arise within the trunk region and commit to endocrine fate. The remaining trunk cells give rise to the ductal lineage.

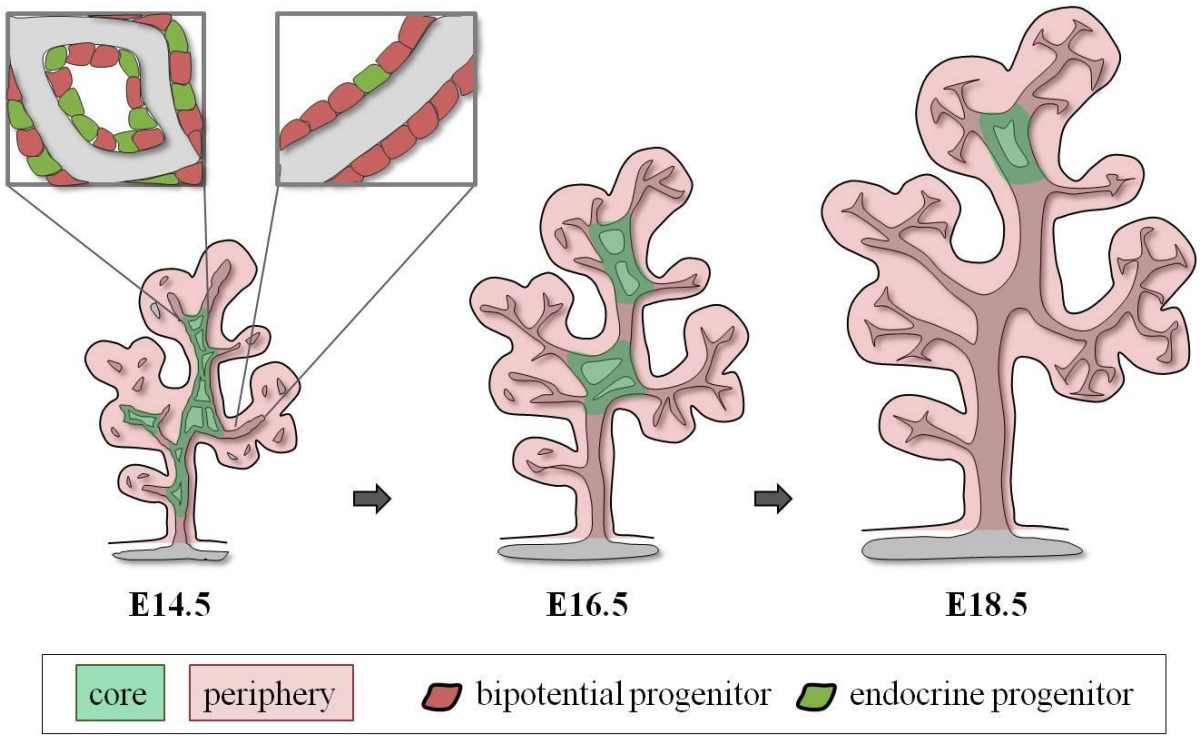

Figure 1.3. Pancreatic core is where most endocrine progenitors reside and is distinguished based on lumenal morphology. Midgestation pancreas is mostly composed of a network of interconnected lumens, or plexus, in the central region of the organ, termed the ‘core’ (E14.5). The remaining outer region is termed the ‘periphery’, which does not go through a plexus state. The core plexus resolves over developmental time, as lumens remodel into a hierarchical tree. This resolution occurs asynchronously, and isolated domains of plexi remain at later stages (E18.5). Core and periphery are not only different in their lumenal morphology, but also cellular composition. Lumens in both regions are lined by bipotential progenitors. However, these bipotential progenitors yield a higher percentage of endocrine progenitors in the core, when compared to the periphery. Thus, the transient core plexus is enriched for endocrine progenitors.

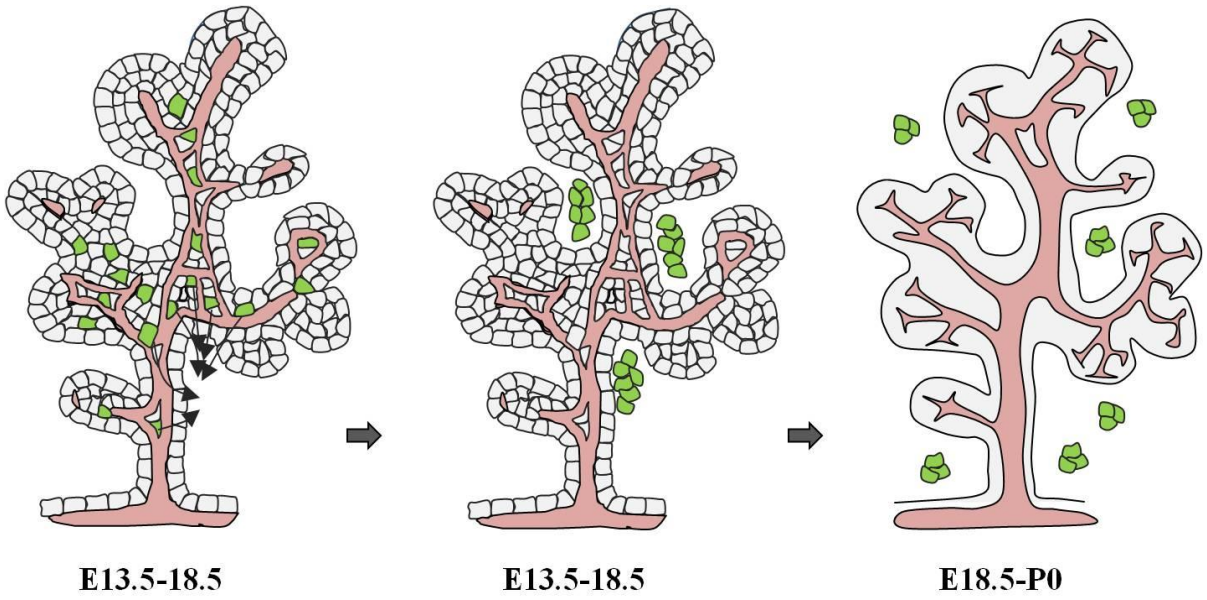

Figure 1.4. Endocrine progenitors delaminate, cluster and form islets of Langerhans. Individual endocrine progenitors leave the ductal epithelium, once they commit to their lineage (left panel). This process is termed ‘delamination’. They then cluster together to form long stretches of endocrine masses, while remaining closely associated with the ductal epithelium (middle panel). Finally, these clusters split and give rise to oval-shaped islets of Langerhans that are now localized away from the ductal epithelium short before birth (right panel).

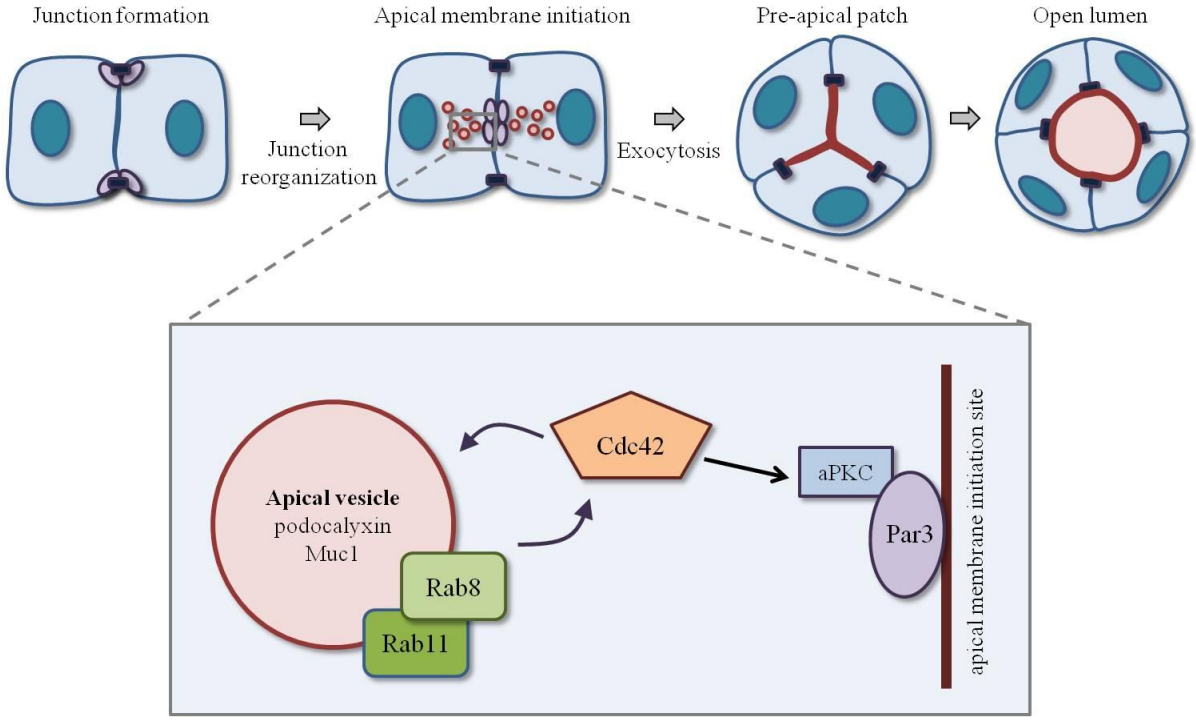

Figure 1.5. Molecular model of *de novo* lumen formation in MDCK system. To form lumens, single MDCK cells aggregate together and form junctions. The Par complex member Par3 (shown in purple) localizes to the junctional foci. As apical membrane formation initiates, Par3 re-localizes to the pre-apical domain between cells. Apically localized Par3 interacts with the other members of the Par complex, aPKC and Par6. This triggers exocytosis of the apical cargo-carrying (Muc1 and podocalyxin-positive) vesicles targeted to the apical membrane. Exocytosis is enabled by vesicular Rab11-Rab8 interaction, which in turn activates the exocytosis master regulator Cdc42. Through these mechanisms, exocytosis of the apical cargo generates the apical membrane and eventually forms a lumen.

CHAPTER TWO

MATERIALS AND METHODS

N.B.: This chapter has been previously published, and is cited as follows: "Azizoglu DB, Braitsch C, Marciano DK, Cleaver O. Afadin and RhoA control pancreatic endocrine mass via lumen morphogenesis. Genes Dev. 2017 Dec 1;31(23-24):2376-2390". The text has been modified accordingly to fit within the dissertation.

Mice and embryo handling

All animal husbandry was performed in accordance with protocols approved by the University of Texas Southwestern Medical Center Institutional Animal Care and Use Committee. E10.5-E18.5 embryos were collected and dissected in PBS buffer. Pancreata were fixed in 4% paraformaldehyde (PFA) in PBS for 3 h at 4°C for section or whole-mount immunostaining. Tissues were washed in PBS, dehydrated, and stored in 70% ethanol at -20°C. Postnatal tissues were collected and fixed in a similar manner.

CD1 mice were used as wild-types. $Afadin^{f/f}$ (Tanaka-Okamoto et al. 2011), $Crb3^{GFP}$ (Pan et al. 2015), $RhoA^{f/f}$ (Barry et al. 2016), $Pdx1^{Cre\text{-}early}$, $Pdx1^{CreERT2}$, $Sox9^{CreERT2}$, and $R26^{tdTomato}$ were used for experiments in this study. Inducible simultaneous deletion of Afadin and RhoA was achieved through mating $Afadin^{f/f}RhoA^{f/f}$ females with $Afadin^{f/+}RhoA^{f/+}Pdx1^{CreERT2}$ males and gavaging of tamoxifen at a dose of 3 mg/40 kg to pregnant mothers at E14.5.

Sectioning

For paraffin sectioning, tissues were rinsed twice in 100% ethanol, twice in xylene for 30 min at room temperature, a mixture of 1:1 paraplast:xylene for 10 min at 60°C, and then a series of 100% paraplast at 60°C (McCormick Scientific). The tissues were then embedded in paraplast and sectioned at 10 μm with a Biocut 2030 microtome. Superfrost Plus glass slides (Fisher) were used. For cryosectioning, tissues were rinsed in PBS and incubated in 30% sucrose overnight at 4°C for cryoprotection. The next day, the tissues were rinsed in OCT twice for 30 min each at room temperature. The tissues were embedded in OCT, snap-frozen on dry ice, and sectioned at 30 μm using a Leica CM-3050S cryostat. Superfrost Plus glass slides (Fisher) were used.

Immunostaining on sections

Paraffin sections were deparaffinized with xylene, rehydrated through ethanol wash series into PBS, permeabilized in PBS + 0.3% Triton X-100 for 10 min, and then treated with R buffer A (nuclear antigens) or R buffer B (cytoplasmic antigens) in a 2100 Retriever (Electron Microscopy Sciences). Slides were incubated in 5% normal donkey serum in PBS for at least 2 h and then in primary antibody overnight at 4°C, washed in PBS, and then incubated in secondary antibody for 2 h at room temperature. Slides were then washed again in PBS and mounted using Prolong Gold (with or without DAPI). For nuclear staining, slides were also incubated in DAPI in PBS for 10 min at room temperature prior to mounting. For cryosections, slides were baked for 10 min at 55°C, rinsed in PBS, and treated for antigen retrieval as above. The following steps were identical to paraffin section staining except that

CAS Block (Invitrogen) was used for blocking and antibody steps. For thick cryosections (30 μm), all washes were performed in 0.1% TritonX in PBS. Slides were permeabilized in 0.3% TritonX in PBS for 30 min, blocked in CAS-Block, and incubated in primary antibody overnight at 4°C. The next day, slides were washed, incubated in secondary antibody for 2 h at room temperature, and washed again. Mounting and nuclear staining were performed as above.

To recognize Rab8, Rab8A and Rab8B antibodies were used in combination. Immunostaining for Cdc42 was performed using Tyramide Signal Amplification, where TSA kit 12 (Invitrogen) was used according to the manufacturer's directions.

The antibodies used were as follows: Afadin (1:100), E-cadherin (1:100), Muc1 (1:200), ZO1 (both antibodies at 1:100), DBA (1:300), Par3 (1:100), aPKC (1:100), Podxl (1:100), occludin (1:100), laminin (1:100), Rab11 (1:50), Rab8A (1:50), Rab8B (1:50), Cdc42 (1:50), Sox9 (1:300), insulin (sections: 1:200 [DAKO]; whole-mount: 1:200 [Cell Signaling]), glucagon (1:200), somatostatin (1:200), ghrelin (1:50), pH3 (1:100), Neurog3 (1:100), and amylase (1:300).

Ex vivo pancreas cultures and inhibitors

E11.5–E12.5 embryonic pancreata were dissected and explanted as described before (Petzold and Spagnoli 2012). Fibronectin coated dishes were used. Culture medium consisted of 5% FBS, 1% penicillin/streptomycin, and gentamicin at 5 μg/mL. Blebbistatin, cytochalasin D, and Y-27632 were used at 10 μM, and 0.1% DMSO (carrier for blebbistatin and cytochalasin D) or dH_20 (carrier for Y-27632) in culture medium was used as control. The day of

dissection was taken as day 0. Drug treatments were initiated at day 1 and carried out for 3 h for explants fixed and stained at day 1 or for 5 d by supplying fresh medium every other day. For staining, explants were fixed in 4% PFA in PBS for 15 min at room temperature, washed in PBS, permeabilized in 0.3% Triton X-100 in PBS for 1 h, washed in PBS, and blocked using CAS-Block. Next, samples were incubated in primary antibody overnight at 4°C, washed in PBS the next day, incubated in secondary antibody overnight at 4°C, washed in PBS the next day, and mounted with Prolong Gold with DAPI on regular slides.

Superresolution microscopy

Paraffin sections immunostained as usual were imaged using a Nikon N-SIM superresolution system.

Whole-mount immunostaining

For embryonic tissues, immunostaining was carried out as described before (Marty-Santos and Cleaver 2016). For postnatal pancreata, tissues were washed in PBS following fixation and stored in PBS overnight at 4°C. Next, tissues were dehydrated into 50% methanol, incubated in 50% methanol for 1 h at room temperature, rehydrated back into PBS, and permeabilized in PBS + 1% Triton X-100 for 2 h at room temperature. Tissues were blocked in CAS-Block for at least 2 h and incubated in primary antibody overnight at 4°C. Tissues were then washed in PBS six times for 1 h each, incubated in secondary antibody overnight at 4°C, and washed in PBS five times for 30 min each. Next, tissues were dehydrated to

100% methanol, washed three times, and mounted in BABB (one-third benzyl alcohol and two-thirds benzyl benzoate) on slides using coverslip spacers.

Live imaging of ex vivo cultures

Afadin$^{f/f}$ females were mated with Afadin$^{f/+}$Crumbs3$^{GFP/+}$Pdx1$^{Cre\text{-}early}$ males. For the indicated experiments, Afadin$^{f/f}$ females were mated with Afadin$^{f/+}$Crumbs3$^{GFP/+}$Sox9^{CreERT2} males, and pregnant mothers were gavaged with tamoxifen at a dose of 3 mg/40 kg at E8.5. E11.5 pancreatic explants positive for the reporter transgene Crumbs3^{GFP} were used for visualization of apically directed vesicles, the apical membrane, and lumens (Pan et al. 2015). The explants were cultured on fibronectin-coated 35-mm glass-bottomed dishes (Greiner Bio- One, 627860). After 16-24 h in culture (indicated as day 1 [d1]), explants were time-lapse imaged (with the z-stack covering the entire tissue) for 3 h every 3 min using an Andor spinning disk confocal microscopy. Data are shown as summed projections of the z-stacks obtained using Imaris.

Hematoxylin and eosin (H&E) staining

Paraffin sections were incubated twice in xylene for 6 min, twice in 100 % ethanol for 2 min, and twice in 95% ethanol for 2 min and washed under running distilled water for 2 min and then with hematoxylin for 7 min. Next, slides were washed under running distilled water for 2 min, submerged in acid alcohol for 5 sec, washed under running distilled water for 5 min, and then stained with eosin for 3 min. The slides were then incubated twice in 95% ethanol

for 2 min, twice in 100% ethanol for 2 min, and twice in xylene for 6 min and mounted using Permount.

TEM

TEM was carried out by the University of Texas Southwestern Electron Microscopy Core Facility per their standard protocols.

Pancreatic sphere assay and immunostaining

Sphere assays were carried out by mating $Afadin^{f/f}R26^{tdTomato+/+}$ females with $Afadin^{f/f}Pdx1^{Cre}$ males, where all and only mutants express tdTomato, eliminating the genotyping step. E10.5-E11.5 pancreata were dissociated into single cells and cultured to form spheres in Matrigel as described by Greggio et al. (2013) with the following exceptions (Greggio et al. 2013): Pancreata of the same genotypes were pooled together in each dissection. Dispase treatment and subsequent mesenchyme removal in PBS were each performed in a small drop of liquid in a regular dissection dish. The pancreata were transferred into 100 µL of DMEM+Trypsin+EDTA using forceps, and 500 µL of DMEM+FBS was used to stop trypsinization. Cell clumps were broken by pipetting up and down, and cells were centrifuged at 300g for 5 min. Cells were then resuspended in an appropriate volume of culture medium described in the original protocol. The Matrigel-cell mix was seeded on coverslips in 96-well plates. Spheres were fixed after 5.5 d in culture. Immunostaining was performed as follows: Spheres were rinsed with PBS on ice and fixed in 4%PFA in PBS for 10 min at room temperature. Next, spheres were washed in PBS + 0.1%

NP40 (PBSN) and permeabilized in PBSN for 15 min at roomtemperature. Spheres were blocked in CAS-Block for 30 min, incubated in primary antibody for 1 h, washed in PBSN, incubated in secondary antibody for 1 h, washed in PBSN again, and mounted upside down onto slides using Prolong Gold with DAPI.

Blood glucose measurement in newborns

P0 DKO litters were decapitated to obtain blood. A TRUEbalance glucose meter and test strips were used for plasma glucose level measurements (n = 30 wild-type; n = 6DKO; n = 4 $Afa^{KO}RhoA^{HET}$; three litters). Statistical analysis was performed using nonparametric one-way ANOVA in GraphPad Prism software. $P < 0.05$ was considered statistically significant.

qPCR on E18.5 pancreata

Real-time qPCR was performed as described previously (Marty-Santos and Cleaver 2016). Briefly, 2 μg of total RNA was isolated from individual E18.5 mouse pancreata (dissected on ice) using RNeasy microkit (Qiagen). cDNA was synthesized using Super-Script III (Invitrogen). One microliter of cDNA in Power SYBR Green Master mix (Applied Biosystems) was used for real-time qPCR analysis (CFX96, Bio-Rad) of gene expression. Primers for Cyclophilin, GAPDH, Sox9, and Neurog3 have been described

previously (Das et al. 2013; Caprioli et al. 2015; Marty-Santos and Cleaver 2016). Gene expression levels were determined by PCR reactions (30 sec at 95°C, 30 sec at 62°C, and 30 sec at 72°C for 35 cycles), and fluorescence was measured at 72°C. Gene expression levels were normalized to Cyclophilin or GAPDH, and the ΔΔCt method was used to calculate fold

change. Data were collected from individual embryos (n = 3–10 per genotype), and samples were analyzed in triplicate. Data are presented as mean (SD).

Western blot on E18.5 pancreata

Individual E18.5 pancreata were dissected on ice under a dissection scope and homogenized in PBS with 10 μg/mL aprotinin, 10 μg/mL leupeptin, and 10 μg/mL pepstatin. Triton X-100 was added to each tube to a final concentration of 1%. Samples were frozen to -80°C, thawed, and centrifuged at 10,000g for 5 min. Supernatants containing protein were analyzed for protein quantification using Pierce BCA protein assay (ThermoScientific) on a 96-well plate. Thirty micrograms of total protein from individual pancreatic lysates was run on a Western blot. Neurog3 primary antibody (F25A1B3-c from Developmental Studies Hybridoma Bank) was used at 1:500.

Quantification and statistical analysis

Data are presented as mean (SD). E12.5 lumen discontinuity quantifications were performed on whole-mount immunostained tissues, where pancreata were analyzed for isolated foci of Muc1 covering ≈80% of the tissue (n = 2 per genotype). Statistical analysis for lumen discontinuity assessment was performed using one-way ANOVA in GraphPad Prism software. E14.5 lumen discontinuity quantifications were performed on 30 μm cryosections, where at least 25 tips per pancreas were analyzed for isolated foci of Muc1 (n = 3 per genotype). The E18.5 core area was measured on head regions of pancreata whole-mount stained for DBA. The core region was identified by using the FilamentTracer function in

Imaris, and the area of this region was calculated using ImageJ measurements (n = 4 per genotype). The core area on E12.5 explants cultured for 6 d was identified by using FilamentTracer. The Surface function was used to create a separate channel for the core region with different color assignment, and this channel was overlaid with the nonmasked surface to visualize the core and the periphery in different colors. The E18.5 $Sox9^{+}$ core volume was calculated on head regions of pancreata whole-mount stained for DBA and Sox9. The core region was identified by using the FilamentTracer function in Imaris, and the Surface function was used to create a separate channel for the core region within the Sox9 channel. The core $Sox9^{+}$ volume was calculated using the Surface function within this channel created for the core (n = 2 wild-type; n = 3 DKO). Quantification of endocrine volume at P0 was performed on whole-mount insulin/glucagon immunostained tissues. Head regions of pancreata were analyzed. To account for the size difference between wild-type and DKO pancreata, z-stack images of whole head regions were taken regardless of the area that they occupied (two z-stacks at 10× magnification and 0.5× digital zoom for wild-type and one z-stack at 10× magnification and 0.5× digital zoom for DKO). The Surface function of Imaris was used to calculate the overall volume of insulin/glucagon-positive cells. The summed volume of two z-stacks for wild-type was compared with one z-stack for DKO. The endocrine area in explants was analyzed in whole-mount immunostained tissue using the Surface function in Imaris (n = 11 wild-type; n = 3 DKO). E17.5 endocrine proliferation was assessed on pH3/endocrine marker costained sections, where at least five sections per pancreas were analyzed (n = 3 per genotype). The E18.5 endocrine yield in the core versus the periphery was analyzed on pancreata whole-mount immunostained for Neurog3 and

Sox9, where at least three different areas for each region (the core or periphery) were analyzed per tissue (n = 2 per genotype). $Sox9^+$ cells were counted using the Spots function in Imaris. $Neurog3^+$ cells were counted manually. The endocrine yield was calculated as $Neurog3^+$ cell number divided by $Sox9^+$ cell number multiplied by 100 to represent percentage. The overall endocrine yield at E15.5 or E17.5 was assessed on sections where $Neurog3^+$ and $Sox9^+$ were counted manually. $Neurog3^+$ cell numbers were analyzed by counting $Neurog3^+$ cells on sections and normalizing these numbers to the $DAPI^+$ pancreatic surface area (the obtained numbers were multiplied by 10^6 for convenience). The endocrine volume at E15.5 was assessed using the same method as at E18.5 except the entire pancreas was analyzed. Unless multiple comparisons were made, all statistical analyses were performed using two-tailed unpaired Student's t-test in GraphPad Prism software. Multiple comparison analyses are described in the relevant Materials and Methods sections. $P < 0.05$ was considered statistically significant.

CHAPTER THREE

AFADIN AND RHOA CONTROL PANCREATIC ENDOCRINE MASS VIA LUMEN MORPHOGENESIS

N.B.: This chapter has been previously published, and is cited as follows: "Azizoglu DB, Braitsch C, Marciano DK, Cleaver O. Afadin and RhoA control pancreatic endocrine mass via lumen morphogenesis. Genes Dev. 2017 Dec 1;31(23-24):2376-2390". The text has been modified accordingly to fit within the dissertation.

Introduction

Extensive efforts have been directed toward developing β-cell replacement therapies for diabetic patients. Although β-cell (or endocrine cell) generation has been accomplished by recapitulating *in vivo* developmental steps, these protocols have yet to be optimized and become therapeutically viable (Pagliuca et al. 2014; Massumi et al. 2016). Several studies suggest that a three-dimensional microenvironment enhances endocrine differentiation (Jiang et al. 2007; Kesavan et al. 2009; Kelly et al. 2011; Greggio et al. 2013; Bankaitis et al. 2015). To date, what this environment entails and how it forms remain unknown. Therefore, a deeper understanding of the endocrine differentiation "niche" will likely propel development of novel treatments for diabetes.

Differentiation of pancreatic progenitors into the endocrine lineage has been thoroughly characterized (Pan and Wright 2011). Endodermal progenitors first transition through a

ducto–endocrine bipotential state, identified by expression of the transcription factor Sox9. A fraction of $Sox9^{+}$ progenitors transiently expresses Neurogenin3 (Neurog3), and a subset of these becomes endocrine progenitors (Pan and Wright 2011). These progenitors then delaminate from the epithelium and differentiate into endocrine cells, including glucagon-producing α and insulinproducing β cells (Pan and Wright 2011). These differentiation events coincide with major morphological changes of the developing pancreatic progenitor epithelium, including lumen morphogenesis.

Close spatiotemporal association between pancreatic lumen formation and cell fate determination brings up the question of whether lumen morphogenesis impacts pancreatic fate. Indeed, loss of Cdc42 in the murine pancreas leads to failure to initiate pancreatic lumens and a concomitant increase in acinar cells at the expense of endocrine differentiation (Kesavan et al. 2009). The investigators noted that the resulting abnormal epithelial morphology increased exposure to laminin, which in turn promoted acinar fate. This work suggests that epithelial morphology and lumen formation profoundly influence pancreatic fate determination.

We and others previously characterized pancreatic lumen morphogenesis in the mouse embryo (Hick et al. 2009; Kesavan et al. 2009; Villasenor et al. 2010). This process can be categorized into four steps. First, microlumens initiate between epithelial cells as isolated foci in the embryonic day 10.5 (E10.5) stratified bud. Next, lumens progressively fuse into longer channels throughout the epithelium by E12.5. These channels take on a three-dimensional (3D) net-like morphology, called a plexus, that undergoes remodeling and extension between E13 and E18.5. By birth, the lumenal plexus resolves into a hierarchical

tree. Recent work by Bankaitis et al. (2015) characterized two distinct compartments in the pancreas at E13.5–E18.5 based on their lumenal/tubular morphology. Regions at the center of the pancreas, which contain a lumenal plexus in the process of remodeling, were termed the core, while regions surrounding the core, which display ramifying branches, were termed the periphery. The core plexus progressively resolves into a ramifying tree at perinatal stages (Bankaitis et al. 2015). Furthermore, the investigators identified the core region as the site of endocrine differentiation. Hence, the core is a transiently formed region distinguished by lumen morphology and differs from the periphery in its cellular composition.

Although the core and periphery are morphologically distinct, it is unknown how these two regions form during pancreas development or how their morphogenesis is influenced by initial lumen formation or subsequent remodeling. The functional relevance of morphogenesis of either region in endocrine differentiation also remains to be determined, as a model that alters either the core or the periphery has not yet been reported. Elucidation of these questions requires a better understanding of pancreatic lumen development.

We took a genetic approach to study pancreatic lumen development and its influence on endocrine cell fate. Given the function of the scaffolding molecule Afadin in kidney tubulogenesis, we hypothesized that Afadin may play a similar role during pancreas development (Takai et al. 2008; Yang et al. 2013; Marciano 2017). We further hypothesized that the Afadin mutant model could be used as a tool to manipulate pancreatic lumens to assess impact on cell fate, including endocrine cells. In this study, we found that pancreas-specific ablation of Afadin results in delayed and discontinuous lumen formation, most prominently in the tip epithelium. We show that Afadin regulates *de novo* lumen formation

through Rab-dependent vesicular trafficking, which can be observed in the tip epithelium during midgestation. Interestingly, Afadin mutants form and resolve the central plexus relatively normally. Through time-lapse imaging and ex vivo studies, we show that, following initial lumen formation, lumen morphogenesis differs in the center versus the tips. In contrast to continuing tip *de novo* lumenogenesis, the central plexus takes shape by lumen extension and anastomosis, processes regulated by actomyosin. Codeletion of Afadin and the master actomyosin regulator RhoA leads to an arrest of central lumenogenesis, resulting in a discontinuous plexus that fails to resolve. This resolution failure causes perdurance of the pancreatic core plexus and an increase in endocrine differentiation of bipotential progenitors, leading to a dramatic increase in endocrine mass by birth. With these findings, we demonstrate that Afadin and RhoA functionally interact to direct morphogenesis of the pancreatic core, which determines endocrine mass.

Results

Afadin is required to form a continuous lumenal network in the developing pancreas

Given the requirement of Afadin in renal vesicle lumen formation, we asked whether it plays a similar role in pancreatic lumenogenesis. Afadin is expressed in many mouse tissues and localizes to the apical membrane in epithelial cells of the renal vesicle (Yang et al. 2013). However, its expression has not been reported in the pancreas. We examined Afadin in the embryonic pancreatic bud and found that it localized to cell–cell boundaries, marked by the adherens junction protein E-cadherin, throughout development **(Figure 3.1A-D')**. At E10.5, Afadin localized along the primary central lumen (data not shown) and showed enrichment at

scattered membrane domains within the stratified epithelium prior to formation of lumens **(Figure 3.1A, A')**. Afadin was also observed adjacent to foci expressing the lumenal glycoprotein Mucin1 (Muc1), suggesting that it marked nascent lumens **(Figure 3.1B, B')**.

At E12.5, Afadin became enriched at junctions flanking the apical membrane **(Figure 3.1C, C')** and restricted to subapical junctions at lumenal boundaries at later stages **(Figure 3.1D, D')**. Superresolution microscopy revealed localization of Afadin at sites with progressive enrichment of E-cadherin or the tight junction (TJ) protein ZO-1, pointing to a function in junction formation in the pancreas, as described previously in other systems **(Figure 3.2A-B')** (Takahashi et al. 1998; Ikeda et al. 1999; Zhadanov et al. 1999). Interestingly, a subset of Afadin foci did not colocalize with either junctional protein, suggesting potential junction-independent functions prior to lumen formation **(Figure 3.2A-B', arrows)**. Thus, Afadin localizes to scattered membrane domains and nonjunctional foci prior to lumen formation and becomes restricted to apical junctions after lumen formation in the developing pancreas. Such dynamics of subcellular localization suggested a potential function of Afadin in pancreatic lumen formation.

To test whether Afadin is required for formation of pancreatic lumens, we deleted Afadin using $Pdx1^{Cre}$ (Afa^{pancKO}) in the early embryonic pancreas (Gu et al. 2002). Deletion efficiency was assessed by Afadin immunostaining and was mostly complete by E11.5 **(Figure 3.2C-D')**. In the absence of Afadin, the developing pancreas failed to form continuous lumens, as shown by Muc1 immunostaining, while control tissue exhibited fine continuous lumens **(Figure 3.1E-F')**. Furthermore, Muc1 was frequently observed in intracellular punctae within mutant epithelial cells but not in controls **(Figure 3.1G-H')**.

Whole-mount immunostaining revealed discontinuous Muc1 foci in the E12.5 Afa^{pancKO} pancreas, in contrast to a mostly continuous network or a plexus in controls **(Figure 3.2E, F, arrows)**. Ex vivo, lumen defects of the mutants were evident in E11.5 pancreatic explants following 1 d in culture **(Figure 3.1I-J')**. Unlike lumen formation failure, epithelial branching occurred normally in the Afa^{pancKO} pancreas **(Figure 3.2G, H)**. The schematic in **Figure 3.1K** illustrates lumen discontinuity in the Afa^{pancKO} pancreas at E12.5 as opposed to a continuous plexus in wild-type. Thus, Afadin is required for lumen continuity in the developing pancreas.

Tip, but not central, lumens develop via Afadin dependent mechanisms

To determine whether lumen defects in Afa^{pancKO} persisted, we analyzed later stages of pancreatic development. We examined epithelial branch tips as well as the center of the epithelium. Afa^{pancKO} pancreas failed to form normal lumens by E15.5 in the tip epithelium **(Figure 3.3A, B)**. Most cells exhibited extensive intracellular Muc1 and discontinuous Muc1 foci between cells, whereas control tissue almost always displayed a single continuous lumen per tip **(Figure 3.3A, B)**. Quantification of lumen continuity using E14.5 thick sections revealed that ~80% of control branch tips had a single lumen per tip, while only ~20% of the Afa^{pancKO} tips had one lumen, and the rest had at least two discontinuous Muc1 foci per tip **(Figure 3.4A)**. Consistent with the E15.5 results, the mutant pancreas failed to form normal lumens at epithelial tips and developed abnormally enlarged lumens after birth **(Figure 3.3C, D; Figure 3.4B, C)**.

Defects in the center of the Afa^{pancKO} epithelium evolved differently than in the tips despite Afadin being expressed equally in both regions **(Figure 3.2C)**. Whole-mount immunostaining revealed a continuous but denser plexus in the bud center at E14.5 relative to controls, suggesting remodeling defects **(Figure 3.3E, F)**. By birth, the pancreatic center recovered from these defects in most cases **(Figure 3.3G, H)**. Furthermore, intracellular Muc1 accumulation was never observed in the Afa^{pancKO} epithelial center, unlike in the epithelial tips **(Figure 3.4D-E')**. Therefore, the Afa^{pancKO} pancreas fails to establish continuous lumens in the tip epithelium by perinatal stages, while the central lumens largely recover from discontinuities and remodeling defects by late gestation.

The striking difference between the tip and central lumen phenotypes in Afa^{pancKO} pancreata suggested that center and tip epithelia might undergo different lumen morphogenesis events at a given time. Previous studies have shown that lumen formation in other systems can occur *de novo* through biogenesis of a new apical membrane and/or via extension of existing lumens (Sigurbjornsdottir et al. 2014). The presence of intracellular Muc1 accumulation in the tip, but not the central, epithelial cells in the Afa^{pancKO} pancreas suggested *de novo* lumen formation in epithelial tips at the time of deletion (E11.5 onward) **(Figure 3.3A-D; Figure 3.4D-E')**. We further hypothesized that central lumen morphogenesis might instead rely on lumen extension following initial lumen formation. To test this idea, we performed time-lapse imaging on pancreatic explants using the Crumbs3^{GFP} (Crb3-GFP) reporter line that marks the apical membrane and apically targeted vesicles (Pan et al. 2015).

Time-lapse imaging of E11.5 day 1 Crb3-GFP pancreata revealed striking differences between the central and tip regions. Extensive vesicular trafficking was directed toward the

apical membrane in cap cells of the pancreatic tips and indicated biogenesis of a new apical membrane (Supplemental Movie S1 in original publication). Furthermore, we observed gradual accumulation of Crb3-GFP at discrete foci in the pancreatic tips that eventually became isolated lumens, suggestive of *de novo* lumenogenesis events **(Figure 3.3I-I'', arrows;** Supplemental Movie S2 in original publication**)**. In contrast, the central epithelium exhibited little noticeable vesicular trafficking at the stages examined (Supplemental Movie S1 in original publication). Additionally, existing central lumens underwent dynamic changes, where they extended and made connections with each other **(Figure 3.3J-J'', arrows;** Supplemental Movie S3 in original publication**)**. These observations suggest that once lumens have appeared and coalesced into a plexus, central lumen morphogenesis occurs primarily through lumen extension as opposed to continuing *de novo* lumenogenesis.

These findings are in line with a model in which the developing pancreas undergoes a centripetal wave of lumen formation and remodeling. Following initial lumen formation in the early E10.5 bud, the central epithelium forms new lumens by extending existing lumens, while the tip epithelium continues to form lumens *de novo* as it grows outward. This gives rise to a central plexus and transiently disconnected tip lumens (E12.5). The central plexus then remodels and resolves into branching lumens as tip lumens fuse with extending branches from the center (E13.5-18.5). This way, the central plexus and tip lumens remodel into a ramifying tree (postnatal day 0 [P0]). In the absence of Afadin, tip lumens fail to form in a timely manner and remain discontinuous. However, the central lumens can remodel and resolve relatively normally **(Figure 3.3K; Figure 3.4F)**.

Afadin is required for coordinated apical membrane formation in epithelial tips

Lumen formation requires apico-basal polarization, and integrity of the apical membrane relies on correct positioning of TJs (Sigurbjornsdottir et al. 2014). In the pancreas, as cells undergo apico-basal polarization, they adopt a bottle shape via apical constriction and organize into rosette structures prior to lumen initiation (Villasenor et al. 2010). Given persistent lumen discontinuity in the Afa^{pancKO} tip epithelium, we asked whether apico-basal polarization or apical membrane formation was affected in the absence of Afadin.

To examine apical polarity, we assessed the Par complex proteins Par3 and aPKC in the E12.5 pancreas and found that they localized to the apical membrane at the center of rosettes **(Figure 3.5A, C)**. In contrast, at the onset of the Afadin mutant phenotype (E12.5), the Afa^{pancKO} epithelium exhibited enrichment of these molecules at scattered membrane domains and in cytoplasmic punctae **(Figure 3.5B, D)**. We also evaluated TJ localization in Afa^{pancKO} and observed ZO1 mislocalized at lateral membranes, in contrast to its normal apical enrichment **(Figure 3.5E-F')**. Furthermore, we observed large vesicles carrying the apical glycoprotein Podocalyxin (Podxl) localized in close proximity to ZO1 enrichment sites in Afa^{pancKO} as opposed to its normal lumenal localization **(Figure 3.5F, arrow)**. Interestingly, E-cadherin was cleared from the membrane between ectopic ZO1 enrichment sites and apposed vesicles, suggesting that this apico-lateral domain is aberrantly determined as the apical membrane in the absence of Afadin **(Figure 3.5F', arrow)**.

At later stages, both apical determinants Par3 and aPKC retained their discontinuous membrane/cytoplasmic localization in Afa^{pancKO} tips **(Figure 3.5G-H'; Figure 3.6A-B')**. Likewise, the transmembrane TJ molecule occludin exhibited mislocalization to lateral

membranes, similar to the early ZO1 pattern **(Figure 3.5I-J')**. Apical constriction and rosette structure were also largely absent in Afa^{pancKO} tip cells **(Figure 3.5G-J')**. Importantly, the basal lamina appeared grossly normal in mutants, as depicted by laminin staining **(Figure 3.6C, D)**. These findings suggest that Afa^{pancKO} cells are able to determine basal polarity; however, they fail to properly segregate apical from lateral/junctional membranes.

Transmission electron microscopy (TEM) analysis at E14.5 confirmed that Afa^{pancKO} tip epithelial cells fail to form a single lumen per tip and revealed an absence of electron-dense TJ structures at cell-cell boundaries facing the rosette centers **(Figure 3.5K-L', arrowheads)**. Moreover, similar to immunostainings, abnormal TJ localization could be observed at scattered membrane domains in Afa^{pancKO}, which occasionally flanked small lumen-like slits between cells **(Figure 3.6E, arrowheads)**. The schematic in **Figure 3.5M** illustrates mislocalized apical membranes, loss of rosette structure, and lumen discontinuity in Afa^{pancKO} pancreatic tips compared with controls. Thus, Afa^{pancKO} pancreata fail to align central TJs and coordinate apical membrane formation across cells of the tip epithelium.

Afadin regulates lumen formation through Rab8-mediated apical membrane docking

To investigate how coordination of apical membrane formation fails in the absence of Afadin, we examined apical membrane biogenesis in the Afa^{pancKO} tips. Intracellular glycoprotein accumulation in close proximity to the membrane **(Figure 3.1H, H', 3.5F, F')** suggested that Afa^{pancKO} tip cells may incur failure of apical membrane biogenesis. In fact, we frequently observed abnormally large vesicles upon loss of Afadin, which were positive for Muc1 **(Figure 3.7A-D')** and ZO1 **(Figure 3.7E-H')**. Notably, these vesicles localized to

the membrane domain near the putative center of rosettes, where apical membranes normally form. These observations indicated that apical vesicle docking/tethering at the plasma membrane is likely to be defective in the absence of Afadin.

Apical membrane docking relies on the small GTPases Rab8, Rab11, and Cdc42 in various systems, including in the developing intestine and pancreas (Sato et al. 2007; Kesavan et al. 2009; Bryant et al. 2010; Khandelwal et al. 2013). *In vitro* studies indicate that Rab11 activates Rab8, which in turn induces Cdc42 activity required for apical vesicle trafficking (Bryant et al. 2010). To determine whether Afadin regulates apical docking machinery, we tested subcellular localization of these factors in the control and Afa^{pancKO} developing pancreas. In line with their roles, Rab8, Rab11, and Cdc42 localized to the apical membrane in control tip epithelia at E14.5-E15.5 **(Fig 3.8A-A', C-C', E)**. In contrast, apical membranes in Afa^{pancKO} displayed no enrichment of Rab11 or Cdc42 **(Figure 3.8B-B', F)**. Although Rab8 did mark the plasma membrane in the putative rosette center, it was not present on Muc1-positive vesicles in Afa^{pancKO}, indicating its loss from apically targeted vesicles **(Figure 3.8D, D')**.

As later defects may result secondarily from failure in lumen formation as opposed to directly from Afadin loss, we analyzed localization of the docking machinery at the onset of the Afa^{pancKO} phenotype. Similar to later stages, early lumens were enriched for Rab11, Rab8, and Cdc42 in controls **(Figure 3.7I, I', K, K', M)**. In Afa^{pancKO}, Rab11 grossly localized to the same cellular domain as Muc1 vesicles **(Figure 3.7J, J')**, in contrast to its absence at later stages. This suggested that the later apical absence of Rab11 is likely to be a result of apical membrane defects and not directly caused by Afadin loss. In contrast, Rab8 failed to

apically enrich and Cdc42 did not colocalize with Muc1-positive vesicles in early mutant cells **(Figure 3.7L, L', N)**. Analysis of immunofluorescence intensity revealed no overall decrease in levels of these proteins (data not shown). These findings suggest that Afadin is needed for proper localization of Rab8 and Cdc42 but not their upstream regulator, Rab11.

To dissect the role of Afadin in localizing the apical docking machinery with high spatial detail and temporal control, we made use of an ex vivo cell-based system. Pancreatic sphere assays developed by Greggio et al. (2013) provide a simplified 3D progenitor expansion system that allows the study of lumen formation (Greggio et al. 2013). We validated the suitability of this system by analyzing Afadin expression and lumen formation in wild-type and Afa^{pancKO} pancreas-derived spheres. Afa^{pancKO} spheres that lacked Afadin expression failed to form proper continuous lumens, recapitulating the *in vivo* phenotype **(Figure 3.7O-P')**. At the two-cell sphere stage, a single Muc1-positive lumen formed between cells in wild-type spheres **(Figure 3.7Q)**. We termed this the nascent lumen. Afa^{pancKO} spheres failed to form a proper nascent lumen and localized Muc1-positive vesicles to the cell-cell boundaries, similar to the *in vivo* phenotype **(Figure 3.7R)**. Rab11 showed enrichment at the nascent lumen and Muc1-positive vesicles in wild-type and Afa^{pancKO} spheres, respectively **(Figure 3.7S, T)**. Rab8 localized to cell-cell boundaries flanking the nascent lumen in wild-type spheres; however, it failed to enrich in Afa^{pancKO} spheres **(Figure 3.7U, V)**. Together, these findings suggest that Afadin is necessary for Rab8-mediated vesicular docking during lumen initiation.

To gain insight into vesicle accumulation in Afadin mutants, we performed time-lapse imaging of control and mutant pancreatic explants. We induced deletion of Afadin in the

early pancreatic epithelium using $Sox9^{CreERT2}$ at E8.5 ($Afa^{pancindKO}$) and analyzed Crb3-GFP-positive E11.5 pancreata following 1 d in culture (Kopp et al. 2011). The control epithelium maintained lumens >3 h **(Figure 3.8G-G'';** Supplemental Movie S4 in original publication**)**. In contrast, $Afa^{pancindKO}$ pancreata showed intracellular apical cargo accumulation in the form of large vesicles, which often dissociated into smaller vesicles over time **(Figure 3.8H-H'';** Supplemental Movie S5 in original publication**)**. Taken together, our data suggest that the Afadin mutant tip epithelium fails to carry out exocytosis due to missing components of the vesicle docking machinery during *de novo* lumen formation **(Figure 3.8I)**.

Central lumen morphogenesis depends on cooperative activity of Afadin and RhoA

Although we show that Afadin directs *de novo* lumen formation in the pancreas tips, its loss within central lumens resulted in only mild morphogenesis defects. Furthermore, Afa^{pancKO} central lumens did not exhibit apical vesicle accumulation. Therefore, our findings indicated that once lumens have formed in the central pancreas, they do not rely on further *de novo* lumenogenesis. These lumens continue to develop via extension and interconnection of existing lumens. RhoA-directed actomyosin machinery is critical to the lumen extension process, and we showed recently that endothelial lumen formation relies on actomyosin activity (Lee and Kolodziej 2002; Denker et al. 2015; Barry et al. 2016). We thus hypothesized that lumen morphogenesis within the central epithelium would also require actomyosin contractility.

To test the function of actomyosin in pancreatic lumen formation, we inhibited components of this machinery (actin and myosin II) in pancreatic explant cultures and assessed lumens.

Indeed, lumen connections were not maintained when myosin II activity was inhibited using blebbistatin **(Figure 3.9A-B', arrowsheads;** Supplemental Movies S6, S7 in original publication**)**. Longer exposure to blebbistatin caused lumens to become discontinuous and enlarged **(Figure 3.9C, D)**. Inhibiting actin polymerization resulted in similar but more robust defects, likely due to actomyosin-independent functions of actin **(Figure 3.10A, A')**.

Since the Afa^{pancKO} pancreas largely recovered from central lumen defects by birth and since lumen continuity depended on actomyosin, we asked whether actomyosin-dependent mechanisms could compensate for Afadin loss in central lumen remodeling. To test this, we ablated the actomyosin regulator RhoA simultaneously with Afadin in a pancreas-specific manner ($Afadin^{f/f}$;$RhoA^{f/f}$;$Pdx1^{Cre}$ [DKO]). This double depletion led to death by P9, in contrast to normal survival of Afadin or RhoA single mutants. At birth, DKO pancreata were smaller compared with controls **(Figure 3.10B, C')**. Glucose measurements in newborns revealed that blood glucose levels of DKOs were significantly lower than their control littermates **(Figure 3.10D)**.

We next asked whether DKO mice suffered from worsened pancreatic lumen discontinuity. Indeed, DKO pancreata displayed exacerbated lumen defects compared with Afa^{pancKO}. Starting as early as E12.5, DKOs exhibited severe lumen discontinuity, incomplete epithelial destratification, and defective apical membrane formation **(Figure 3.10E-M')**. Similar to Afa^{pancKO}, DKOs exhibited no initial branching defects (data not shown). Unlike Afa^{pancKO}, DKO pancreata showed persistent central lumen morphogenesis failure. Central lumens of E15.5 DKO pancreata were discontinuous and enlarged, in contrast to the continuous plexus in controls or Afa^{pancKO} **(Figure 3.9E-G)**.

$Afa^{KO}RhoA^{HET}$ pancreata also exhibited a worsened central lumen phenotype compared with Afa^{pancKO}, albeit considerably milder than DKO **(Figure 3.9F)**. Notably, $Afa^{HET}RhoA^{KO}$ pancreata displayed no abnormalities **(Figure 3.10N, O)**. In line with this, no effect on lumen formation or continuity was observed upon depletion of either RhoA (data not shown) or the Rho kinase ROCK **(Figure 3.10P, Q)**, both of which are activators of myosin II. Thus, the actomyosin machinery is required for pancreatic lumen continuity but is likely regulated by additional upstream factors independent of Rho signaling.

At E18.5, a hierarchical ductal tree could be distinguished in controls where Dolichos biflorus agglutinin (DBA) staining labeled large and mid-sized branching ducts **(Figure 3.9H)**. $Afa^{KO}RhoA^{HET}$ pancreata displayed slight discontinuity as well as nonhierarchical arrangement, with all lumens increased in diameter compared with controls **(Figure 3.9H, I)**. E18.5 DKO pancreata had severe discontinuity and failed to form proper ducts **(Figure 3.9J)**. Therefore, Afadin and RhoA act together to ensure central lumen morphogenesis and remodeling in the developing pancreas **(Figure 3.9K)**.

Arrest of lumen morphogenesis results in perdurance of the pancreatic core

Our analysis of lumen development in DKOs revealed a failure of continuous lumen formation throughout the pancreas and, as a result, widespread arrest in central lumen morphogenesis and remodeling. Importantly, recent work by Bankaitis et al. (2015) described two distinct and transiently formed regions in the developing pancreas: the core and the periphery. The periphery consists of terminal branch tips, where lumens have completed remodeling, while the core consists of lumens interconnected as a plexus with ongoing lumen

remodeling. As the plexus remodels into hierarchical ducts and branches (plexus-to-duct remodeling), the core region disappears (Bankaitis et al. 2015). The schematic in **Figure 3.11A** illustrates this transient core-periphery distinction. An example of a core region is shown by DBA staining on the E18.5 wild-type pancreas, where the core can be architecturally distinguished by looping of nonhierarchical lumens (of similar or irregular thickness) **(Figure 3.11B)**. Looping can be identified by tracing lumens: Whenever a lumen being traced connects with an already traced lumen, this architecture is defined as looping. To understand how lumen morphogenesis arrest affected core-periphery regionalization, we examined DKO pancreata stained for Muc1 and DBA. At E18.5, the wild-type pancreatic trunk consisted of one main duct and smaller hierarchically organized branches; however, a narrow region of core lumens around the main duct could be distinguished **(Figure 3.11C)**. In contrast, the DKO pancreatic trunk consisted of nonhierarchical longitudinal tubes connected by horizontal lumens with a few discontinuities **(Figure 3.11D)**. The DKO core region was therefore expanded compared with the wild-type **(Figure 3.11C, D)**. Likewise, the control pancreatic head consisted of a main duct, hierarchically organized branching lumens, and only a few distributed core regions **(Figure 3.11E)**. In contrast, DKO lumens appeared nonhierarchical and mostly discontinuous **(Figure 3.11F)**. Analysis with FilamentTracer (Imaris) enabled tracking and generation of a continuous counterpart of the lumens in the DKO pancreatic head **(Figure 3.11E-F'')**. This analysis showed that most DKO lumens were organized into loops, although they remained discontinuous **(Figure 3.11F', F'')**. Based on the lack of hierarchical/ramifying organization and the presence of loop conformation, we quantified the area of the core region and found that it is dramatically

expanded in the DKO **(Figure 3.11G)**. Ex vivo pancreatic cultures showed a similar expansion of the core region **(Figure 3.11H-I')**. Thus, DKO lumens fail to undergo plexus remodeling and remain as nonhierarchical lumens, leading to prolonged maintenance of the core region.

Developing pancreatic lumens are lined by a $Sox9^+$ bipotential population that gives rise to endocrine and mature ductal cells (Pan and Wright 2011). Given the aberrant maintenance of the core plexus in DKOs due to blocked lumen resolution, we predicted an expansion in the $Sox9^+$ population associated with core lumens. Indeed, using whole-mount Sox9/DBA costaining, we found a dramatic expansion of the $Sox9^+$ population associated with the core plexus **(Figure 3.11J-L)**. Therefore, arrest in lumen morphogenesis leads to ectopic maintenance of the core and expansion of the core-resident bipotential progenitor population.

Core perdurance promotes endocrine commitment and increases endocrine mass

Next, we asked how defects in the DKO pancreas affected differentiation of pancreatic lineages. Strikingly, DKOs displayed a significant increase in endocrine mass by birth. Both whole-mount and section insulin/glucagon stainings revealed dramatic expansion of endocrine cells in the DKO pancreas at P0 **(Figure 3.12A-D)**. Both β and α cells were increased in number, and islet morphology was severely disrupted **(Figure 3.12B, D)**. DKO explants similarly exhibited increased endocrine mass **(Figure 3.12E, F)**. Quantification of endocrine volume *in vivo* and ex vivo revealed a significant increase in DKOs **(Figure 3.12G, H)**. Notably, the relative contribution of each endocrine lineage to the islet mass was

not altered compared with controls **(Figure 3.13A-D)**. Unlike endocrine mass, acinar and ductal differentiation remained unaffected in DKOs **(Figure 3.13E, F)**.

To understand how the DKO pancreas promotes endocrine differentiation, we asked what causes the increase in endocrine cell numbers. We tested whether this increase derives from an increase in the number of $Sox9^+$ bipotential progenitors or $Neurog3^+$ committed endocrine progenitors or the proliferation of differentiated endocrine cells. DKO pancreata showed no significant increase in endocrine cell proliferation as assessed by insulin/glucagon/phosphorylated histone H3 (pH3) immunostaining on sections at E16.5 and E17.5 **(Figure 3.12I-K; data not shown)**. Quantification of whole-mount stains and sections at E16.5, E17.5, and E18.5 also showed no difference in the total (core- and periphery-resident) number of $Sox9^+$ cells in DKO pancreata compared with controls (data not shown). Neurog3 immunostaining showed grossly normal numbers of endocrine progenitors in any given field of view within the core area in DKOs **(Fig 3.12L, M)**. However, the overall core area was expanded in DKOs.

Given that the core has been identified as the birthplace of endocrine cells, we asked whether core perdurance in DKOs can promote endocrine fate. We reasoned that if the increase in endocrine mass is due to the core acting as a supportive microenvironment, we might expect no difference in $Neurog3^+$ cell numbers in a given area but an increase in overall $Neurog3^+$ cell number in DKOs. To quantify gross Neurog3 expression in the pancreas, we assessed mRNA levels by quantititaive PCR (qPCR). Indeed, qPCR analysis revealed significant elevation in Neurog3, and not Sox9, expression in DKO pancreata **(Figure 3.12N; Figure**

3.13G). Neurog3 protein levels were also elevated in the E18.5 DKO pancreas **(Figure 3.12O)**, in line with increased overall endocrine progenitor numbers.

In order to assess the commitment capacity of $Sox9^{+}$ bipotential progenitors toward endocrine lineage in DKOs, we calculated the percentage of $Neurog3^{+}$ cells out of the total $Sox9^{+}$ population (termed endocrine yield). When analyzed separately for the core and periphery, the endocrine yield was not altered in DKOs relative to controls at E18.5 (representative images in **Figure 3.12L, M; Figure 3.13H)**. As reported previously, core bipotential progenitors did show a higher endocrine yield than the periphery-resident population in both controls and DKOs **(Figure 3.13H)** (Bankaitis et al. 2015). The endocrine yield (or volume) was not altered before E18.5 in the DKOs **(Figure 3.13I-L; data not shown)**. Together, these data suggest that the observed endocrine increase **(Figure 3.12A-H)** is not due to the altered differentiation capacity of either the core-resident or the periphery-resident bipotential population but the perdurance of the high-endocrine-yielding core-resident bipotential cells.

To confirm that core perdurance results in an endocrine mass increase, we examined the small percentage of Afa^{pancKO} pancreata with core perdurance (Afa^{pancKO} severe) resembling the DKO phenotype **(Figure 3.13M-O)**. Supporting our hypothesis, only those Afa^{pancKO} with core perdurance, but not those without, displayed an increase in endocrine mass **(Figure 3.13P-R)**. This correlation strongly suggested that core perdurance leads to increased endocrine differentiation. Altogether, these findings indicate that progenitors have a higher potential to give rise to endocrine cells when exposed to the core environment rather than the periphery, thereby attributing niche properties to the core.

To rule out the possibility that Afadin and/or RhoA act cell-intrinsically to direct endocrine differentiation, and independent of core morphogenesis, we carried out inducible deletion of Afadin and RhoA at the onset of endocrine differentiation (E14.5) using $Pdx1^{CreErt2}$ ($AfaRhoA^{indDKO}$). Deletion of Afadin in epithelial cells was evident by the loss of Afadin from Muc1-positive lumens **(Figure 3.13S, T)**. $AfaRhoA^{indDKO}$ pancreata exhibited lumen defects only in the outermost tip epithelium (i.e., the growing tips) **(Figure 3.13U-V')** and displayed normal core lumen morphology **(Figure 3.12P, Q)**. $AfaRhoA^{indDKO}$ pancreata had normal endocrine mass, suggesting that Afadin and RhoA do not function cell-autonomously to regulate endocrine mass **(Figure 3.12R, S; Figure 3.13W–X')**. Therefore, Afadin or RhoA do not regulate endocrine mass through an endocrine progenitor cell-intrinsic mechanism but through core morphogenesis.

Together, these findings uncover the reliance of endocrine cell differentiation on its cellular context. We propose a model for lumen morphogenesis defects caused by the absence of Afadin and RhoA and the resulting phenotypes in cellular differentiation **(Figure 3.12T)**. Only the DKO model exhibits a persistent central lumen morphogenesis failure. The resulting distribution of bipotential progenitors **(Figure 3.12T, red)** and the endocrine progenitor population therein **(Figure 3.12T, green)** is critical to ultimate endocrine mass. Notably, the total number of bipotential progenitors remains the same in all models, as depicted by the equal summed number of $Sox9^{+}$ and $Neurog3^{+}$ cells. However, failure of central lumen morphogenesis in DKO leads to remodeling arrest and prolonged progenitor exposure to the core region relative to controls. This in turn leads to increased endocrine

mass, as the core provides a niche for endocrine differentiation. Altogether, Afadin and RhoA control endocrine mass through remodeling of the core niche.

Discussion

Recent work by Bankaitis et al. (2015) distinguished core and periphery regions in the embryonic pancreas and characterized the core as the birthplace for endocrine progenitors. Here, we identify Afadin and RhoA as key regulators of pancreatic core and peripheral lumen formation and remodeling **(Figure 3.14A)**. By generating novel mouse models of pancreatic lumen remodeling failure, we show that perdurance of the pancreatic core can drive increased endocrine differentiation. Overall, we show that Afadin and RhoA are required for normal remodeling dynamics of the pancreas core, which in turn functions as a niche for endocrine differentiation.

Our studies reveal that Afadin is a critical regulator of lumen morphogenesis during pancreas development. Previously, we showed that Afadin is required for kidney tubulogenesis (Yang et al. 2013). Together, these findings suggest that the role of Afadin in lumen formation is conserved across tissues. Furthermore, the delay in continuous lumen formation that we identified in the center of Afadin mutants closely resembles the lumen formation/fusion delay seen in the renal vesicle. These data indicate that Afadin is required for coordination of lumen initiation and fusion in both tissues. However, most cells can compensate for the loss of Afadin and eventually proceed through developmental events. Our double deletion of Afadin and RhoA shows that this compensation occurs through a RhoA-dependent cellular mechanism.

We also show that early branch formation is not affected by depletion of Afadin or of Afadin and RhoA combined. Our previous work showed that branch formation results from the splitting of branch tips and remodeling of the underlying epithelium (Villasenor et al. 2010). We found that, following the emergence of lumen defects in both Afa^{pancKO} and DKO pancreata, mutant branches progressively and abnormally enlarge. These findings suggest that underlying lumen continuity is required for proper branch formation.

In this study, we also show that formation of continuous pancreatic lumens occurs via apical membrane biogenesis in a manner that is exquisitely coordinated between epithelial cells. Afadin loss causes mislocalized apical domains relative to epithelial rosette structures. Interestingly, single cells are able to generate distinct apical and basal membrane regions but fail to synchronize and align with neighboring cells. Afadin thus promotes coordinated apical membrane formation across multicellular tubules. Such coordination may depend in part on timely lumen initiation. Indeed, Afadin loss leads to a delay in lumen initiation, which may result from subapical vesicle accumulation due to loss of Rab8 and Cdc42 recruitment to the preapical domain **(Figure 3.14B)**. Thus, our data suggest a novel role for Afadin in Rab8-dependent apical vesicular trafficking.

In line with these findings, Rab8 mutant epithelia display intracellular accumulation of apical components, very similar to Afa^{pancKO} (Sato et al. 2007). Further studies are needed to determine how Afadin regulates apical docking. Given that Afadin localizes subapically, binds F-actin, and carries a myosin-like Dilute domain, it may act as an anchor for apically directed vesicles at the subapical actin network (Mandai et al. 2013). Alternatively, it might help regulate exocytic Rab activation or expression levels. Interestingly, ADIP (Afadin DIL

domain-interacting protein), which binds Afadin, has been shown to be essential for Rab8 enrichment during cilia formation and therefore might provide a link between Afadin and Rab8 recruitment (Klinger et al. 2014). We note that Afadin is the epithelial counterpart of Rasip1, which we showed to be an endothelial-specific molecule required for continuous vascular lumen formation (Xu et al. 2011). Our previous findings also suggest that Rasip1 is involved in vesicular trafficking (Barry et al. 2016). Therefore, Afadin and Rasip1 may represent analogous molecules that carry out similar cellular functions to direct coordinated lumenogenesis in the epithelium and endothelium, respectively.

Recent work by Bankaitis et al. (2015) characterized the core and the periphery as distinct regions in the developing pancreas based on lumen architecture. Here, we further demonstrate that prior to core-periphery regionalization, early central and tip lumens start using distinct cellular and molecular mechanisms to develop once initial lumens are formed. We note that *de novo* lumens can also be observed at earlier stages (E10.0-E11.5) in the bud center (data not shown), suggesting a temporal centripetal wave of *de novo* lumen formation as the bud grows. However, at the stages that we focused on (E11.5-E18.5), during which endocrine cell differentiation accelerates, lumens in the central region form mainly through extension and fusion of existing lumens.

The spatiotemporal distinction of *de novo* lumen formation versus extension of lumens throughout pancreas development is also made evident by subapical vesicle trapping exclusively in epithelial tips of the E18.5 Afadin-RhoA-ablated pancreas ($AfaRhoA^{indDKO}$). This suggests that timely and proper *de novo* lumen formation clearly requires Afadin-mediated vesicular trafficking. On the other hand, central lumen extension and remodeling

depend on RhoA-mediated actomyosin contractility. Afadin activity can compensate for this function in the RhoA mutant pancreas. The molecular role of Afadin in this compensation remains to be determined. Afadin has been implicated in the regulation of actomyosin in other systems, indicating that it may regulate central lumen morphogenesis through actomyosin contractility, similar to its ortholog, Rasip1 (Sawyer et al. 2009; Sawyer et al. 2011). In line with this idea, blebbistatin treatment of pancreatic explants disrupts lumen continuity, while depletion of RhoA or ROCK does not, indicating likely contribution of other actomyosin regulators.

Proper lumen morphogenesis has been linked previously to pancreatic differentiation (Kesavan et al. 2009; Bankaitis et al. 2015). However, which aspect of lumenogenesis regulates endocrine differentiation has remained elusive. Importantly, the study of the pancreas-specific Cdc42 mutant model revealed that loss of this molecule leads to a near-complete loss of lumens in the pancreas epithelium, disintegration of the epithelium, and suppression of endocrine fate. This morphogenetic phenotype appears severe enough to abolish core region formation in the Cdc42 mutant altogether. In contrast, the DKO model is able to initiate lumenogenesis with a delay but fails to undergo lumen extension, fusion, and, later, remodeling. Additionally, the core region displays distinct phenotypes in our two models (mild Afa^{pancKO} and DKO), enabling us to ask how core-periphery regionalization impacts cell fate. Our results suggest that peripheral lumen morphogenesis is dispensable for proper cellular differentiation, including acinar or ductal lineage. Given that endocrine cells emerge within the core, it is not unexpected that peripheral morphogenesis has little impact on this lineage. In contrast, arrest in lumen remodeling leads to perdurance of the core region

in severe Afa^{pancKO} and DKO and results in increased endocrine differentiation. Other cell types, such as exocrine acinar and ductal cells, display no gross abnormalities in DKOs. Furthermore, lumen continuity per se is not required for differentiation of pancreatic lineages, as lumens display discontinuity in Afa^{pancKO} and DKO, but cell differentiation is not hampered in these models.

It remains to be determined how exactly the core supports endocrine differentiation: What cellular neighbors are required within the niche? What signals do they transmit? Importantly, continuous plexus conformation is not a required property of the core to act as a niche, suggesting that the core is unlikely to act through a lumen-derived signal. Our data indicate that total bipotential progenitor number or endocrine cell proliferation was not altered upon core perdurance in DKOs, while Neurog3 levels were elevated. We propose that this is due to prolonged exposure of progenitors to the core niche, likely inducing/stabilizing Neurog3 expression in bipotential progenitors. **Figure 3.14C** illustrates the distinction between cellular organizations in a core versus a periphery epithelial unit. Closed conformation of lumens in the core may provide concentrated signaling that promotes endocrine fate. In DKOs, lumens are discontinuous, leading to a block in core plexus remodeling; however, overall cellular organization in the core unit is maintained.

Altogether, our study uncovers the pancreatic core as a functional niche for endocrine progenitors and advances our understanding of endocrine differentiation during pancreas development. Importantly, we uncouple lumen formation from lumen extension and plexus remodeling and show that endocrine progenitors are influenced by cellular context created by the latter processes. Elucidating properties of the pancreatic core will provide a better

understanding of *in vivo* β-cell differentiation, which will improve *in vitro* β-cell differentiation attempts to treat diabetes patients.

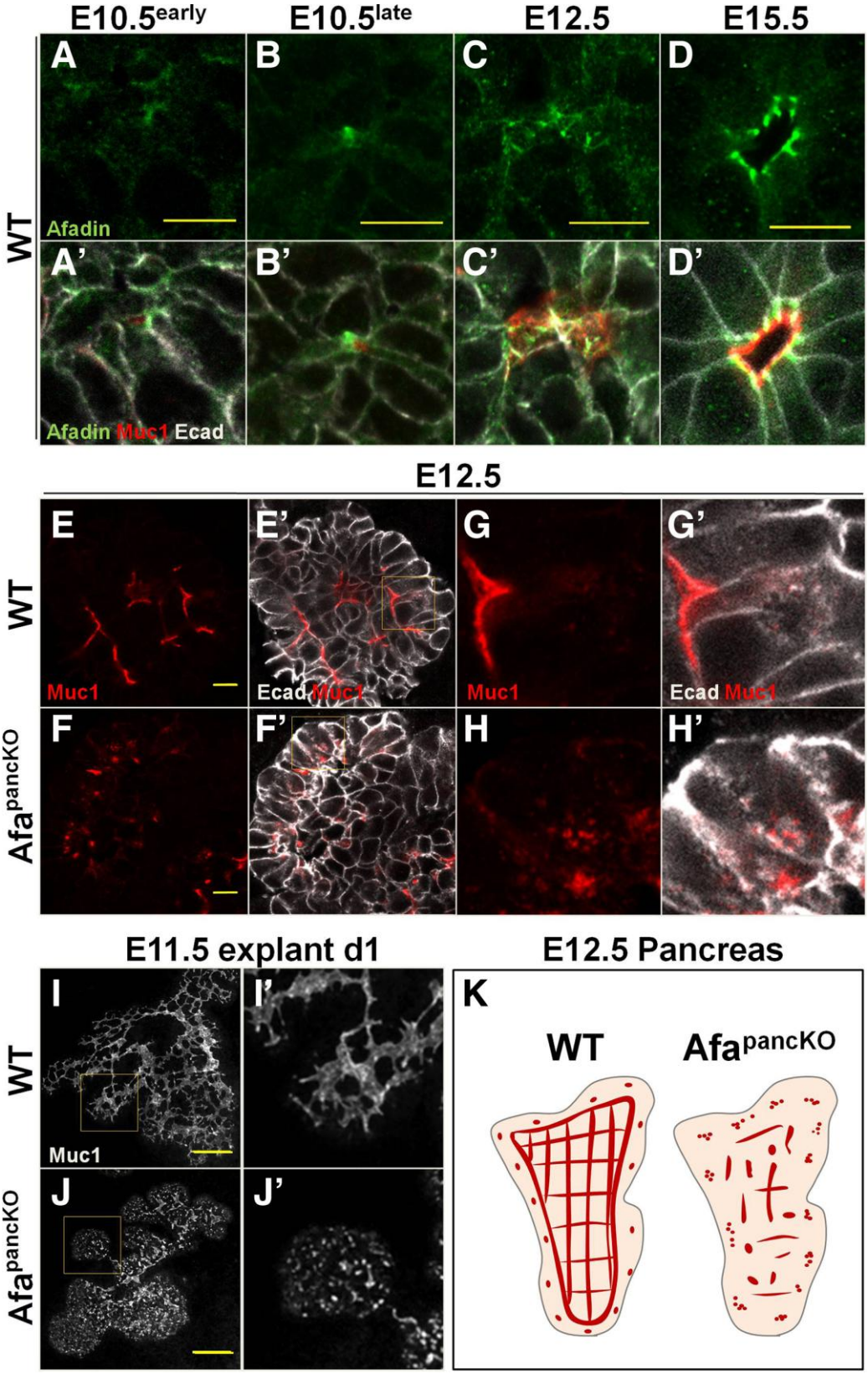
E10.5early
E10.5late
E12.5
E15.5
WT
A
B
C
D
Afadin
A'
B'
C'
D'
Afadin Muc1 Ecad
E12.5
WT
E
E'
G
G'
Muc1
Ecad Muc1
Muc1
Ecad Muc1
Afa pancKO
F
F'
H
H'
E11.5 explant d1
E12.5 Pancreas
WT
I
I'
Muc1
Afa pancKO
J
J'
K
WT
Afa pancKO

Figure 3.1. Early Afadin mutant pancreas fails to form a continuous lumenal network. **(A-D')** Paraffin sections from wild type (WT) embryonic pancreata at indicated stages were immunostained for Afadin, Muc1 (lumens) and E-cadherin (Ecad, epithelial membranes). "Early" and "late" refer to the timing with respect to microlumen formation based on Muc1 enrichment. Scale bars 10μm. **(E-H')** Paraffin sections from E12.5 WT and $Afadin^{f/f}Pdx1^{Cre}$ (Afa^{pancKO}) embryonic pancreata were immunostained for Muc1 and Ecad. Representative images from 5 independent experiments (n=5 embryos per genotype). Insets in **E'** and **F'** are shown at higher magnification in **G-H'**. Scale bars 10μm. **(I-J')** E11.5 WT and Afa^{pancKO} pancreatic explants were cultured for 1 day (d1) and whole mount immunostained for Muc1. Representative images from 6 independent experiments (n=7 embryos per genotype). Insets in **I** and **J** are shown at higher magnification in **I'** and **J'**, respectively. Scale bars 100μm. **(K)** Schematic illustrates lumen discontinuity in the Afa^{pancKO} pancreas compared to the continuous lumen network, or plexus, in WT at E12.5. Red lines represent continuous or semi-continuous lumens, while red dots indicate discontinuous lumen foci. Grey outlined pink region represents the pancreatic epithelium.

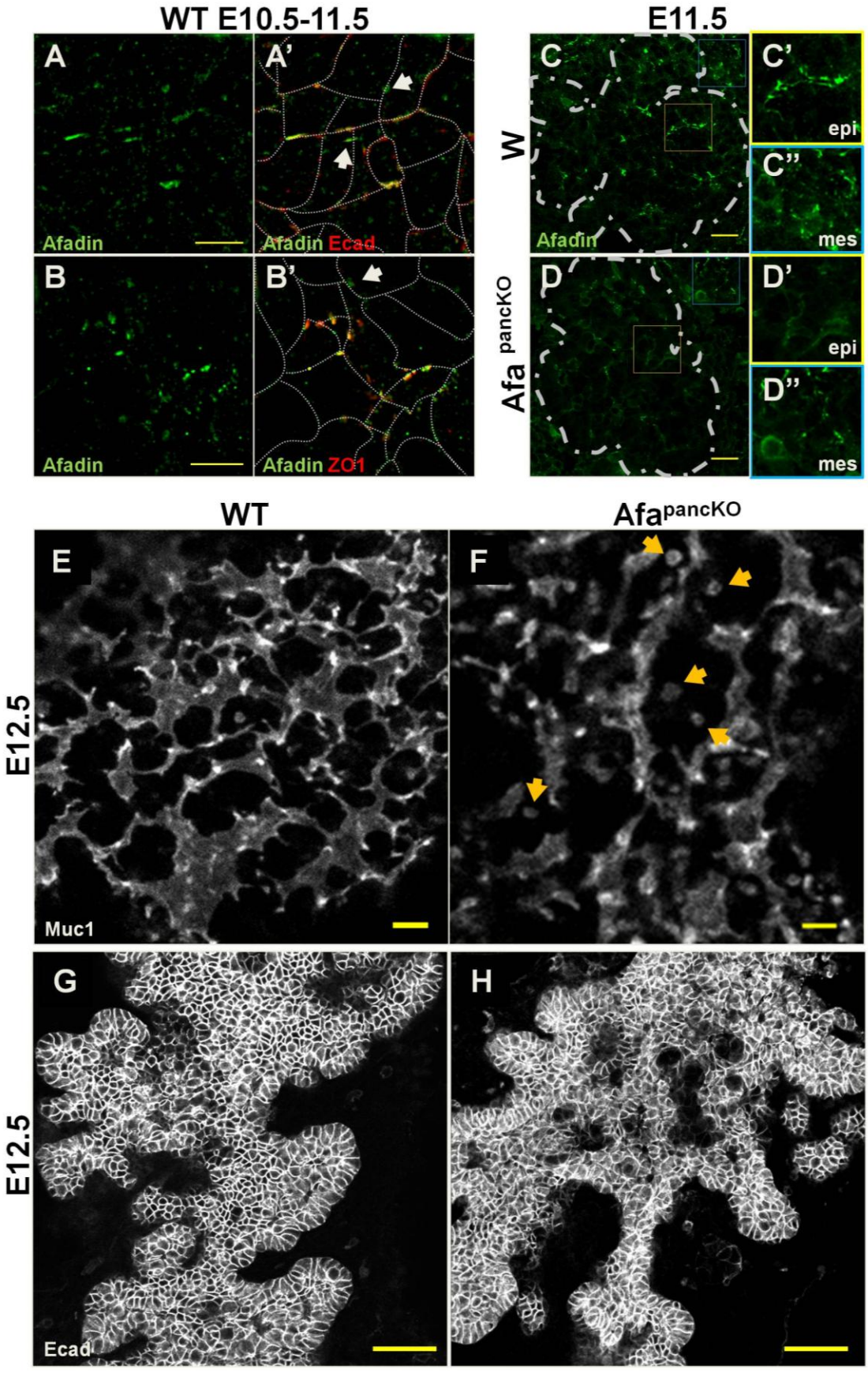
WT E10.5-11.5
E11.5
A
A'
Afadin
Afadin Ecad
B
B'
Afadin
Afadin ZO1
C
C'
epi
C''
mes
W
Afadin
D
D'
epi
D''
mes
Afa pancKO
WT
Afa pancKO
E
F
Muc1
E12.5
G
H
Ecad
E12.5

Figure 3.2. Afadin loss by E12.5 leads to pancreatic lumen discontinuity. (A-B') Paraffin sections of E10.5 (in **A-A'**) and E11.5 (in **B-B'**) WT pancreata were immunostained for Afadin, Ecad (AJs) and ZO1 (TJs), and imaged using a structured illumination microscopy-based super-resolution system. Arrows indicate foci of Afadin enrichment not colocalizing with Ecad (in **A'**) or ZO1 (in **B'**). Dotted lines outline cell membranes. Representative images from 3 independent experiments on n=3 embryos. Scale bars 5 μm. **(C-D'')** Paraffin sections of WT and Afa^{pancKO} pancreata at indicated stages were immunostained for Afadin. Dotted lines outline the pancreatic epithelium. Insets in **C** and **D** are shown at high magnification in **C'-C''** and **D'-D''**. Epi, epithelium; mes, mesenchyme. Representative images from 3 independent experiments on n=3 embryos per genotype. Scale bars 20 μm. **(E-F)** E12.5 WT and Afa^{pancKO} pancreata were whole mount immunostained for Muc1 to mark lumens. Summed slices of same thickness are shown for each whole mount. Arrows indicate isolated Muc1 foci. Representative images from 3 independent experiments on n=3 embryos per genotype. Scale bars 50 μm. **(G-H)** E12.5 WT and Afa^{pancKO} pancreata were whole mount immunostained for E-cad to mark the epithelium. Visual sections through the whole mount are shown. Scale bars 50 μm.

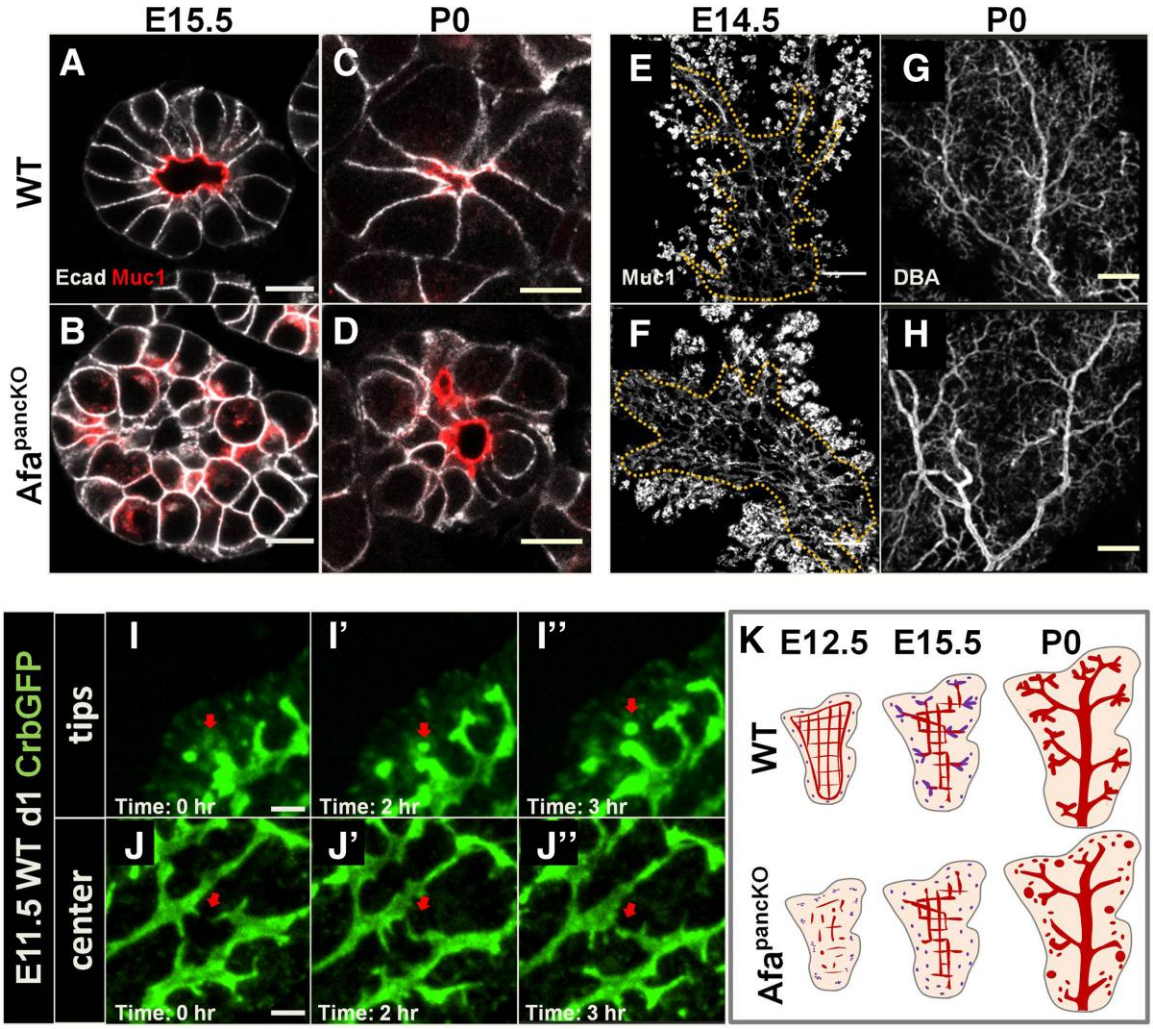

Figure 3.3. Afadin regulates *de novo* lumenogenesis in the tips, but is dispensable for remodeling in the center. (A-D) Paraffin sections of WT and Afa^{pancKO} pancreata at indicated stages were immunostained for Muc1 (lumens) and Ecad (epithelial membranes). Representative images from 5 independent experiments (n=5 embryos per genotype) in **A-B**, and 3 independent experiments (n=3 embryos per genotype) in **C-D**. Scale bars 10μm. **(E-H)** E14.5 and postnatal day (P) 0 WT and Afa^{pancKO} pancreata were whole mount immunostained for Muc1 to mark lumens, and *Dolichos biflorus* agglutinin (DBA) to mark large and mid-

sized branching ducts. Summed slices of same thickness are shown for each whole mount. Dotted line shows the central region in **E-F**. Head regions shown in **G-H**. Representative images from 3 independent experiments (n=3 embryos per genotype). Scale bars 100μm in **E-F** and 200μm in **G-H**. **(I-J'')** Snapshots from time-lapse imaging of E11.5 WT pancreatic explants on day 1 (d1) in culture. The pancreata express $Crumsb3^{GFP}$ (Crb3-GFP) that localizes to lumens and apical vesicles. Red arrow indicates a *de novo* lumen formation event in **I-I''** and a lumen fusion event in **J-J''**. Representative images from 8 independent experiments (n=8 embryos). Scale bars 10μm. **(K)** Schematic illustrates lumen morphogenesis events throughout development in WT and defects in Afa^{pancKO}. At E12.5, central lumens (red) in WT pancreas are in plexus conformation, while *de novo* lumens (purple) are forming in the tip epithelium. At midgestation, central lumens remodel into branches, while tip lumens fuse with these branches (purple branches). *De novo* lumens continue to form in tip epithelium (purple dots). By birth, a hierarchical tree is formed. Afa^{pancKO} pancreas fails to form continuous lumens at E12.5 in both central and tip epithelia. By midgestation, the mutant central lumens remodel, while *de novo* lumens continue to form but remain discontinuous. This gives rise to an Afa^{pancKO} prenatal pancreas with a relatively normal central lumenal tree, but discontinuous and enlarged tip lumens.

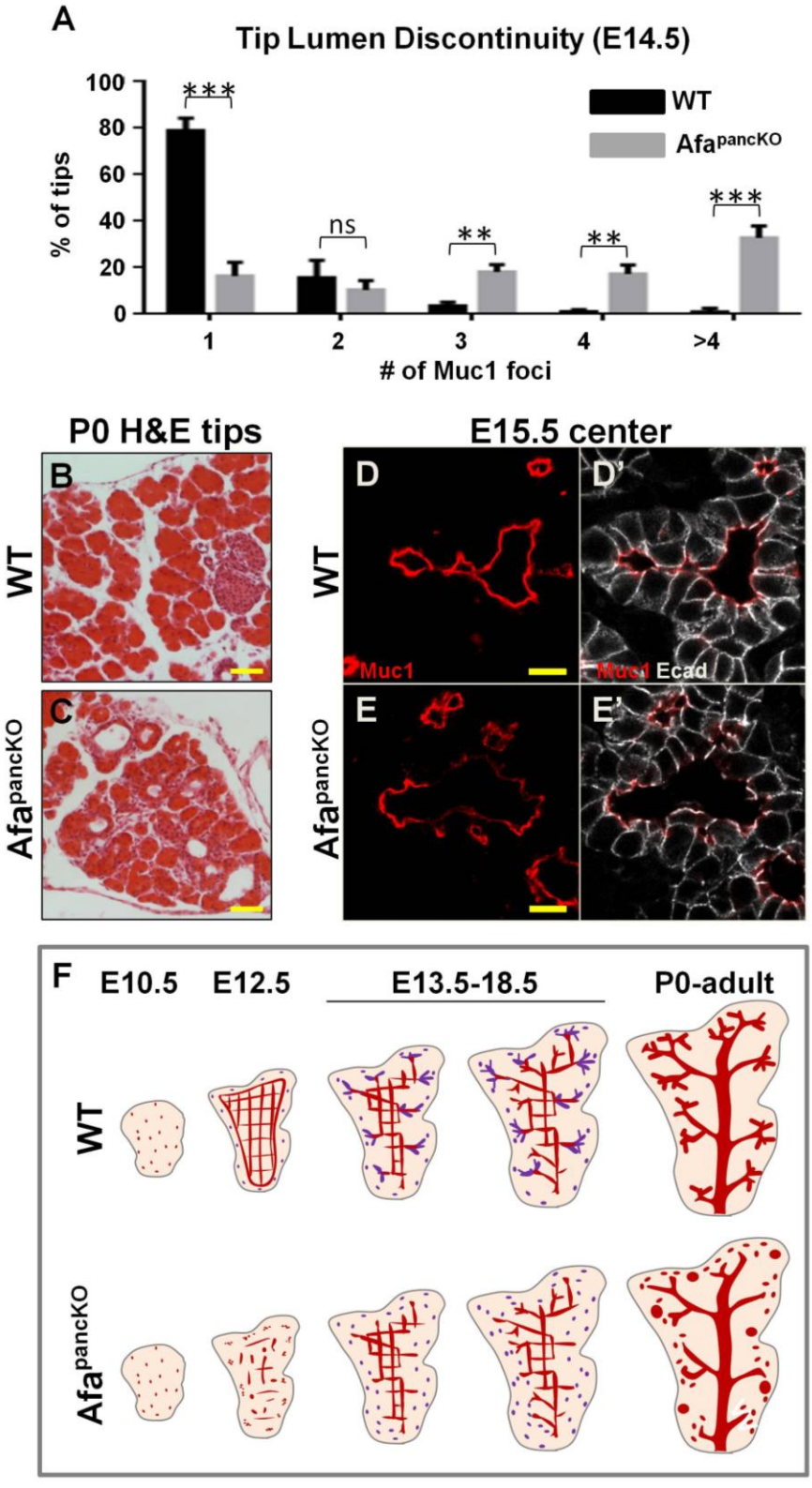
A
Tip Lumen Discontinuity (E14.5)
% of tips
100
80
60
40
20
0
***
ns
**
**
***
WT
Afa pancKO
1
2
3
4
>4
# of Muc1 foci
P0 H&E tips
E15.5 center
B
C
D
D'
E
E'
WT
Afa pancKO
Muc1
Muc1 Ecad
F
E10.5
E12.5
E13.5-18.5
P0-adult
WT
Afa pancKO

Figure 3.4. Afadin loss affects central and tip lumens differentially. (A) E14.5 30 μm sections immunostained for Muc1 and Ecad were analyzed for discontinuous foci of Muc1 in epithelial tips on n=3 embryos per genotype. Data are represented as mean (S.D.). ns, nonsignificant. **(B-C)** Paraffin sections of P0 WT and Afa^{pancKO} were stained with hematoxylin and eosin (H&E). Representative images from 3 independent experiments on n=3 embryos per genotype. Scale bars 100 μm. **(D-E')** Paraffin sections of E15.5 WT and Afa^{pancKO} pancreata were immunostained with Muc1 (lumens) and Ecad (epithelial membranes). Central epithelium is shown with normal lumens. Representative images from 5 independent experiments on n=5 embryos per genotype. Scale bars 10 μm. **(F)** The schematic illustrates the lumen morphogenesis events throughout development in WT and defects in this process in Afa^{pancKO}. At E10.5, microlumens are forming in both WT and Afa^{pancKO}. By E12.5, central lumens (red) in WT pancreas form a continuous plexus, as *de novo* lumens (purple) form in the tip epithelium. Then, central plexus undergoes remodeling into branches, and tip lumens fuse with these branches (purple branches). Meanwhile, lumens continue to form in the tip epithelium *de novo* (purple dots). This gives rise to a hierarchical tree by birth. Afa^{pancKO} pancreas fails to form continuous lumens at E12.5. The Afa^{pancKO} central lumens remodel relatively normally, and lumens continue to form *de novo* in the tip epithelium but remain discontinuous. As a result, perinatal Afa^{pancKO} pancreas has a relatively normal central lumenal tree, but discontinuous and cystic lumens at the tips.

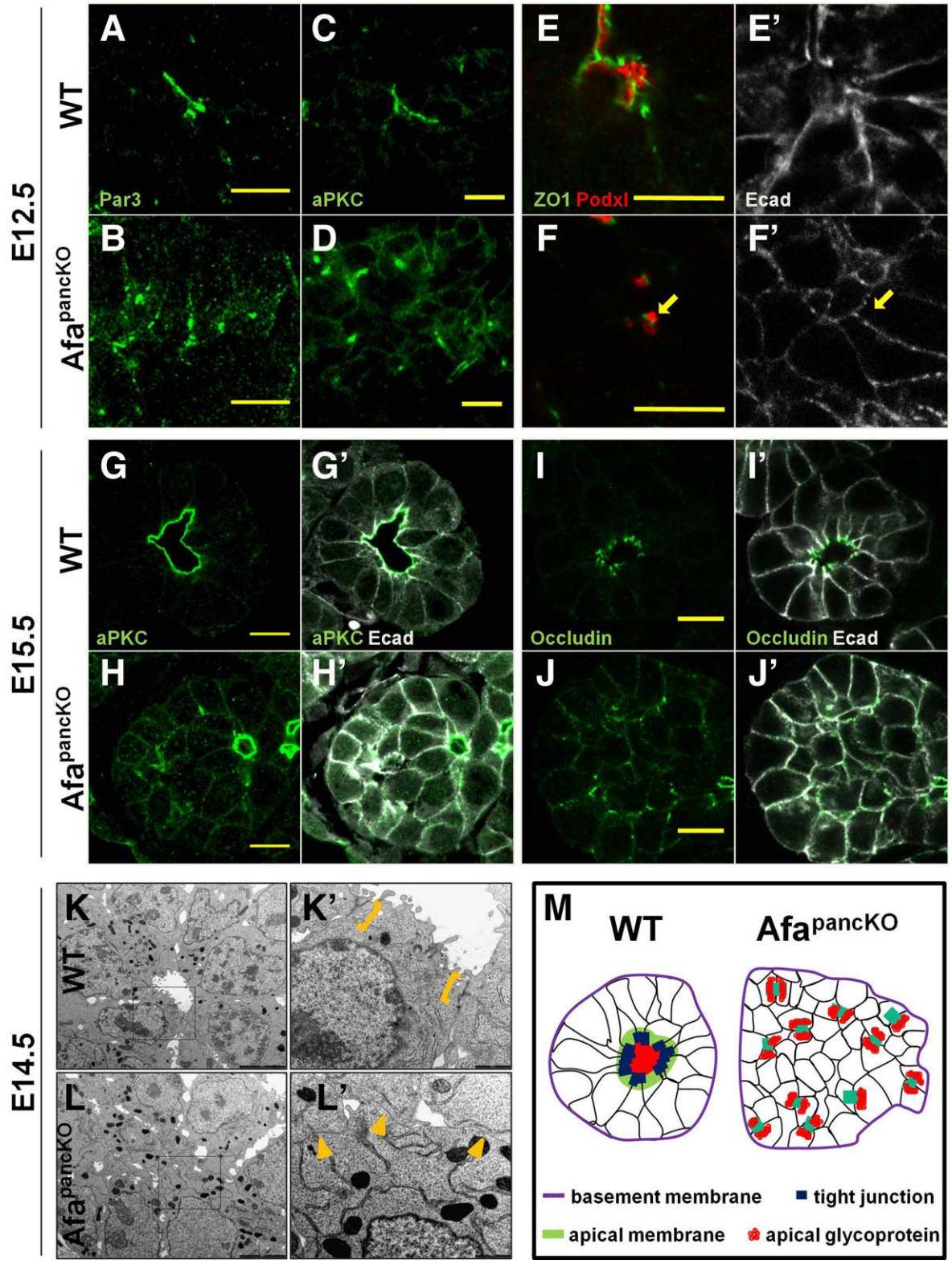
E12.5
WT
Afa pancKO
A
B
C
D
E
E'
F
F'
Par3
aPKC
ZO1 Podxl
Ecad
E15.5
G
G'
H
H'
I
I'
J
J'
aPKC
aPKC Ecad
Occludin
Occludin Ecad
E14.5
K
K'
L
L'
M
WT
Afa pancKO
basement membrane
tight junction
apical membrane
apical glycoprotein

Figure 3.5. Apical membrane formation is not coordinated in Afadin mutant tip epithelium. (A-J') Paraffin sections of WT and Afa^{pancKO} embryonic pancreata at indicated stages were immunostained for apical determinants Par3 and aPKC, TJ proteins ZO1 and occludin, and apical glycoprotein podocalyxin (Podxl). Arrow in **F'** indicates membrane region cleared from E-cadherin. Representative images from 3 independent experiments (n=3 embryos per genotype) in **A-H'** and 6 independent experiments (n=6 embryos per genotype) in **I-J'**. Scale bars 10μm. **(K-L')** Transmission electron microscopy images on sections of E14.5 WT and Afa^{pancKO} pancreata. Insets in **K** and **L** are shown at high magnification in **K'** and **L'**. Brackets indicate electron dense TJ structures at the subapical membrane. Arrowheads designate regions of cell-cell contact in the rosette center lacking TJ structures. Representative images from 2 independent experiments (n=2 embryos per genotype). Scale bars 5μm in **K, L** and 1μm in **K', L'**. **(M)** Schematic of WT and Afa^{pancKO} tip epithelia: basement membrane, purple; epithelial membranes, black; lumenal glycoproteins, red; apical determinant enrichment, green (WT only); TJ enrichment, dark blue (WT only); colocalization of TJ proteins and apical determinants, light blue (Afa^{pancKO} only).

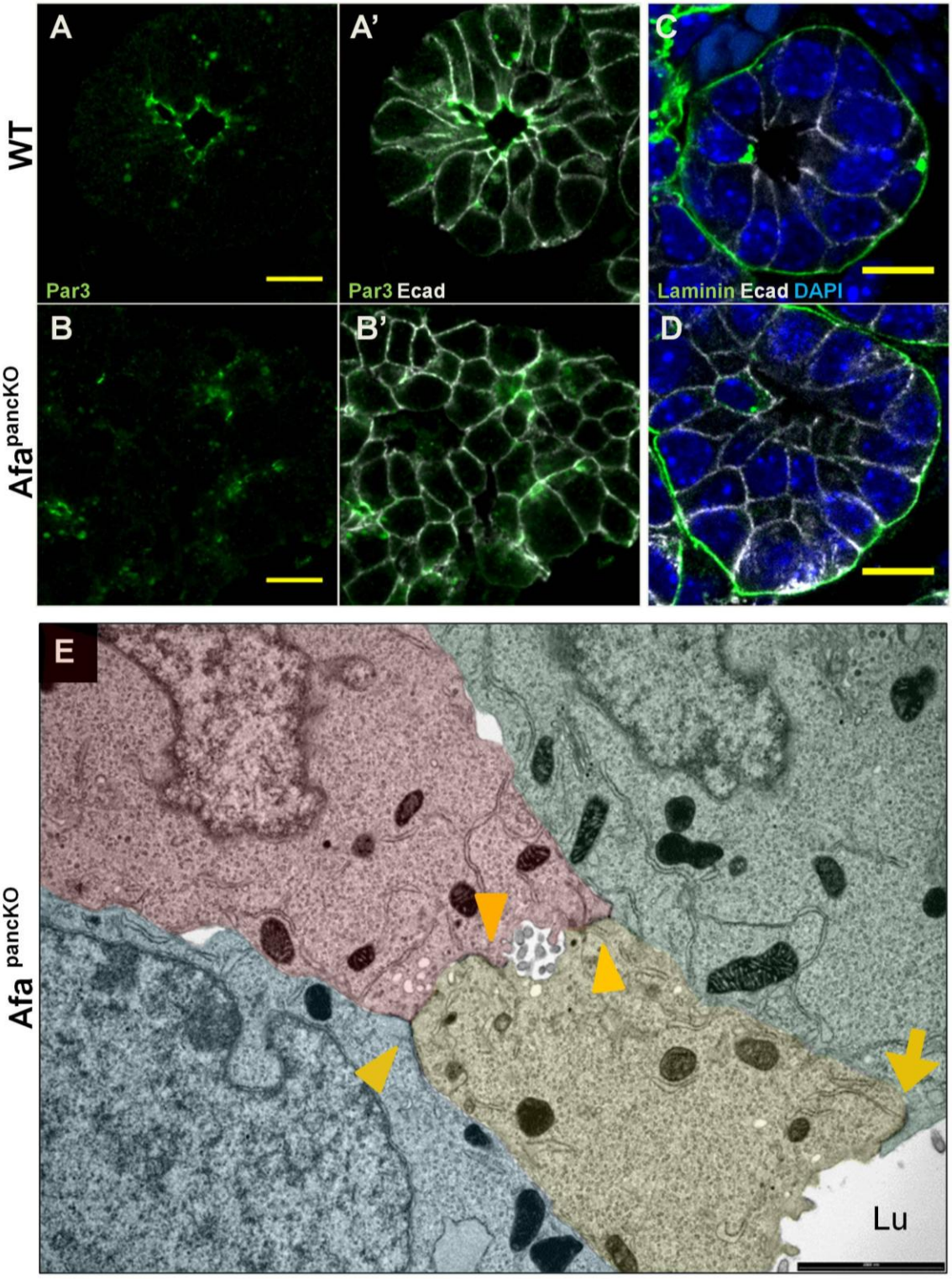
WT
Afa pancKO
A
A'
C
Par3
Par3 Ecad
Laminin Ecad DAPI
B
B'
D
E
Lu

Figure 3.6. Afadin loss causes apical junction mislocalization while basal membrane remains unaffected. (A-D) Paraffin sections of WT and Afa^{pancKO} embryonic pancreata at indicated stages were immunostained for apical determinant Par3 in **A-B'** and basement membrane marker laminin in **C-D** along with Ecad. DAPI in **C-D** marks the nuclei. Representative images from 3 independent experiments on n=3 embryos per genotype. Scale bars 10 μm. **(E)** Transmission electron microscopy image of Afa^{pancKO} showing mislocalization of TJs. Each cell is pseudo-colored. Arrow indicates a normally localized electron dense TJ at the subapical membrane. Arrowheads indicate such structures abnormally found at non-central membrane, towards the basal side of a cell facing a lumen (Lu). Also, note the presence of an abnormal slit in between two cells flanked by TJs. Scale bar 2 μm.

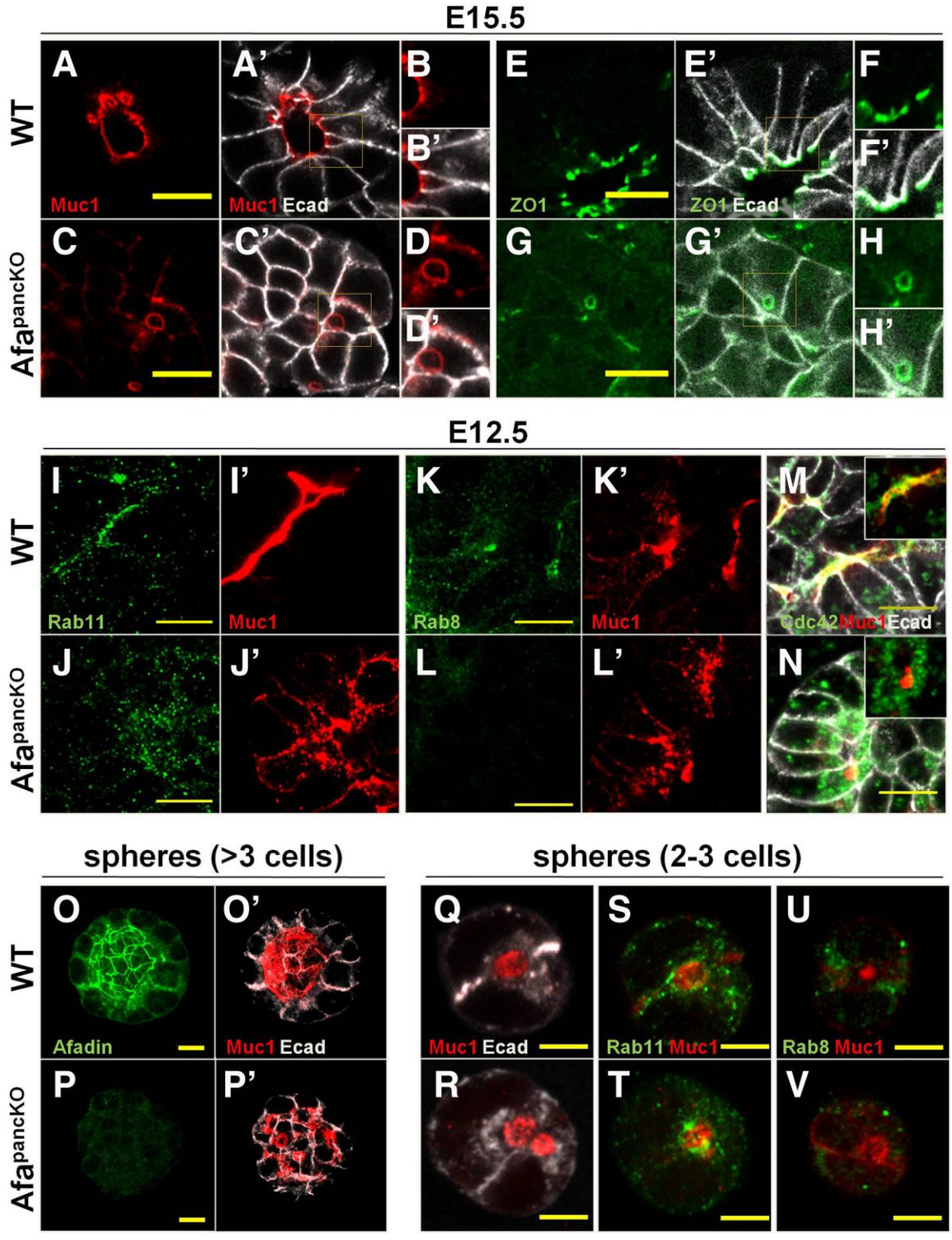
E15.5
WT
Afa pancKO
A
A'
B
B'
E
E'
F
F'
C
C'
D
D'
G
G'
H
H'
Muc1
Muc1 Ecad
ZO1
ZO1 Ecad
E12.5
I
I'
K
K'
M
J
J'
L
L'
N
Rab11
Muc1
Rab8
Cdc42 Muc1 Ecad
spheres (>3 cells)
spheres (2-3 cells)
O
O'
Q
S
U
P
P'
R
T
V
Afadin
Muc1 Ecad
Rab11 Muc1
Rab8 Muc1

Figure 3.7. Afadin regulates Rab8-mediated apical docking during *de novo* lumen formation. (A-N) Paraffin sections of E15.5 and E12.5 WT and Afa^{pancKO} pancreata immunostained for lumenal Muc1, TJ protein ZO1, vesicular GTPases Rab11 and Rab8, and Cdc42, and Ecad (epithelial membranes). **B-B', D-D'**, **F-F'** and **H-H'** show high magnification images of insets in **A-A', C-C'**, **E-E'**, and **G-G'**, respectively. Insets in **M** and **N** show Cdc42 and Muc1 staining, excluding Ecad. Representative images from 5 independent experiments (n=5 embryos per genotype) in **A-D'**, 4 independent experiments (n=4 embryos per genotype) in **E-H'** and 3 independent experiments (n=3 embryos per genotype) in **I-N**. Scale bars 10μm. **(O-V)** Pancreatic sphere assays seeded with cells from E10.5-E11.5 WT and Afa^{pancKO}. Post 5 days (**O-P'**) or 1 day (**Q-V)** in culture, spheres were immunostained. Representative images from 4 independent experiments (n=4 embryos per genotype). Scale bars 10μm in **O-P'** and 5μm in **Q-V**.

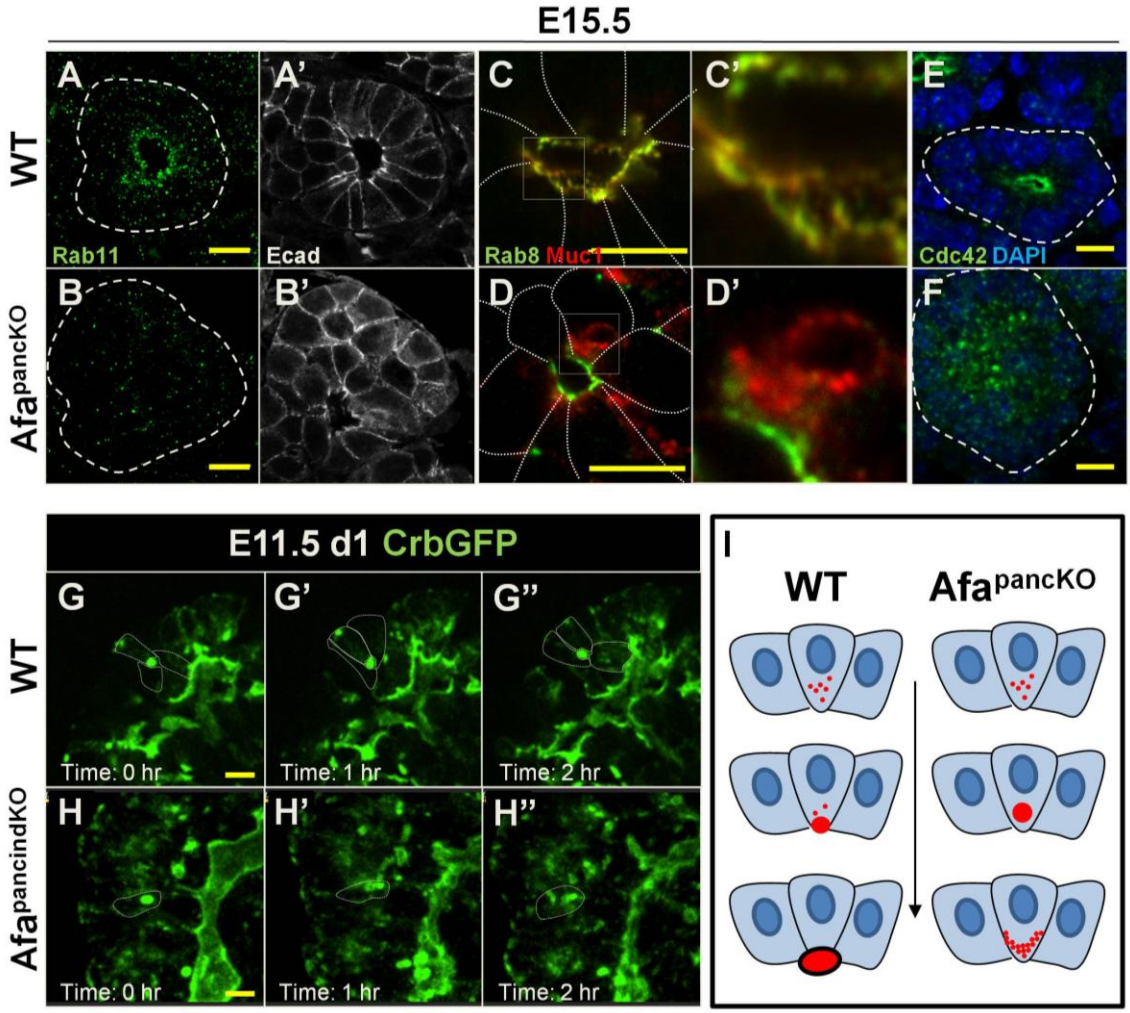

Figure 3.8. Apical vesicles fail to exocytose in the absence of Afadin. (A-F) Paraffin sections of E15.5 WT and Afa^{pancKO} pancreata were immunostained for vesicular small GTPases Rab11 and Rab8, and exocytosis master regulator Cdc42. Muc1 and Ecad mark lumens and epithelial membranes, respectively. Dotted lines in **A, B, E** and **F** outline tip epithelia. Insets in **C** and **D** are shown at high magnification in **C'** and **D'**. Dotted lines in **C** and **D** outline cell membranes (recognized by trafficking of Crb3-GFP along the cell membranes combined with inducible cytoplasmic TdTomato expression not shown here).

Representative images from 3 independent experiments on n=3 embryos per genotype. Scale bars 10 μm. **(G-H'')** Snapshots from time-lapse imaging of E11.5 WT and Afa^{pancKO} pancreatic explants on day 1 (d1) in culture. The pancreata express $Crumsb3^{GFP}$ (Crb3-GFP) that localizes to lumens, apical membrane and vesicles. Dotted lines outline WT cells facing a lumen in **G-G''** or an Afa^{pancKO} cell with intracellular Crumbs3 accumulation in **H-H''**. Note dissociation of intracellular Crumbs3 foci over time in the mutant. Dotted lines outline relevant cellular membranes. Representative images from 4 independent experiments on n=4 embryos per genotype. Scale bars 5μm. **(I)** Schematic summarizing apical membrane biogenesis failure in Afa^{pancKO} during lumen formation. On the left, three WT neighboring cells (light blue, membranes in black) initiate lumen formation, as the middle cell undergoes apical membrane biogenesis. Vesicles (red) carrying apical components are directed towards the pre-apical membrane and are exocytosed to form a lumen. On the right, the middle Afa^{pancKO} cell fails to undergo proper apical membrane biogenesis, and accumulates the apically-directed vesicles by the membrane. These vesicles do not get exocytosed, and often dissociate into smaller vesicles instead.

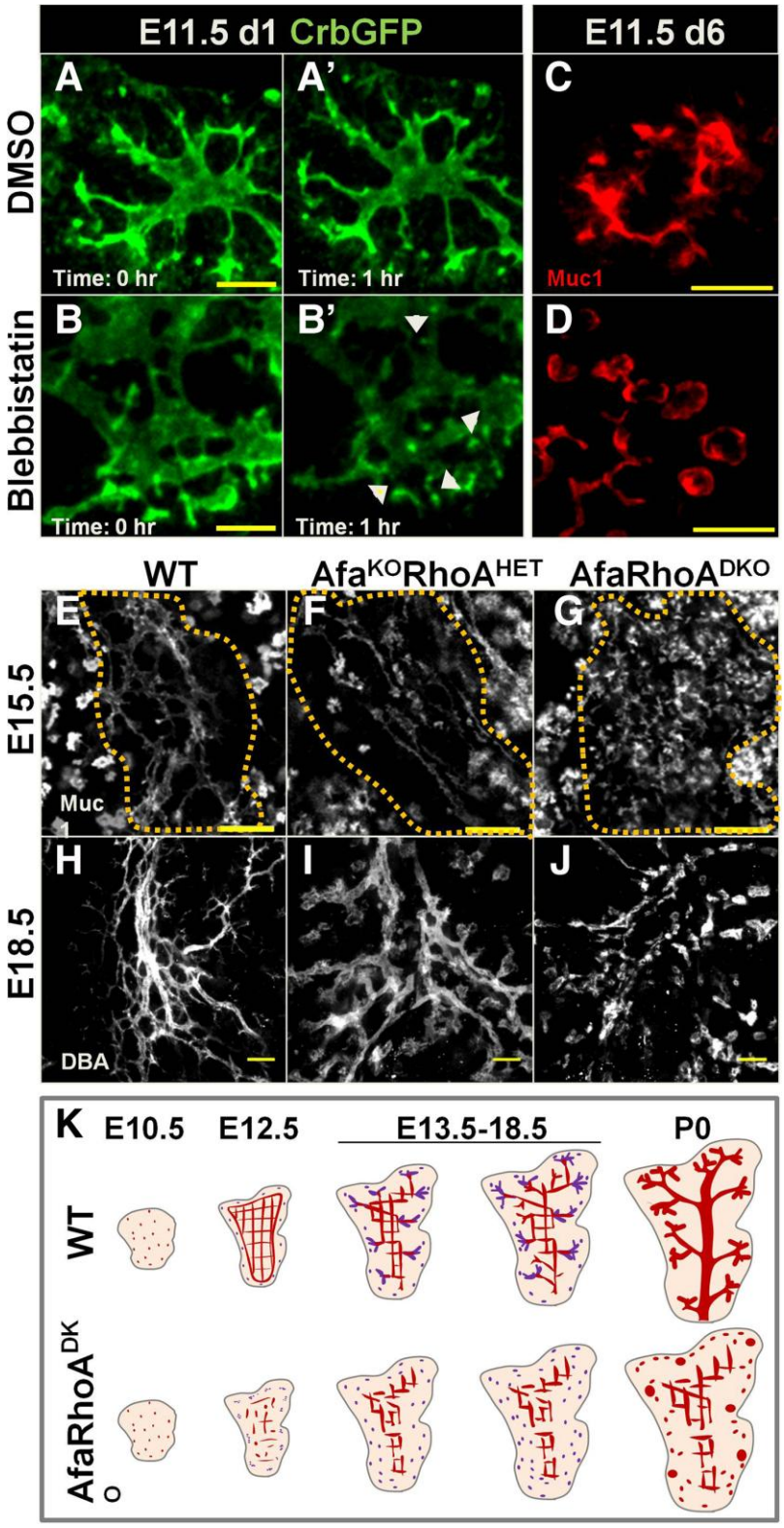
E11.5 d1 CrbGFP
E11.5 d6
A
A'
C
DMSO
Time: 0 hr
Time: 1 hr
Muc1
B
B'
D
Blebbistatin
Time: 0 hr
Time: 1 hr
WT
AfaKORhoAHET
AfaRhoADKO
E
F
G
E15.5
Muc
H
I
J
E18.5
DBA
K
E10.5
E12.5
E13.5-18.5
P0
WT
AfaRhoADKO

Figure 3.9. Lumen morphogenesis in the pancreas center depends on cooperative activity of Afadin and RhoA. (A-B') Snapshots from time-lapse imaging of DMSO- or Blebbistatin-treated Crb3-GFP E11.5 pancreatic explants on day 1 (d1) in culture. Arrowheads in **B'** indicate points of disconnection in lumens. Representative images from 3 independent experiments (n=3 embryos). Scale bars 20μm. **(C-D)** E11.5 WT pancreatic explants treated with DMSO or Blebbistatin for 5 days, fixed and immunostained for Muc1. Representative images from 2 independent experiments (n=8 embryos). Scale bars 20μm. **(E-J)** E15.5 WT, $Afadin^{f/f}RhoA^{f/+}Pdx1^{Cre}$ ($Afa^{KO}Rho^{HET}$) and $Afadin^{f/f}RhoA^{f/f}Pdx1^{Cre}$ ($AfaRho^{DKO}$, DKO) pancreata were whole mount stained for Muc1 (all lumens) or DBA (l-large and mid-sized branching ducts, excluding tips). Dotted lines in **E-G** delineate central region. Head regions at E18.5 in **H-J**. Summed slices of same thickness for each whole mount. Representative images from 3 independent experiments (n=5 embryos per genotype) in **E-G** and 3 independent experiments (n=4 embryos per genotype) in **H-J**. Scale bars 50μm in **E-G** and 100μm in **H-J**. **(K)** Schematic illustrates lumen morphogenesis defects in DKO. At E10.5, lumens are discontinuous in both WT and DKO pancreata. Later (E12.5), DKO pancreas fails to form a continuous plexus. While WT central lumens remodel at midgestation, DKO central lumens remain discontinuous and fail to undergo remodeling into branches. As a result, central lumens of the prenatal DKO pancreas remain in plexus conformation. In DKO tip epithelium, *de novo* lumens (purple) remain discontinuous and become enlarged perinatally.

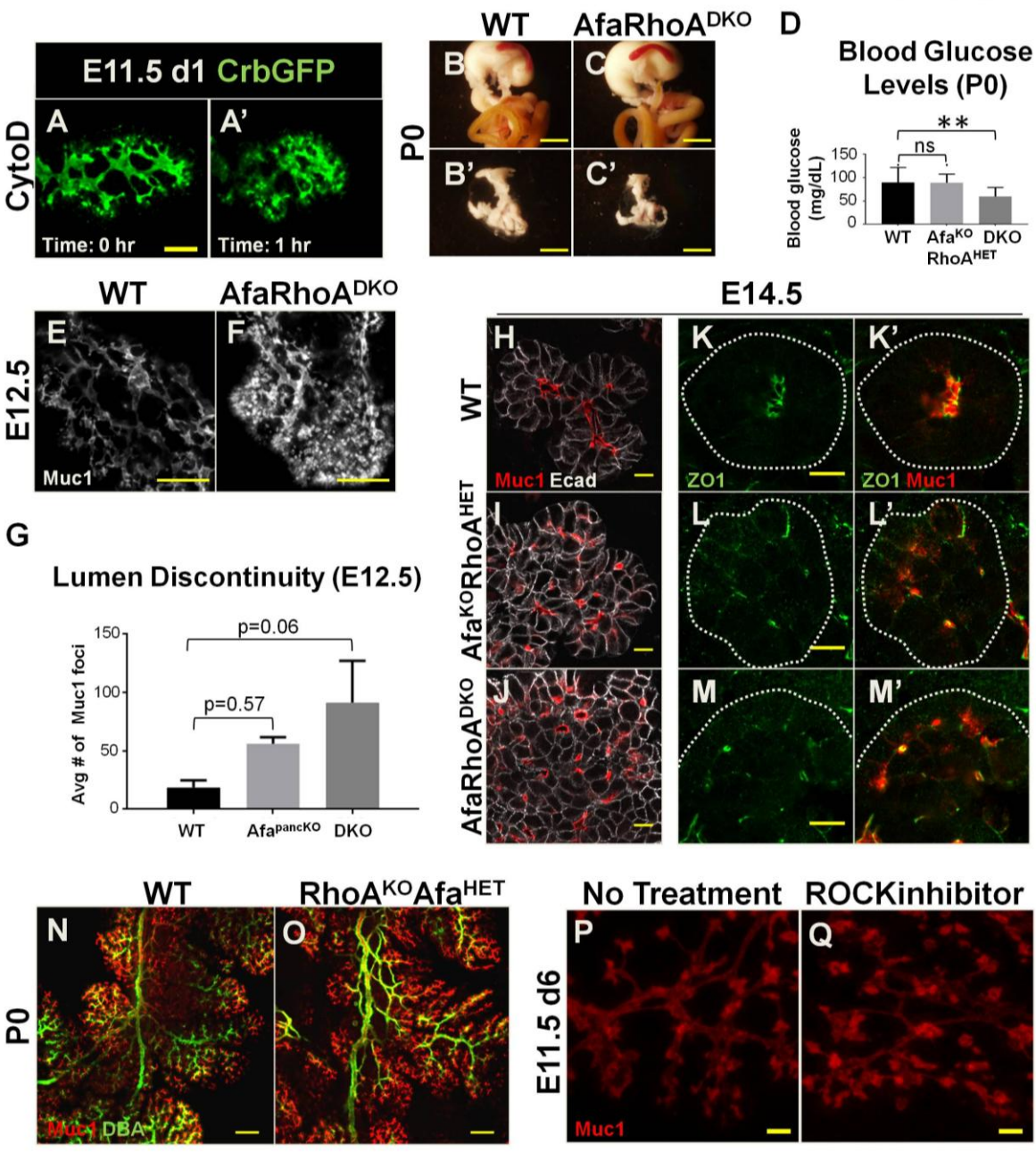
E11.5 d1 CrbGFP
CytoD
A
A'
Time: 0 hr
Time: 1 hr
WT
AfaRhoA^DKO
P0
B
C
B'
C'
D
Blood Glucose Levels (P0)
Blood glucose (mg/dL)
150
100
50
0
**
ns
WT
Afa^KO RhoA^HET
DKO
E12.5
E
F
Muc1
E14.5
WT
H
Muc1 Ecad
K
K'
ZO1
ZO1 Muc1
Afa^KO RhoA^HET
I
L
L'
AfaRhoA^DKO
J
M
M'
G
Lumen Discontinuity (E12.5)
Avg # of Muc1 foci
150
100
50
0
p=0.06
p=0.57
WT
Afa^pancKO
DKO
P0
WT
RhoA^KO Afa^HET
N
O
Muc1 DBA
E11.5 d6
No Treatment
ROCKinhibitor
P
Q
Muc1

Figure 3.10. Loss of RhoA activity exacerbates the lumen phenotype of Afadin mutants. **(A-A')** Snapshots from time-lapse imaging of Cytochalasin D-treated Crb3-GFP E11.5 pancreatic explants on day 1 (d1) in culture. Representative images from 3 independent experiments on n=3 embryos. Scale bar 50 μm. **(B-C')** Images of stomach and pancreas together and pancreas alone from P0 WT and AfaRhoA^{DKO} are shown. Representative images from 4 independent experiments on n=6 embryos per genotype. Scale bars 500 μm. **(D)** Blood glucose levels of P0 WT (n=30), Afa^{KO}RhoA^{HET} (n=4), and AfaRhoA^{DKO} (DKO, n=6) pups were measured. Data are represented as mean (S.D.). ns, nonsignificant. **(E-G)** E12.5 WT, Afa^{pancKO} and DKO pancreata were whole mount immunostained for Muc1 and analyzed for isolated Muc1 foci on n=2 embryos per genotype. Summed slices of 20 μm thickness are shown in **E-F**. Scale bars 50 μm. Data are represented as mean (S.D.). **(H-M')** Paraffin sections of E14.5 WT, Afa^{KO}RhoA^{HET} and DKO pancreata were immunostained for Muc1 (lumens), Ecad (epithelial membranes) and ZO1 (tight junctions). Dotted lines outline tip epithelia. Representative images from 3 independent experiments on n=3 embryos per genotype. Scale bars 10 μm. **(N-O)** P0 WT and RhoA^{KO}Afa^{HET} were whole mount immunostained for Muc1 and DBA. Maximum projections are shown. Representative images from 4 independent experiments on n=4 embryos per genotype. Scale bars 100 μm. **(P-Q)** E11.5 WT pancreatic explants were treated with dH_20 or ROCK inhibitor Y-27632 for 5 days, fixed and immunostained for Muc1 to assess lumen morphology. Representative images from 3 independent experiments on n=6 embryos. Scale bars 20μm.

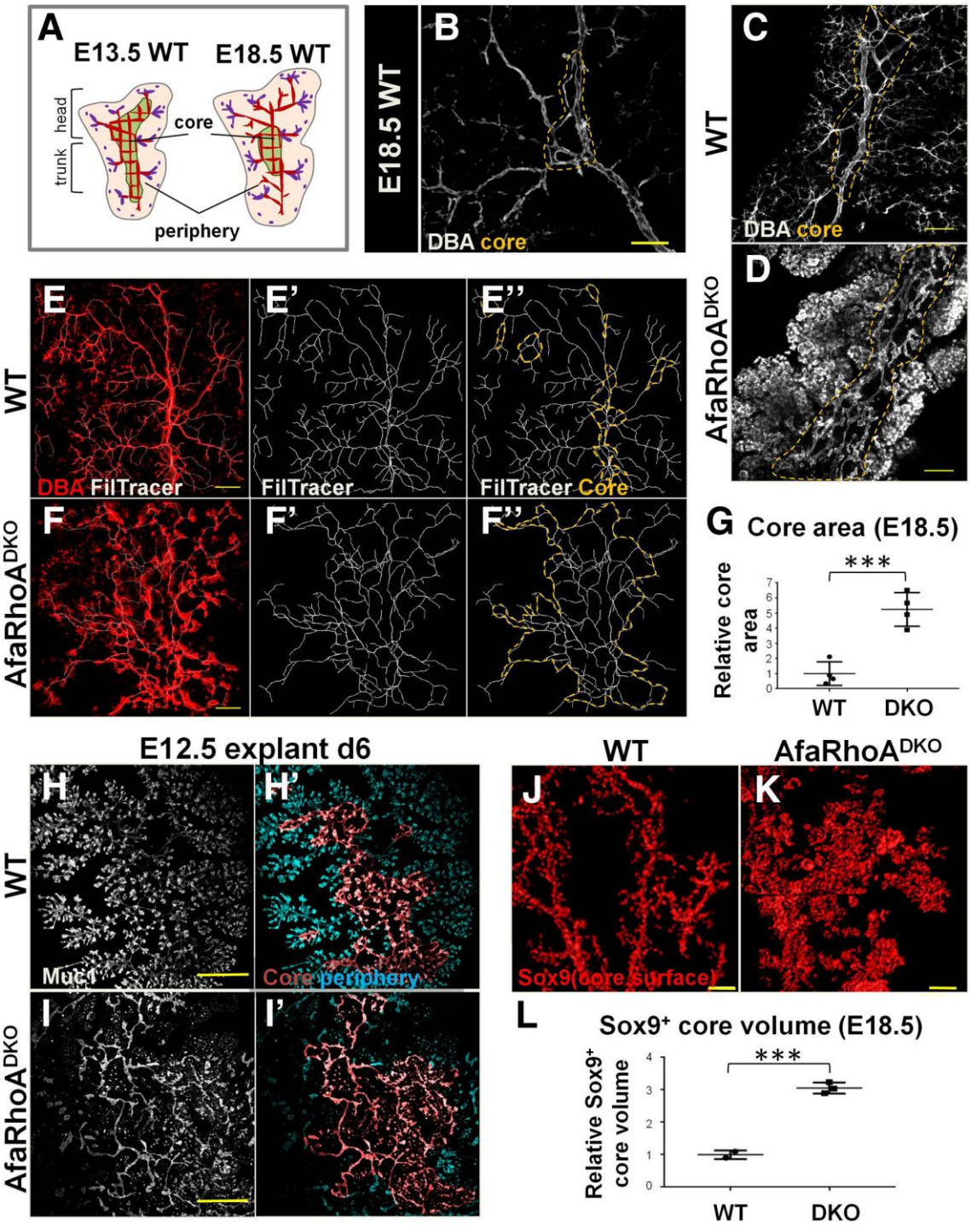
A
E13.5 WT
E18.5 WT
head
trunk
core
periphery
B
E18.5 WT
DBA core
C
WT
DBA core
D
AfaRhoA^DKO
E
E'
E''
WT
DBA FilTracer
FilTracer
FilTracer Core
F
F'
F''
AfaRhoA^DKO
G Core area (E18.5)
***
Relative core area
WT
DKO
E12.5 explant d6
H
H'
WT
Muc1
Core periphery
I
I'
AfaRhoA^DKO
WT
AfaRhoA^DKO
J
K
Sox9(core surface)
L
Sox9+ core volume (E18.5)
***
Relative Sox9+ core volume
WT
DKO

Figure 3.11. Arrest of lumen morphogenesis leads to ectopic perdurance of the core. (A) Schematic illustrates the distinction between core and periphery in the murine embryonic pancreas, and transient nature of the core-periphery regionalization. The pink region corresponds to the periphery with lumen branches, while the green region represents the core with an interconnected plexus (red) midst remodeling. The central plexus undergoes remodeling to form branches, as the tips continue to form *de novo* lumens and fuse with the lumen branches arising from the center. Red lumens in the periphery represent lumens arising from remodeling of central lumens and purple lumens represent lumens arising *de novo*. Purple dots indicate the most recent, yet discontinuous, *de novo* lumens. Plexus remodeling takes place gradually encompassing inwards to the center of the tissue, as more central plexus lumens become hierarchical branches. Thus, the core region becomes gradually smaller relative to the periphery. **(B)** E18.5 WT pancreata whole mount immunostained for DBA to mark large and mid-sized ducts. Maximum projection of the z-stack is shown. Dotted line outlines core lumens. Scale bar 40µm. **(C-D)** E18.5 WT and AfaRho^{DKO} (DKO) pancreata whole mount immunostained for DBA. Pancreatic trunk is shown. Summed slices (50µm) through z-stack are shown. Dotted line outlines core lumens. Representative images from 4 independent experiments (n=4 embryos per genotype). Scale bars 100µm. **(E-F'')** E18.5 WT and DKO pancreata whole mount immunostained for DBA. Pancreatic head is shown. Maximum projection of z-stacks are shown in **E** and **F**. Filament Tracer function on Imaris tracks lumens and creates a continuous counterpart of lumens in **E** and **F**. Orange dotted line indicates core region in **E''** and **F''**. Representative images from 4 independent experiments (n=4 embryos per genotype). Scale bars 150µm. **(G)** Quantification of core area

using Filament Tracer analysis on pancreata from WT (n=3) and DKO (n=3) embryos per genotype (representative images in **E-F''**). **(H-I')** E12.5 WT and DKO pancreatic explants cultured for 6 days (d6), then fixed and immunostained for Muc1. Lumens were traced using Filament Tracer. Core and peripheral lumens are highlighted in different colors by using the Surface function of Imaris. Representative images from 3 independent experiments (n=4 embryos per genotype). Scale bars 300μm. **(J-K)** E18.5 WT and DKO pancreata were whole mount immunostained for Sox9. Surface function on Imaris used to visualize total $Sox9^{+}$ surface area in the core region. Head region of the pancreas is shown. Representative images from 3 independent experiments (n=4 embryos per genotype). Scale bars 150μm. **(L)** E18.5 core volume calculated on Sox9 whole mount stained WT (n=2) and DKO (n=3) pancreas head regions using surface function of Imaris (representative images in **J-K**).

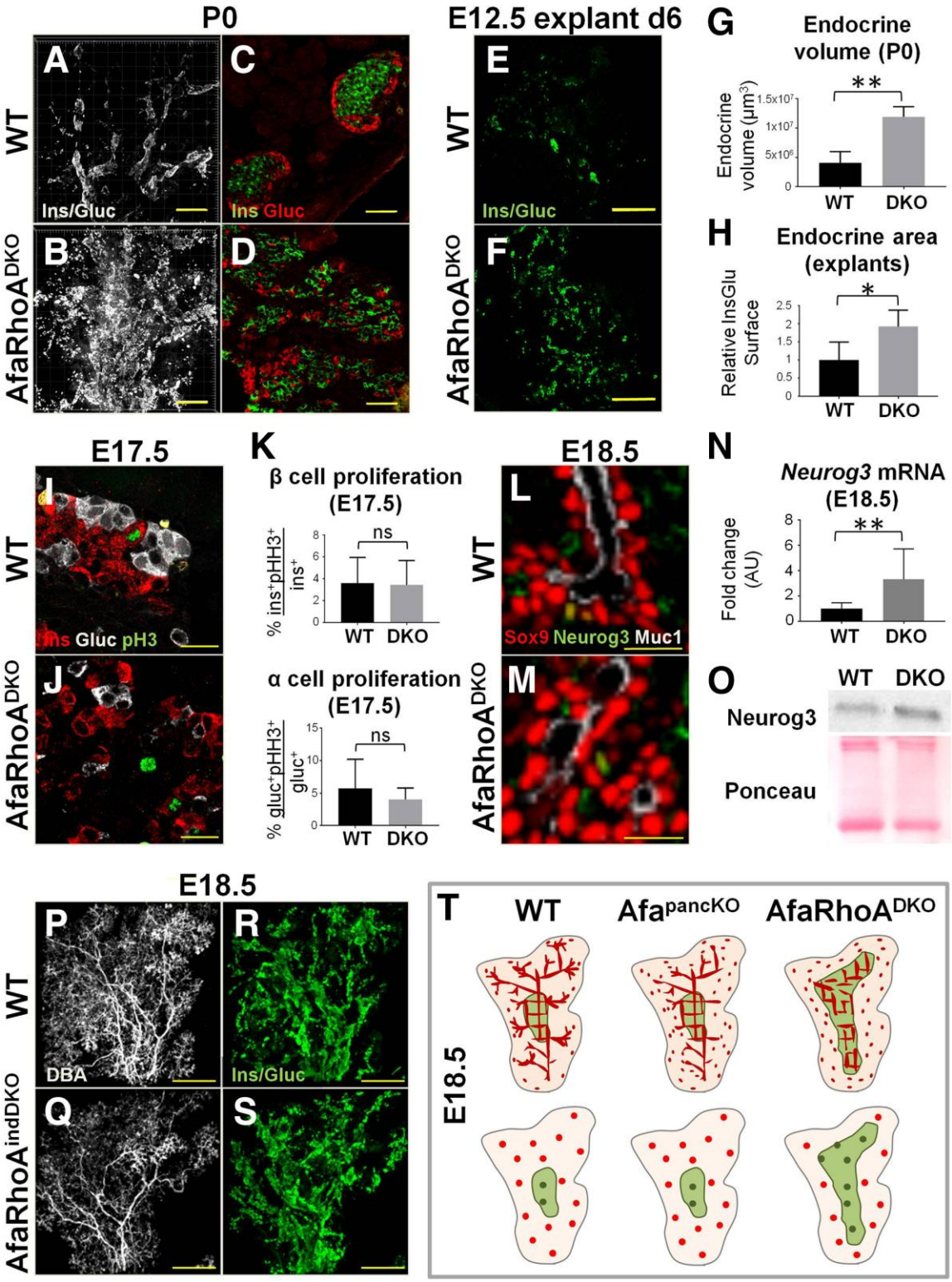
P0
E12.5 explant d6
WT
AfaRhoA DKO
A
B
C
D
E
F
Ins/Gluc
Ins Gluc
G
Endocrine volume (P0)
Endocrine volume (µm3)
1.5x10^7
1x10^7
5x10^6
0
**
WT
DKO
H
Endocrine area (explants)
Relative InsGlu Surface
2.5
2
1.5
1
0.5
0
*
WT
DKO
E17.5
I
J
Ins Gluc pH3
K
β cell proliferation (E17.5)
% ins+pHH3+ / ins+
8
6
4
2
0
ns
WT
DKO
α cell proliferation (E17.5)
% gluc+pHH3+ / gluc+
15
10
5
0
ns
WT
DKO
E18.5
L
M
Sox9 Neurog3 Muc1
N
Neurog3 mRNA (E18.5)
Fold change (AU)
8
6
4
2
0
**
WT
DKO
O
WT
DKO
Neurog3
Ponceau
E18.5
P
Q
R
S
DBA
Ins/Gluc
AfaRhoA indDKO
T
WT
AfapancKO
AfaRhoADKO
E18.5

Figure 3.12. Core perdurance promotes endocrine commitment in bipotential progenitors. (A-B) P0 WT and AfaRho^{DKO} (DKO) pancreata whole mount immunostained for insulin and glucagon in the same channel as a proxy for endocrine content. Maximum projections of the head regions are shown. Representative images from 4 independent experiments (n=6 embryos per genotype). Scale bars 200µm. **(C-D)** P0 WT and DKO pancreas paraffin sections immunostained for insulin and glucagon to label beta and alpha cells, respectively. Representative images from 3 independent experiments (n=3 embryos per genotype). Scale bars 50µm. **(E-F)** E12.5 WT and DKO pancreatic explants cultured for 6 days (d6), then fixed and immunostained for insulin/glucagon in the same channel. Representative images from 3 independent experiments on pancreata from WT (n=11) and DKO (n=3) embryos. Scale bars 300µm. **(G)** Quantification of endocrine volume at P0 using Surface function of Imaris (n=4 embryos per genotype) (representative images in **A-B**). **(H)** Surface function of Imaris was used to quantify endocrine area on E12.5 WT and DKO pancreatic explants cultured for 6 days from WT (n=3) and DKO (n=3) embryos (representative images in **E-F**). **(I-J)** Paraffin sections of E17.5 WT and DKO pancreata were immunostained for insulin (Ins), glucagon (Gluc) and pH3 to assess endocrine cell proliferation. Representative images from 3 independent experiments (n=3 embryos per genotype). Scale bars 20µm. **(K)** α and β cell proliferation assessed on E17.5 WT and DKO pancreas sections stained for insulin, glucagon and pH3 (representative images in **I-J**). Data are represented as mean (S.D.). ns, nonsignificant. **(L-M)** E18.5 WT and DKO pancreata whole mount immunostained for Sox9 (bipotential progenitors), Neurog3 (endocrine progenitors) and Muc1 (lumens). A visual section through the whole mount is shown.

Representative images from 3 independent experiments (n=3 embryos per genotype). Scale bars 20μm. **(N)** qPCR data from E18.5 WT and DKO pancreata shows fold change in mRNA levels for *Neurog3* WT (n=10) and DKO (n=4) embryos. Data are shown as mean (S.D.) **(O)** Western Blotting from E18.5 WT and DKO pancreata using a Neurog3 antibody. Ponceau staining serves as loading control. Representative images of membranes are shown (n=3 embryos per genotype, 2 independent experiments). **(P-S)** E18.5 WT and Tamoxifen-induced $Afadin^{f/f}RhoA^{f/f}Pdx1Cre^{ERT2}$ ($AfaRho^{indDKO}$) pancreata whole mount stained for DBA (large and mid-sized branching ducts) and Insulin/Glucagon (in the same channel). Maximum projections of the head regions are shown. Representative images from 3 independent experiments (n=3 embryos per genotype). Scale bars 300μm. **(T)** Schematic illustrates core-periphery regionalization (top row) and resulting cellular differentiation phenotype at E18.5 (bottom row) in Afa^{pancKO} and DKO pancreata compared to the WT. Top row: Core region (green) and the periphery (pink). Peripheral lumen discontinuity is designated by isolated apical/lumenal foci (red). Lumen plexus in the core is normal in Afa^{pancKO}, but remains discontinuous and fails to resolve in DKO. As a result, the core region perdures in DKO pancreas. Bottom row: Bipotential (red) and endocrine progenitors (green). Progenitor distribution is similar in WT and Afa^{pancKO} pancreata. By contrast, most bipotential progenitors reside in the core in DKOs due to perdurance of this region. As a result, DKOs generate more endocrine progenitors. (N.B.: Caitlin Braitsch performed the RNA isolation and qPCR to generate the data presented in panel **N**.)

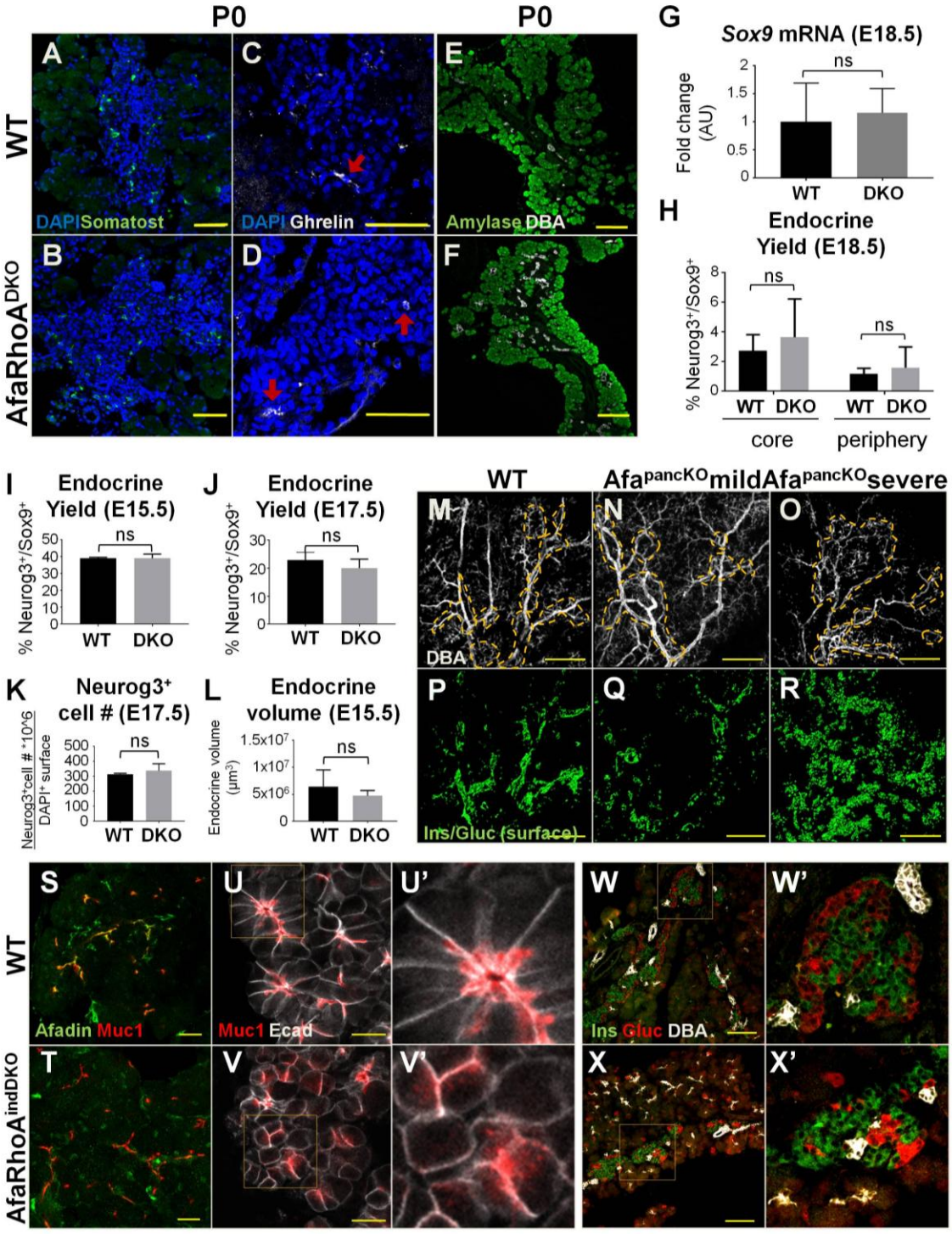
P0
P0
WT
AfaRhoA^DKO
A
B
C
D
E
F
DAPI Somatost
DAPI Ghrelin
Amylase DBA
G
Sox9 mRNA (E18.5)
Fold change (AU)
ns
WT
DKO
H
Endocrine Yield (E18.5)
% Neurog3+/Sox9+
ns
WT DKO WT DKO
core
periphery
I
Endocrine Yield (E15.5)
J
Endocrine Yield (E17.5)
K
Neurog3+ cell # (E17.5)
L
Endocrine volume (E15.5)
Endocrine volume (μm3)
WT
AfapancKO mild
AfapancKO severe
M
N
O
DBA
P
Q
R
Ins/Gluc (surface)
S
U
U'
W
W'
Afadin Muc1
Muc1 Ecad
Ins Gluc DBA
T
V
V'
X
X'

Figure 3.13. Endocrine mass increase correlates with core expansion independent of endocrine-cell intrinsic roles of Afadin-RhoA. (A-D) Paraffin sections of P0 WT and AfaRhoA^{DKO} pancreata were immunostained for somatostatin (somatost) and ghrelin to mark δ and ε cells, respectively. DAPI marks the nuclei. Arrows show cells positive for ghrelin in **C-D**. Representative images from 3 independent experiments on n=3 embryos. Scale bars 50 μm. **(E-F)** Paraffin sections of P0 WT and AfaRhoA^{DKO} (DKO) pancreata were immunostained for amylase to mark acinar cells, and DBA to mark ductal cells. Scale bars 200 μm. **(G)** qPCR data from E18.5 WT and DKO pancreata shows fold change in mRNA levels for *Sox9* on n=10 WT and n=4 DKO embryos. Data are shown as mean (S.D.). **(H)** Endocrine yield (Neurog3^{+}/Sox9^{+} %) was calculated on E18.5 WT and DKO pancreata whole mount immunostained for Neurog3, Sox9 and DBA with n=2 embryos per genotype (representative images in **Figure 3.12L-M**). DBA was used to identify core and periphery lumens. **(I-J)** Endocrine yield was calculated on sections on WT and DKO pancreata immunostained for Neurog3 and Sox9 (n=2 embryos per genotype). **(K)** Neurog3^{+} cells were counted on E17.5 WT and DKO sections relative to the DAPI^{+} pancreatic surface area (n=2 embryos per genotype). **(L)** E15.5 endcorine volume was calculated on whole mount insulin/glucagon immunostained WT and DKO tissues using Surface function of Imaris (n=2 embryos per genotype). **(M-R)** P0 Afa^{pancKO} pancreata were whole mount stained for DBA to assess ductal continuity and for insulin/glucagon to assess endocrine mass. Dotted lines outline large ducts and core regions with incomplete remodeling. Surface function of Imaris was used to create a surface for insulin/glucagon positive areas. Representative images from 3 independent experiments on n=3 embryos per genotype. Scale bars 300 μm. **(S-V')** E18.5

AfaRhoA^{indDKO} paraffin sections were immunostained for Afadin, Muc1 and Ecad. Insets in **U** and **V** are shown at high magnification in **U'** and **V'**, respectively. Representative images from 3 independent experiments on n=3 embryos per genotype. Scale bars 20 μm. **(W-X')** E18.5 AfaRhoA^{indDKO} paraffin sections were immunostained for insulin, glucagon and DBA. Insets in **S** and **T** are shown at high magnification in **S'** and **T'**. Representative images from 3 independent experiments on n=3 embryos per genotype. Scale bars 100 μm. (N.B.: Caitlin Braitsch performed the RNA isolation and qPCR to generate the data presented in panel **G**.)

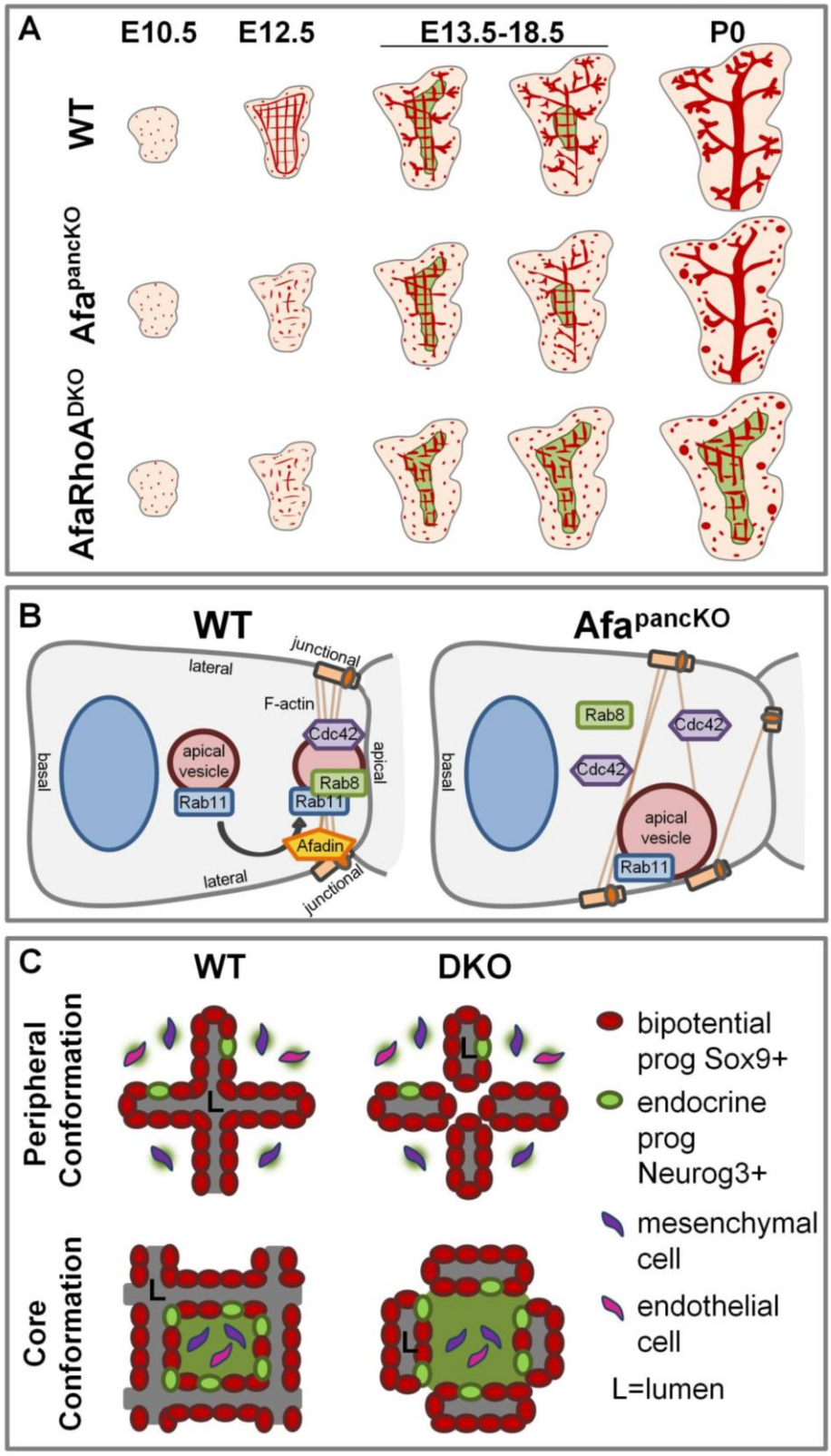
A
E10.5
E12.5
E13.5-18.5
P0
WT
Afa pancKO
AfaRhoA DKO
B
WT
junctional
lateral
F-actin
Cdc42
apical vesicle
Rab11
Rab8
Afadin
basal
apical
lateral
junctional
Afa pancKO
Rab8
Cdc42
Cdc42
basal
apical vesicle
Rab11
C
WT
DKO
Peripheral Conformation
Core Conformation
L
bipotential prog Sox9+
endocrine prog Neurog3+
mesenchymal cell
endothelial cell
L=lumen

Figure 3.14. Afadin and RhoA regulate lumen morphogenesis and control endocrine mass. (A) Schematic illustrates a comparison of the lumen morphogenesis defects and resulting core-periphery regionalization in Afa^{pancKO} and $AfaRhoA^{DKO}$ relative to the WT pancreas. Afa^{pancKO} fails to form normal peripheral lumens, while core plexus remodels relatively normally, giving rise to a relatively normal lumenal tree by birth. By contrast, plexus remodeling defects in $AfaRhoA^{DKO}$ lead to ectopic perdurance of the core region by birth. **(B)** Schematic shows a model for WT and Afa^{pancKO} cells in the process of making an apical membrane to form a lumen. In WT cells, Afadin likely acts as a scaffold to localize Rab8 and Cdc42 to the pre-apical domain, and thereby facilitates their loading onto the apical vesicles. Proper localization of these molecules drives trafficking and exocytosis of the apical vesicle at the pre-apical membrane. Loss of Afadin in Afa^{pancKO} cells leads to mislocalization of tight junctions, as well as disruption of Rab8 and Cdc42 recruitment to their proper loci. As a result, apical vesicles are targeted nearby junctional domains, but fail to exocytose presumably due to absence of Rab8 and Cdc42, factors required for exocytosis. **(C)** Schematics illustrate the organization of bipotential progenitors and nearby cell types in a peripheral versus core unit. Endocrine progenitors mostly arise in the core region as opposed to the periphery. Core conformation may concentrate signaling events required for endocrine fate by enclosing cells in the space within plexus (shown in green). $AfaRhoA^{DKO}$ pancreas maintains these lumen conformations despite lumen discontinuity, and promotes endocrine differentiation due to perdurance of core conformation (latter concept not shown in figure).

CHAPTER FOUR

CONCLUSIONS AND FUTURE DIRECTIONS

Lumen morphogenesis is crucial to pancreas development and has been suggested to impact pancreatic lineage allocation. To date, molecular mechanisms underlying pancreatic lumen morphogenesis and what aspect of lumen morphogenesis determines pancreatic lineage allocation have remained elusive. My studies identify genetic factors needed for two distinct lumen morphogenesis events during pancreas development, and uncover a role for the transient lumenal network, i.e. the plexus, in endocrine differentiation. Here, I discuss these findings in the context of the current knowledge in the field, address major caveats and challenges of the presented study and propose future directions for a better understanding of pancreatic lumen morphogenesis and endocrine differentiation.

Afadin as a 'lumen master'

My study presented here identified a role for Afadin in *de novo* lumen formation during pancreas development. Afadin plays a similar role in the developing kidney, and so does its cousin molecule Rasip1 in the vasculature (Xu et al. 2011; Yang et al. 2013). Thus, Afadin (and Rasip1) emerges as a master regulator of *de novo* lumen formation. My work suggests that Afadin loss leads to junction misorganization, apical determinant mislocalization and failure in exocytosis. However, how Afadin regulates these processes remains unknown.

Afadin was discovered as a junctional molecule and its depletion leads to junction misorganization, in particular of tight junctions (Ikeda et al. 1999). Similarly, my work showed that the pancreatic epithelium mislocalizes tight junctional complexes in the absence of Afadin. These findings together suggest that one important function of Afadin in lumen formation is junction assembly.

In addition to forming ectopic junctions, the *Afadin* mutant epithelium fails to properly localize apical determinants. Proper localization of apical determinants and tight junction organization are two highly inter-dependent processes (Shin et al. 2006). Indeed, a subset of apical determinants first localize to the junctional foci, before re-locating to the pre-apical membrane. Therefore, apical determinant localization may be affected due to abnormal junction organization in the absence of Afadin (Zhadanov et al. 1999).

What about the role of Afadin in apical vesicle exocytosis? Afadin may regulate this process also through junction assembly. In the absence of Afadin, apical vesicles abnormally localize near ectopic tight junctional foci. Since these sites are ectopic, they lack the exocytosis mediators, such as Cdc42 and Rab8. This can explain failure of exocytosis followed by accumulation of vesicles in the *Afadin* mutant nearby junctions. Thus, exocytosis failure may be secondary to ectopic localization of junctions and junction-directed targeting of vesicles to loci that lack exocytosis mediators.

Localization of apical vesicles near ecoptic tight junctional complexes in *Afadin* mutants brings up an important question beyond Afadin function: Are these junctional complexes the targeting site for apical vesicle exocytosis? Does such vesicle targeting occur only in the absence of Afadin, or also in a wild type cell? Suggesting that the latter may be the case, tight

junctional complexes have been previously proposed as target sites for exocytosis (Zahraoui et al. 2000). Furthermore, apical components such as Par3 or the exocyst first enrich at junctional foci during apical membrane initiation, and then re-localize to the pre-apical membrane (Bryant et al. 2010). Thus, junctional complexes provide the first assembly point for apical components at the plasma membrane, and may do the same for exocytosis of apical vesicles.

As an alternative to a junction-dependent role, Afadin may regulate exocytosis directly, independently of junction assembly. The domain structure of Afadin provides clues as to how this could work: Afadin has an F-actin binding domain and a dilute (DIL) domain, the cargo-binding domain in the MyosinV family (Mandai et al. 2013). Using these domains, Afadin can potentially link its "cargo" to the actin cytoskeleton. Intriguingly, DIL domain-containing MyosinV has been shown to interact with the vesicular GTPase Rab11, and function in exocytosis (Muller et al. 2008; Roland et al. 2011; Khandelwal et al. 2013). Therefore, Afadin may similarly bind vesicular GTPases, such as Rab11, through the DIL domain, and thereby facilitate apical vesicle targeting and exocytosis.

I speculate that Afadin plays an at least partially junction-independent role in exocytosis. I propose a model where MyosinV is responsible for trafficking apically-targeted vesicles to the correct membrane site (presumably junctional) through its DIL domain **(Figure 4)**. Once at the membrane, MyosinV may transfer its cargo, the apically targeted vesicle, over to Afadin, which may also bind to the vesicle through its DIL domain (and maybe the RA domain). This could ensure proper targeting and tethering of the vesicles at junctional foci near the pre-apical membrane. Next, with the help of exocytosis mediators Cdc42 and Rabs,

the apical vesicle is exocytosed at the pre-apical membrane. Further studies focused on domain deletions of Afadin, particularly F-actin binding, RA and DIL domains, will be crucial to determine the extent to which this speculation holds true.

Altogether, these findings indicate a dual role for Afadin in lumen formation. Afadin coordinates junction assembly and exocytosis in the right place at the right time for proper apical membrane formation. Elucidating the molecular mechanisms underlying this regulation will provide insight into pancreatic lumen morphogenesis, and also generally into tube development.

Building the plexus

Initial lumen formation is followed by lumen coalescence and remodeling in the developing pancreas. Through the work presented here, I identified RhoA as a crucial partner of Afadin in lumen coalescence and remodeling processes, once initial lumens have formed. While single *Afadin* or *RhoA* mutants do not display any major defects in plexus formation and remodeling, double depletion of these factors causes a dramatic arrest in plexus morphogenesis. These findings reveal a novel partnership between Afadin and RhoA during pancreatic plexus development, which is critical for proper pancreatic differentiation. Dissecting mechanisms of this partnership will shed light on lumen coalescence and pancreas morphogenesis.

What cellular and molecular mechanisms coalesce lumens and build the plexus? In the pancreas, this question has not been investigated. In other systems, lumen coalescence depends on junction formation and the activities of actin, actomyosin and RhoA (Lee and

Kolodziej 2002). Therefore, it is not entirely surprising that RhoA and actomyosin play a similar role in the developing pancreas. However, their exact molecular functions here are unclear. In Drosophila trachea, junction formation occurs between cells at their basolateral side to establish a track of actin that marks where the lumens will fuse. RhoA is thought to regulate formation of the actin track (Lee and Kolodziej 2002). It would be interesting to determine whether similar actin tracks form prior to lumen coalescence in the pancreas.

How does Afadin come into play during lumen coalescence? The answer may be through its known functions, its suggested functions, or its yet unknown functions implied by its domain structure. As discussed in "Afadin as a lumen master" section of this chapter, Afadin is required for junction assembly (Ikeda et al. 1999). If junction formation is necessary for lumen coalescence in the developing pancreas similar to other systems, Afadin may facilitate this process through its known role in junction assembly. RhoA is also a regulator of junction assembly and may co-function with Afadin to assemble junctions for proper lumen coalescence (Terry et al. 2011).

Another potential synergy point for Afadin and RhoA is actomyosin. As my work showed, actomyosin activity is necessary for lumen coalescence in the pancreas. RhoA is a master regulator of actoymosin activity (Zaidel-Bar et al. 2015). Afadin also binds to F-actin, and has been shown to be involved in actomyosin constriction (Sawyer et al. 2011). Thus, Afadin and RhoA may synergize during lumen coalescence through their effect on actomyosin.

Lastly, Afadin and RhoA may act together in more complicated ways than having a common cellular job. It is possible that RhoA directs one cellular event, while Afadin coordinates another, together needed for lumen coalescence. Failure of one of these cellular events may

be compensated for in the absence of Afadin or RhoA. By contrast, when both factors are absent, the cell may lose its compensatory mechanisms and fail to participate in lumen coalescence.

Further studies are needed to determine how Afadin and RhoA act together to build a plexus during pancreas development. Identifying the molecular basis of plexus formation will advance our understanding of pancreas morphogenesis and how it is coordinated with differentiation.

Plexus as an endocrine niche

The developing pancreas forms a transient plexus of lumens. This plexus is where most endocrine progenitors reside. When the plexus forms, endocrine differentiation initiates. With complete resolution of the plexus, endocrine differentiation terminates (Bankaitis et al. 2015). Could the plexus be acting as a niche for endocrine cell differentiation? My work presented here shows that, when the plexus is maintained longer without resolving, endocrine cell production is dramatically increased. Together, these findings strongly suggest that the plexus serves as a niche for endocrine differentiation.

Although the pancreatic plexus has not been the focus of previous studies until recently, there have been reports of mutants with plexus resolution defects. *Nr5a2* mutant pancreas is one of the most clear examples, where the plexus is maintained longer than normal (Hale et al. 2014). Interestingly, these mutants did not display any increase in endocrine mass. This may seem contradictory to my findings at first sight. However, there is one major caveat of concluding a role for plexus from this study (this was not the focus of the study, and neither

did the authors make any such conclusions): Nr5a2 plays important roles early during pancreas development. As a result, Nr5a2 depletion affects pancreatic progenitors well before tip-trunk compartmentalization, plexus resolution, or endocrine fate induction. Thus, it will be dfficult to interpret the resulting differentiation defects as a consequence of alterations in plexus. Nonetheless, generation of other models with prolonged plexus maintenance will be crucial to independently test the function of the plexus in endocrine cell generation.

One puzzling finding from my studies was the late increase in DKO endocrine mass, only starting past E18.5. This late increase may suggest that 1. endocrine progenitor numbers are only increased right before E18.5, or 2. more endocrine progenitors arise at earlier stages, but do not differentiate until E18.5. If the former was correct, one would expect to find subtype bias towards the PP lineage in the DKO pancreas. This is because committed endocrine progenitors are unipotent, and mostly differentiate to PP cells if committing close to birth (Yamaoka and Itakura 1999; Desgraz and Herrera 2009). By contrast, there was no bias towards PP or any other endocrine subtype in the DKO. This finding argues that an increased number of endocrine progenitors is generated starting at earlier stages; however, these progenitors do not differentiate until E18.5. Such delayed burst of differentiation could be explained by a negative feedback mechanism exerted by the differentiating endocrine cells (or other cell types) on endocrine progenitors until late gestation, i.e. until the normal differentiation period of endocrine cells comes to an end. Indeed, a similar idea of negative feedback on endocrine differentiation has been previously proposed by others (Pan and

Wright 2011). Based on these findings, I argue that the plexus niche can promote endocrine fate induction, but is not sufficient to force endocrine differentiation until late gestation.

The idea of a delayed burst of endocrine differentiation in DKO pancreas is in line with the isletogenesis defects seen in these mutants. Isletogenesis requires delamination and coordinated clustering of cells (Bouwens and De Blay 1996; Yamaoka and Itakura 1999; Miller et al. 2009). When a sudden burst of differentiation occurs and the cells delaminate all at once, they would be predicted to fail in coordinating their delamination and clustering. It would be informative, in this context, to determine whether DKO pups at later stages (by P9, as they survive only until then) can cluster these burst-generated endocrine cells and form proper islets with a delay. Identification of the contributing factors behind late endocrine mass increase and isletogenesis defects in DKOs will require further studies.

One major challenge in my studies has been to distinguish bipotential progenitors from differentiated ductal cells. Ductal cells retain the bipotential markers Sox9, Hnf1b, Hnf6 and Nkx6.1; however, there are no known molecular markers specific to these cells (Larsen and Grapin-Botton 2017). Due to lack of such tools, my work was unable to definitively address whether there is any impact of Afadin;RhoA double depletion on the number of bipotential cells or ductal cells. Indeed, my findings do not rule out the possibility that the plexus may impact ductal fate, rather than endocrine fate per se. The plexus may act inhibitory on ductal fate determination, maintaining the trunk cells in the bipotential state, and indirectly promoting endocrine fate.

A role for plexus in blocking ductal differentiation would make sense from the perspective of the ductal cell. These cells line lumens in the mature pancreas, where they function to

maintain the lumens and mediate digestion. It is highly likely that ductal differentiation and lumen maturation are inter-dependent. Indeed, supporting this idea, mutants for transcription factors that lead to ductal differentiation defects very frequently display cystic duct phenotypes (Larsen and Grapin-Botton 2017). Thus, plexus-to-duct maturation may be required for bipotential cells to turn on ductal fate. Further studies are needed to make the distinction between bipotential versus committed ductal states, and to identify the precise role of the plexus in pancreatic lineage determination.

What makes the plexus a niche, whether it is for bipotential state maintenance or endocrine fate induction? One potentially relevant feature of the plexus is its distance from the outer mesenchyme surrounding the periphery that is thought to promote acinar differentiation (Kesavan et al. 2009). The plexus still makes contact with the extracellular matrix and presumably mesenchymal cells; however, this mesenchymal population could be different than the peripheral population. Therefore, it is possible that the plexus acts a barrier between distinct mesenchymal populations in the core versus periphery (from here on referred to as mesenchymal barrier hypothesis).

Vascular endothelial cells are emerging as master regulators of organ development and regeneration through their angiocrine roles in many tissues (Azizoglu and Cleaver 2016). Likewise, vasculature was identified to regulate pancreatic progenitor maintenance and differentiation (Pierreux et al. 2010; Magenheim et al. 2011; Kao et al. 2015). Similar to the mesenchymal barrier hypothesis, it is possible that the plexus builds a barrier between distinct endothelial populations in the core versus periphery (endothelial barrier hypothesis).

Being away from acinar cells is another main feature of the plexus in contrast with the peripheral lumens. Acinar cells may act inhibitory in endocrine fate induction, or promote ductal differentiation. In this scenario, the plexus may "protect" the bipotential progenitors from the acinar environment, supporting endocrine differentiation (acinar protection hypothesis). My preliminary data (not shown) based on genetic induction of acinar cell death suggests that ablating acinar cells does not promote endocrine cell production. However, likely leakiness of the used genetic induction complicates interpretation of these results. Thus, acinar protection hypothesis needs to be further tested to determine whether acinar cells play any role in endocrine differentiation.

Finally, the plexus may serve as a niche by simply concentrating signaling events needed for endocrine fate induction or bipotential state maintenance (as proposed in Chapter 3). With recent work, cell cycle dynamics is emerging as a key contributor to endocrine fate induction. Thus, it will be interesting to analyze such dynamics in the plexus cells to determine whether the plexus acts through regulation of cell cycle length. These and other hypotheses need to be tested to uncover how the plexus may facilitate endocrine differentiation during pancreas development. Investigating the mechanism of plexus-mediated endocrine differentiation will undoubtedly advance our understanding of *in vivo* endocrine differentiation, and guide *in vitro* attempts to generate endocrine cells for potential cell replacement therapies.

Future Directions

My studies identified a novel cellular function for Afadin in exocytosis during lumen formation and a role for lumen coalescence in building a transient plexus. My work also

suggests that this plexus may serve as a niche for endocrine fate induction. Based on this work, future studies could focus on three novel directions: 1. identification of the molecular role of Afadin in exocytosis, 2. elucidating cellular and molecular mechanisms of lumen coalescence, a poorly understood developmental process that gives rise to the plexus niche, and 3. investigating how the plexus may serve as a niche for endocrine cell generation.

How apical membrane is targeted and exocytosed during lumen formation is poorly understood. Studying the role of Afadin in this process will likely provide insight into how apical exocytosis occurs. It will be crucial to dissect the function of Afadin domains, particularly F-actin binding, RA and DIL domains, in this context. Carrying out domain deletions in *in vitro* lumen formation assays, such as in the MDCK system, would be a good starting point to address these questions. Likewise, identifying binding partners of Afadin in the context of lumen formation is likely to provide cues on Afadin function in exocytosis. Afadin is expressed in most epithelia and participates in junction formation; however, it may play independent roles and bind distinct sets of proteins during lumen formation (Mandai et al. 2013). Therefore, it will be key to carry out these experiments in *de novo* lumen forming systems and strictly during lumen formation, not before or after. Addressing these questions is prone to uncover mechanisms of exocytosis during *de novo* lumen formation.

Lumen coalescence has primarily been studied in lower vertebrates or invertebrates, and its mechanisms remain mostly unknown (Bagnat et al. 2007; Alvers et al. 2014). A major challenge in studying lumen coalescence is the lack of an *in vitro* model system. While *de novo* lumen formation has been investigated in the well-established three dimensional MDCK cultures, no model systems have been used for study of lumen coalescence.

Establishing such an *in vitro* system will undoubtedly provide a useful tool for visualizing and manipulating cellular and molecular events needed for lumen coalescence. In addition, time-lapse imaging of actin dynamics and junctional reorganization during lumen coalescence will be highly informative. Such time-lapse imaging of lumens can be performed on pancreatic explants, as presented through my work. When combined with pharmacological manipulations of RhoA or other signaling pathways, these approaches can uncover the molecular machinery behind regulation of actin dynamics to coalesce lumens. Future studies focused on these questions will facilitate dissection of mechanisms underlying lumen coalescence, and will help us gain insight into the formation of a rarely discussed, but clearly important, plexus state during development.

The last main direction will be to investigate how the plexus serves as a niche for endocrine cell generation. Simply identifying cell types or signaling factors enriched in the plexus will be crucial to this investigation. This may be achieved by transcriptomic analysis of plexus- versus periphery-associated bipotential cells through RNA-Sequencing. Making use of more advanced tools, single cell RNA-Sequencing can be performed on the heterogeneous cell populations microdissected from plexus versus periphery. These analyses may identify plexus-enriched cell types or subtypes, or molecular factors at the trancript level, with potential functions in endocrine fate induction. Further, a focus on endocrine-committed (high Neurog3^{+}) versus non-committed populations (low Neurog3^{+}) may uncover the pathways altered upon endocrine commitment.

The composition and conformation of cells required for endocrine fate can be further identified through quasi "*in vitro* reconstitution" studies using isolated cells and three

dimensional (3D) printing.. Recent technological advances in biophysics has made it possible to print cells in desired compositions and geometrical spaces in 3D (Visser et al. 2018). Furthermore, studies from the Grapin-Botton lab have identified media conditions required to culture pancreatic progenitors *in vitro* for both progenitor maintenance and differentiation towards major pancreatic lineages, including the endocrine lineage (Greggio et al. 2013). 3D-printing and culturing bipotential cells in core plexus (square) versus peripheral (linear) conformations may reveal whether the plexus serves as a niche by concentrating signaling events. These experiments can also be performed in the presence of other, mesenchymal or endothelial, subtypes. Such studies may uncover the cell types or subtypes, and geometrical conformation of these cells required for endocrine fate induction.

I predict that, making use of today's technology, future studies addressing these questions are likely to uncover mechanisms of endocrine fate induction that has, to date, remained elusive.

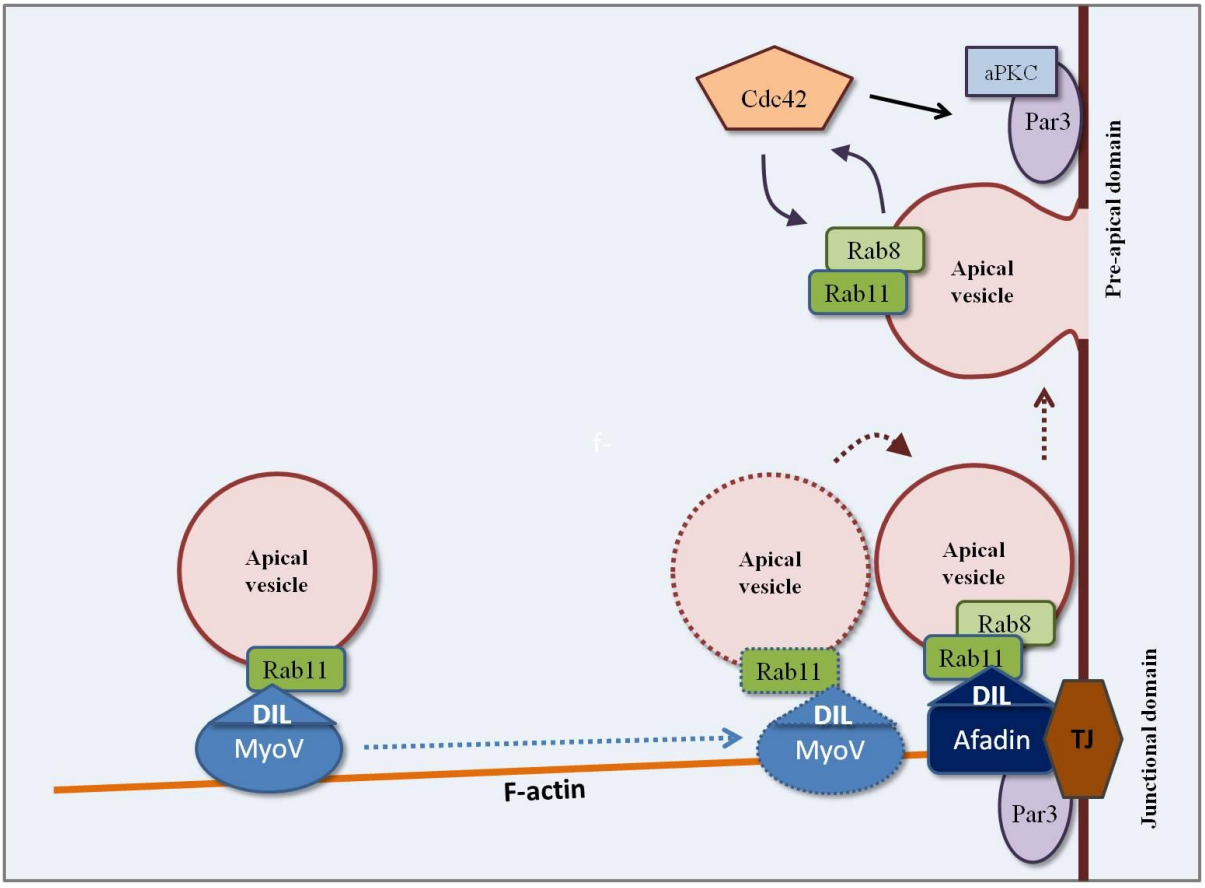

Figure 4. Speculative model on apical vesicle exocytosis during lumen formation. Apical vesicles carry the small GTPase Rab11 that helps targeting the vesicle to the proper membrane domain. Rab11 binds to the motor protein MyosinV (MyoV) through the MyoV DIL domain. Thus, MyoV may traffick apical vesicles on F-actin to the membrane. The target membrane domain may be tight junctional (TJ) foci, where Afadin resides. Afadin also carries a DIL domain with potential to bind Rab11. This potential binding may facilitate transfer of the apical vesicle from the motor protein MyoV over to the junctional protein Afadin. The vesicle may then be tethered to the junctional membrane. Afadin is also required for Rab8 loading onto the vesicle. Finally, action of nearby exocytosis mediators, including Cdc42 and Rab8, can result in exocytosis of the apical vesicle at the pre-apical membrane.

APPENDIX A
Antibody List

Antibody	Company	Catalog number
Afadin	Sigma	A0224
E-cadherin	BDBiosciences	610182
Muc1	ThermoFisher	HM-1630-P
ZO1	Invitrogen	33-9100
ZO1	Invitrogen	40-2200
DBA	VectorLabs	B-1035
Par3	Millipore	07-330
aPKC	SantaCruz	sc-216
Podocalyxin	R&DSystems	AF1556
Occludin	Invitrogen	71-1500
Laminin	Sigma	L9393
Rab11	Invitrogen	71-5300
Rab8A	ProteinTech	55296-1-AP
Rab8B	ProteinTech	55295-1-AP
Cdc42	CellSignaling	2462S
Sox9	Millipore	AB5535
Insulin	DAKO	A0564
Insulin	CellSignaling	4590
Glucagon	Millipore	4030-01F
Somatostatin	Immunostar	20067
Ghrelin	SantaCruz	sc-293422
pH3	Millipore	06-570
Neurog3	DSHB	F25A1B3-c
Amylase	Sigma	A8273

BIBLIOGRAPHY

Alvers AL, Ryan S, Scherz PJ, Huisken J, Bagnat M. 2014. Single continuous lumen formation in the zebrafish gut is mediated by smoothened-dependent tissue remodeling. *Development* **141**: 1110-1119.

Apelqvist A, Li H, Sommer L, Beatus P, Anderson DJ, Honjo T, Hrabe de Angelis M, Lendahl U, Edlund H. 1999. Notch signalling controls pancreatic cell differentiation. *Nature* **400**: 877-881.

Azizoglu DB, Cleaver O. 2016. Blood vessel crosstalk during organogenesis-focus on pancreas and endothelial cells. *Wiley interdisciplinary reviews Developmental biology* **5**: 598-617.

Azzarelli R, Hurley C, Sznurkowska MK, Rulands S, Hardwick L, Gamper I, Ali F, McCracken L, Hindley C, McDuff F et al. 2017. Multi-site Neurogenin3 Phosphorylation Controls Pancreatic Endocrine Differentiation. *Developmental cell* **41**: 274-286 e275.

Bagnat M, Cheung ID, Mostov KE, Stainier DY. 2007. Genetic control of single lumen formation in the zebrafish gut. *Nature cell biology* **9**: 954-960.

Bankaitis ED, Bechard ME, Wright CVE. 2015. Feedback control of growth, differentiation, and morphogenesis of pancreatic endocrine progenitors in an epithelial plexus niche. *Genes & development* **29**: 2203-2216.

Barry DM, Koo Y, Norden PR, Wylie LA, Xu K, Wichaidit C, Azizoglu DB, Zheng Y, Cobb MH, Davis GE et al. 2016. Rasip1-Mediated Rho GTPase Signaling Regulates Blood Vessel Tubulogenesis via Nonmuscle Myosin II. *Circulation research* **119**: 810-+.

Bonello TT, Perez-Vale KZ, Sumigray KD, Peifer M. 2018. Rap1 acts via multiple mechanisms to position Canoe and adherens junctions and mediate apical-basal polarity establishment. *Development* **145**.

Bouwens L, De Blay E. 1996. Islet morphogenesis and stem cell markers in rat pancreas. *The journal of histochemistry and cytochemistry : official journal of the Histochemistry Society* **44**: 947-951.

Bryant DM, Datta A, Rodriguez-Fraticelli AE, Peranen J, Martin-Belmonte F, Mostov KE. 2010. A molecular network for de novo generation of the apical surface and lumen. *Nature cell biology* **12**: 1035-1045.

Caprioli A, Villasenor A, Wylie LA, Braitsch C, Marty-Santos L, Barry D, Karner CM, Fu S, Meadows SM, Carroll TJ et al. 2015. Wnt4 is essential to normal mammalian lung development. *Developmental biology* **406**: 222-234.

Carminati M, Gallini S, Pirovano L, Alfieri A, Bisi S, Mapelli M. 2016. Concomitant binding of Afadin to LGN and F-actin directs planar spindle orientation. *Nature structural & molecular biology* **23**: 155-163.

Citi S, Guerrera D, Spadaro D, Shah J. 2014. Epithelial junctions and Rho family GTPases: the zonular signalosome. *Small GTPases* **5**: 1-15.

Dahl U, Sjodin A, Semb H. 1996. Cadherins regulate aggregation of pancreatic beta-cells in vivo. *Development* **122**: 2895-2902.

Das A, Tanigawa S, Karner CM, Xin M, Lum L, Chen C, Olson EN, Perantoni AO, Carroll TJ. 2013. Stromal-epithelial crosstalk regulates kidney progenitor cell differentiation. *Nature cell biology* **15**: 1035-1044.

Datta A, Bryant DM, Mostov KE. 2011. Molecular regulation of lumen morphogenesis. *Curr Biol* **21**: R126-136.

De Vas MG, Kopp JL, Heliot C, Sander M, Cereghini S, Haumaitre C. 2015. Hnf1b controls pancreas morphogenesis and the generation of Ngn3+ endocrine progenitors. *Development* **142**: 871-882.

Denker E, Sehring IM, Dong B, Audisso J, Mathiesen B, Jiang D. 2015. Regulation by a TGF beta-ROCK-actomyosin axis secures a non-linear lumen expansion that is essential for tubulogenesis. *Development* **142**: 1639-1650.

Desgraz R, Herrera PL. 2009. Pancreatic neurogenin 3-expressing cells are unipotent islet precursors. *Development* **136**: 3567-3574.

Drake CJ, Brandt SJ, Trusk TC, Little CD. 1997. TAL1/SCL is expressed in endothelial progenitor cells/angioblasts and defines a dorsal-to-ventral gradient of vasculogenesis. *Developmental biology* **192**: 17-30.

Drake CJ, Fleming PA. 2000. Vasculogenesis in the day 6.5 to 9.5 mouse embryo. *Blood* **95**: 1671-1679.

Gannon M, Ray MK, Van Zee K, Rausa F, Costa RH, Wright CV. 2000. Persistent expression of HNF6 in islet endocrine cells causes disrupted islet architecture and loss of beta cell function. *Development* **127**: 2883-2895.

Gao L, Yang Z, Hiremath C, Zimmerman SE, Long B, Brakeman PR, Mostov KE, Bryant DM, Luby-Phelps K, Marciano DK. 2017. Afadin orients cell division to position the tubule lumen in developing renal tubules. *Development* **144**: 3511-3520.

Gingras AR, Puzon-McLaughlin W, Bobkov AA, Ginsberg MH. 2016. Structural Basis of Dimeric Rasip1 RA Domain Recognition of the Ras Subfamily of GTP-Binding Proteins. *Structure* **24**: 2152-2162.

Gittes GK, Galante PE, Hanahan D, Rutter WJ, Debase HT. 1996. Lineage-specific morphogenesis in the developing pancreas: role of mesenchymal factors. *Development* **122**: 439-447.

Gouzi M, Kim YH, Katsumoto K, Johansson K, Grapin-Botton A. 2011. Neurogenin3 initiates stepwise delamination of differentiating endocrine cells during pancreas development. *Developmental dynamics : an official publication of the American Association of Anatomists* **240**: 589-604.

Gradwohl G, Dierich A, LeMeur M, Guillemot F. 2000. neurogenin3 is required for the development of the four endocrine cell lineages of the pancreas. *Proceedings of the National Academy of Sciences of the United States of America* **97**: 1607-1611.

Greggio C, De Franceschi F, Figueiredo-Larsen M, Gobaa S, Ranga A, Semb H, Lutolf M, Grapin-Botton A. 2013. Artificial three-dimensional niches deconstruct pancreas development in vitro. *Development* **140**: 4452-4462.

Gu G, Dubauskaite J, Melton DA. 2002. Direct evidence for the pancreatic lineage: NGN3+ cells are islet progenitors and are distinct from duct progenitors. *Development* **129**: 2447-2457.

Hale MA, Swift GH, Hoang CQ, Deering TG, Masui T, Lee YK, Xue J, MacDonald RJ. 2014. The nuclear hormone receptor family member NR5A2 controls aspects of multipotent progenitor cell formation and acinar differentiation during pancreatic organogenesis. *Development* **141**: 3123-3133.

Hao Y, Du Q, Chen X, Zheng Z, Balsbaugh JL, Maitra S, Shabanowitz J, Hunt DF, Macara IG. 2010. Par3 controls epithelial spindle orientation by aPKC-mediated phosphorylation of apical Pins. *Curr Biol* **20**: 1809-1818.

Herrera PL, Huarte J, Sanvito F, Meda P, Orci L, Vassalli JD. 1991. Embryogenesis of the murine endocrine pancreas; early expression of pancreatic polypeptide gene. *Development* **113**: 1257-1265.

Hick AC, van Eyll JM, Cordi S, Forez C, Passante L, Kohara H, Nagasawa T, Vanderhaeghen P, Courtoy PJ, Rousseau GG et al. 2009. Mechanism of primitive duct formation in the pancreas and submandibular glands: a role for SDF-1. *BMC developmental biology* **9**: 66.

Hieda Y, Iwai K, Morita T, Nakanishi Y. 1996. Mouse embryonic submandibular gland epithelium loses its tissue integrity during early branching morphogenesis. *Developmental dynamics : an official publication of the American Association of Anatomists* **207**: 395-403.

Hogan BL, Kolodziej PA. 2002. Organogenesis: molecular mechanisms of tubulogenesis. *Nature reviews Genetics* **3**: 513-523.

Horne-Badovinac S, Lin D, Waldron S, Schwarz M, Mbamalu G, Pawson T, Jan Y, Stainier DY, Abdelilah-Seyfried S. 2001. Positional cloning of heart and soul reveals multiple roles for PKC lambda in zebrafish organogenesis. *Curr Biol* **11**: 1492-1502.

Hoshino T, Sakisaka T, Baba T, Yamada T, Kimura T, Takai Y. 2005. Regulation of E-cadherin endocytosis by nectin through afadin, Rap1, and p120ctn. *The Journal of biological chemistry* **280**: 24095-24103.

Ikeda W, Nakanishi H, Miyoshi J, Mandai K, Ishizaki H, Tanaka M, Togawa A, Takahashi K, Nishioka H, Yoshida H et al. 1999. Afadin: A key molecule essential for structural organization of cell-cell junctions of polarized epithelia during embryogenesis. *Journal of Cell Biology* **146**: 1117-1131.

Iruela-Arispe ML, Beitel GJ. 2013. Tubulogenesis. *Development* **140**: 2851-2855.

Jaffe AB, Kaji N, Durgan J, Hall A. 2008. Cdc42 controls spindle orientation to position the apical surface during epithelial morphogenesis. *The Journal of cell biology* **183**: 625-633.

Jennings RE, Berry AA, Strutt JP, Gerrard DT, Hanley NA. 2015. Human pancreas development. *Development* **142**: 3126-3137.

Jensen J. 2004. Gene regulatory factors in pancreatic development. *Developmental dynamics : an official publication of the American Association of Anatomists* **229**: 176-200.

Jensen J, Heller RS, Funder-Nielsen T, Pedersen EE, Lindsell C, Weinmaster G, Madsen OD, Serup P. 2000. Independent development of pancreatic alpha- and beta-cells from neurogenin3-expressing precursors: a role for the notch pathway in repression of premature differentiation. *Diabetes* **49**: 163-176.

Jiang JJ, Au M, Lu KH, Eshpeter A, Korbutt G, Fisk G, Majumdar AS. 2007. Generation of insulin-producing islet-like clusters from human embryonic stem cells. *Stem cells* **25**: 1940-1953.

Kang HS, Kim YS, ZeRuth G, Beak JY, Gerrish K, Kilic G, Sosa-Pineda B, Jensen J, Pierreux CE, Lemaigre FP et al. 2009. Transcription factor Glis3, a novel critical player in the regulation of pancreatic beta-cell development and insulin gene expression. *Molecular and cellular biology* **29**: 6366-6379.

Kao DI, Lacko LA, Ding BS, Huang C, Phung K, Gu G, Rafii S, Stuhlmann H, Chen S. 2015. Endothelial cells control pancreatic cell fate at defined stages through EGFL7 signaling. *Stem Cell Rep* **4**: 181-189.

Kelly OG, Chan MY, Martinson LA, Kadoya K, Ostertag TM, Ross KG, Richardson M, Carpenter MK, D'Amour KA, Kroon E et al. 2011. Cell-surface markers for the isolation of pancreatic cell types derived from human embryonic stem cells. *Nat Biotechnol* **29**: 750-U114.

Kesavan G, Sand FW, Greiner TU, Johansson JK, Kobberup S, Wu X, Brakebusch C, Semb H. 2009. Cdc42-mediated tubulogenesis controls cell specification. *Cell* **139**: 791-801.

Khandelwal P, Prakasam HS, Clayton DR, Ruiz WG, Gallo LI, van Roekel D, Lukianov S, Peranen J, Goldenring JR, Apodaca G. 2013. A Rab11a-Rab8a-Myo5B network promotes stretch-regulated exocytosis in bladder umbrella cells. *Mol Biol Cell* **24**: 1007-1019.

Kim YH, Larsen HL, Rue P, Lemaire LA, Ferrer J, Grapin-Botton A. 2015. Cell cycle-dependent differentiation dynamics balances growth and endocrine differentiation in the pancreas. *PLoS biology* **13**: e1002111.

Klinger M, Wang W, Kuhns S, Barenz F, Drager-Meurer S, Pereira G, Gruss OJ. 2014. The novel centriolar satellite protein SSX2IP targets Cep290 to the ciliary transition zone. *Mol Biol Cell* **25**: 495-507.

Konstantinova I, Nikolova G, Ohara-Imaizumi M, Meda P, Kucera T, Zarbalis K, Wurst W, Nagamatsu S, Lammert E. 2007. EphA-Ephrin-A-mediated beta cell communication regulates insulin secretion from pancreatic islets. *Cell* **129**: 359-370.

Kopp JL, Dubois CL, Schaffer AE, Hao E, Shih HP, Seymour PA, Ma J, Sander M. 2011. Sox9+ ductal cells are multipotent progenitors throughout development but do not produce new endocrine cells in the normal or injured adult pancreas. *Development* **138**: 653-665.

Krentz NAJ, van Hoof D, Li Z, Watanabe A, Tang M, Nian C, German MS, Lynn FC. 2017. Phosphorylation of NEUROG3 Links Endocrine Differentiation to the Cell Cycle in Pancreatic Progenitors. *Developmental cell* **41**: 129-142 e126.

Landsman L, Nijagal A, Whitchurch TJ, Vanderlaan RL, Zimmer WE, Mackenzie TC, Hebrok M. 2011. Pancreatic mesenchyme regulates epithelial organogenesis throughout development. *PLoS biology* **9**: e1001143.

Larsen HL, Grapin-Botton A. 2017. The molecular and morphogenetic basis of pancreas organogenesis. *Seminars in cell & developmental biology* **66**: 51-68.

Lee S, Kolodziej PA. 2002. The plakin Short Stop and the RhoA GTPase are required for E-cadherin-dependent apical surface remodeling during tracheal tube fusion. *Development* **129**: 1509-1520.

Magenheim J, Ilovich O, Lazarus A, Klochendler A, Ziv O, Werman R, Hija A, Cleaver O, Mishani E, Keshet E et al. 2011. Blood vessels restrain pancreas branching, differentiation and growth. *Development* **138**: 4743-4752.

Mandai K, Rikitake Y, Shimono Y, Takai Y. 2013. Afadin/AF-6 and Canoe: Roles in Cell Adhesion and Beyond. *Prog Mol Biol Transl* **116**: 433-454.

Marciano DK. 2017. A holey pursuit: lumen formation in the developing kidney. *Pediatric nephrology* **32**: 7-20.

Marty-Santos L, Cleaver O. 2016. Pdx1 regulates pancreas tubulogenesis and E-cadherin expression. *Development* **143**: 101-112.

Massarwa R, Schejter ED, Shilo BZ. 2009. Apical secretion in epithelial tubes of the Drosophila embryo is directed by the Formin-family protein Diaphanous. *Developmental cell* **16**: 877-888.

Massumi M, Pourasgari F, Nalla A, Batchuluun B, Nagy K, Neely E, Gull R, Nagy A, Wheeler MB. 2016. An Abbreviated Protocol for In Vitro Generation of Functional Human Embryonic Stem Cell-Derived Beta-Like Cells. *PloS one* **11**.

Miettinen PJ, Huotari M, Koivisto T, Ustinov J, Palgi J, Rasilainen S, Lehtonen E, Keski-Oja J, Otonkoski T. 2000. Impaired migration and delayed differentiation of pancreatic islet cells in mice lacking EGF-receptors. *Development* **127**: 2617-2627.

Miller K, Kim A, Kilimnik G, Jo J, Moka U, Periwal V, Hara M. 2009. Islet formation during the neonatal development in mice. *PloS one* **4**: e7739.

Miralles F, Battelino T, Czernichow P, Scharfmann R. 1998a. TGF-beta plays a key role in morphogenesis of the pancreatic islets of Langerhans by controlling the activity of the matrix metalloproteinase MMP-2. *The Journal of cell biology* **143**: 827-836.

Miralles F, Czernichow P, Scharfmann R. 1998b. Follistatin regulates the relative proportions of endocrine versus exocrine tissue during pancreatic development. *Development* **125**: 1017-1024.

Muller T, Hess MW, Schiefermeier N, Pfaller K, Ebner HL, Heinz-Erian P, Ponstingl H, Partsch J, Rollinghoff B, Kohler H et al. 2008. MYO5B mutations cause microvillus inclusion disease and disrupt epithelial cell polarity. *Nat Genet* **40**: 1163-1165.

Nanba D, Nakanishi Y, Hieda Y. 2001. Changes in adhesive properties of epithelial cells during early morphogenesis of the mammary gland. *Development, growth & differentiation* **43**: 535-544.

Pagliuca FW, Millman JR, Gurtler M, Segel M, Van Dervort A, Ryu JH, Peterson QP, Greiner D, Melton DA. 2014. Generation of Functional Human Pancreatic beta Cells In Vitro. *Cell* **159**: 428-439.

Pan FC, Wright C. 2011. Pancreas Organogenesis: From Bud to Plexus to Gland. *Dev Dynam* **240**: 530-565.

Pan XC, Schnell U, Karner CM, Small EV, Carroll TJ. 2015. A Cre-Inducible Fluorescent Reporter for Observing Apical Membrane Dynamics. *Genesis* **53**: 285-293.

Petzold KM, Spagnoli FM. 2012. A system for ex vivo culturing of embryonic pancreas. *Journal of visualized experiments : JoVE*: e3979.

Pictet RL, Clark WR, Williams RH, Rutter WJ. 1972. An ultrastructural analysis of the developing embryonic pancreas. *Developmental biology* **29**: 436-467.

Pierreux CE, Cordi S, Hick AC, Achouri Y, Ruiz de Almodovar C, Prevot PP, Courtoy PJ, Carmeliet P, Lemaigre FP. 2010. Epithelial: Endothelial cross-talk regulates exocrine differentiation in developing pancreas. *Developmental biology* **347**: 216-227.

Post A, Pannekoek WJ, Ross SH, Verlaan I, Brouwer PM, Bos JL. 2013. Rasip1 mediates Rap1 regulation of Rho in endothelial barrier function through ArhGAP29. *Proceedings of the National Academy of Sciences of the United States of America* **110**: 11427-11432.

Pulkkinen MA, Spencer-Dene B, Dickson C, Otonkoski T. 2003. The IIIb isoform of fibroblast growth factor receptor 2 is required for proper growth and branching of pancreatic ductal epithelium but not for differentiation of exocrine or endocrine cells. *Mechanisms of development* **120**: 167-175.

Qin Y, Meisen WH, Hao Y, Macara IG. 2010. Tuba, a Cdc42 GEF, is required for polarized spindle orientation during epithelial cyst formation. *The Journal of cell biology* **189**: 661-669.

Rakotomamonjy J, Brunner M, Juschke C, Zang K, Huang EJ, Reichardt LF, Chenn A. 2017. Afadin controls cell polarization and mitotic spindle orientation in developing cortical radial glia. *Neural development* **12**: 7.

Rodriguez-Fraticelli AE, Vergarajauregui S, Eastburn DJ, Datta A, Alonso MA, Mostov K, Martin-Belmonte F. 2010. The Cdc42 GEF Intersectin 2 controls mitotic spindle orientation to form the lumen during epithelial morphogenesis. *The Journal of cell biology* **189**: 725-738.

Roland JT, Bryant DM, Datta A, Itzen A, Mostov KE, Goldenring JR. 2011. Rab GTPase-Myo5B complexes control membrane recycling and epithelial polarization. *Proceedings of the National Academy of Sciences of the United States of America* **108**: 2789-2794.

Rukstalis JM, Habener JF. 2007. Snail2, a mediator of epithelial-mesenchymal transitions, expressed in progenitor cells of the developing endocrine pancreas. *Gene expression patterns : GEP* **7**: 471-479.

Santosa MM, Low BS, Pek NM, Teo AK. 2015. Knowledge Gaps in Rodent Pancreas Biology: Taking Human Pluripotent Stem Cell-Derived Pancreatic Beta Cells into Our Own Hands. *Frontiers in endocrinology* **6**: 194.

Sato T, Fujita N, Yamada A, Ooshio T, Okamoto R, Irie K, Takai Y. 2006. Regulation of the assembly and adhesion activity of E-cadherin by nectin and afadin for the formation of adherens junctions in Madin-Darby canine kidney cells. *The Journal of biological chemistry* **281**: 5288-5299.

Sato T, Mushiake S, Kato Y, Sato K, Sato M, Takeda N, Ozono K, Miki K, Kubo Y, Tsuji A et al. 2007. The Rab8 GTPase regulates apical protein localization in intestinal cells. *Nature* **448**: 366-369.

Sawyer JK, Choi W, Jung KC, He L, Harris NJ, Peifer M. 2011. A contractile actomyosin network linked to adherens junctions by Canoe/afadin helps drive convergent extension. *Mol Biol Cell* **22**: 2491-2508.

Sawyer JK, Harris NJ, Slep KC, Gaul U, Peifer M. 2009. The Drosophila afadin homologue Canoe regulates linkage of the actin cytoskeleton to adherens junctions during apical constriction. *Journal of Cell Biology* **186**: 57-73.

Schaffer AE, Freude KK, Nelson SB, Sander M. 2010. Nkx6 transcription factors and Ptf1a function as antagonistic lineage determinants in multipotent pancreatic progenitors. *Developmental cell* **18**: 1022-1029.

Schwitzgebel VM, Scheel DW, Conners JR, Kalamaras J, Lee JE, Anderson DJ, Sussel L, Johnson JD, German MS. 2000. Expression of neurogenin3 reveals an islet cell precursor population in the pancreas. *Development* **127**: 3533-3542.

Seymour PA, Freude KK, Tran MN, Mayes EE, Jensen J, Kist R, Scherer G, Sander M. 2007. SOX9 is required for maintenance of the pancreatic progenitor cell pool. *Proceedings of the National Academy of Sciences of the United States of America* **104**: 1865-1870.

Shin K, Fogg VC, Margolis B. 2006. Tight junctions and cell polarity. *Annu Rev Cell Dev Biol* **22**: 207-235.

Sigurbjornsdottir S, Mathew R, Leptin M. 2014. Molecular mechanisms of de novo lumen formation. *Nat Rev Mol Cell Bio* **15**: 665-676.

Solar M, Cardalda C, Houbracken I, Martin M, Maestro MA, De Medts N, Xu X, Grau V, Heimberg H, Bouwens L et al. 2009. Pancreatic exocrine duct cells give rise to insulin-producing beta cells during embryogenesis but not after birth. *Developmental cell* **17**: 849-860.

Stanger BZ, Tanaka AJ, Melton DA. 2007. Organ size is limited by the number of embryonic progenitor cells in the pancreas but not the liver. *Nature* **445**: 886-891.

Takahashi K, Matsuo T, Katsube T, Ueda R, Yamamoto D. 1998. Direct binding between two PDZ domain proteins Canoe and ZO-1 and their roles in regulation of the Jun N-terminal kinase pathway in Drosophila morphogenesis. *Mechanisms of development* **78**: 97-111.

Takai Y, Ikeda XA, Ogita H, Rikitake Y. 2008. The Immunoglobulin-Like Cell Adhesion Molecule Nectin and Its Associated Protein Afadin. *Annu Rev Cell Dev Bi* **24**: 309-342.

Tanaka-Okamoto M, Hori K, Ishizaki H, Itoh Y, Onishi S, Yonemura S, Takai Y, Miyoshi J. 2011. Involvement of afadin in barrier function and homeostasis of mouse intestinal epithelia. *Journal of cell science* **124**: 2231-2240.

Tawk M, Araya C, Lyons DA, Reugels AM, Girdler GC, Bayley PR, Hyde DR, Tada M, Clarke JD. 2007. A mirror-symmetric cell division that orchestrates neuroepithelial morphogenesis. *Nature* **446**: 797-800.

Terry SJ, Zihni C, Elbediwy A, Vitiello E, Leefa Chong San IV, Balda MS, Matter K. 2011. Spatially restricted activation of RhoA signalling at epithelial junctions by

p114RhoGEF drives junction formation and morphogenesis. *Nature cell biology* **13**: 159-166.

Thompson BJ. 2013. Cell polarity: models and mechanisms from yeast, worms and flies. *Development* **140**: 13-21.

Villasenor A, Chong DC, Henkemeyer M, Cleaver O. 2010. Epithelial dynamics of pancreatic branching morphogenesis. *Development* **137**: 4295-4305.

Visser CW, Kamperman T, Karbaat LP, Lohse D, Karperien M. 2018. In-air microfluidics enables rapid fabrication of emulsions, suspensions, and 3D modular (bio)materials. *Science advances* **4**: eaao1175.

Wang S, Yan J, Anderson DA, Xu Y, Kanal MC, Cao Z, Wright CV, Gu G. 2010. Neurog3 gene dosage regulates allocation of endocrine and exocrine cell fates in the developing mouse pancreas. *Developmental biology* **339**: 26-37.

Wilson CW, Parker LH, Hall CJ, Smyczek T, Mak J, Crow A, Posthuma G, De Maziere A, Sagolla M, Chalouni C et al. 2013. Rasip1 regulates vertebrate vascular endothelial junction stability through Epac1-Rap1 signaling. *Blood* **122**: 3678-3690.

Xu K, Sacharidou A, Fu S, Chong DC, Skaug B, Chen ZJ, Davis GE, Cleaver O. 2011. Blood Vessel Tubulogenesis Requires Rasip1 Regulation of GTPase Signaling. *Developmental cell* **20**: 526-539.

Yamaoka T, Itakura M. 1999. Development of pancreatic islets (review). *International journal of molecular medicine* **3**: 247-261.

Yang ZF, Zimmerman S, Brakeman PR, Beaudoin GM, Reichardt LF, Marciano DK. 2013. De novo lumen formation and elongation in the developing nephron: a central role for afadin in apical polarity. *Development* **140**: 1774-1784.

Zahraoui A, Louvard D, Galli T. 2000. Tight junction, a platform for trafficking and signaling protein complexes. *The Journal of cell biology* **151**: F31-36.

Zaidel-Bar R, Zhenhuan G, Luxenburg C. 2015. The contractome--a systems view of actomyosin contractility in non-muscle cells. *Journal of cell science* **128**: 2209-2217.

Zhadanov AB, Provance DW, Speer CA, Coffin JD, Goss D, Blixt JA, Reichert CM, Mercer JA. 1999. Absence of the tight junctional protein AF-6 disrupts epithelial cell-cell junctions and cell polarity during mouse development. *Curr Biol* **9**: 880-888.

Zhang H, Ables ET, Pope CF, Washington MK, Hipkens S, Means AL, Path G, Seufert J, Costa RH, Leiter AB et al. 2009. Multiple, temporal-specific roles for HNF6 in pancreatic endocrine and ductal differentiation. *Mechanisms of development* **126**: 958-973.

Zhou Q, Law AC, Rajagopal J, Anderson WJ, Gray PA, Melton DA. 2007. A multipotent progenitor domain guides pancreatic organogenesis. *Developmental cell* **13**: 103-114.